CODEN:LUTEDX/(TEIE-5421)/1-88/(2019)

Industrial Electrical Engineering and Automation

# Battery energy storage design and operation in an HVDC-system with WPP clusters



**Harald Åkesson**

Division of Industrial Electrical Engineering and Automation
Faculty of Engineering, Lund University

# Abstract

The electricity sector is in the beginning of a large shift from centralized dispatchable production to distributed variable production. With this necessary change, new challenges arise. One crucial challenge is related to upholding the system balance in the power grid. In this master thesis, a Battery Energy Storage System (BESS) has been implemented in an HVDC-system with large amounts of Wind Power Plant (WPP) clusters, for performing the primary control, to see if this could contribute to the development of renewables. The purpose of this work is to find out what control strategy could be used to balance the DC-grid both short-term and long-term as well as in what capacity range the BESS would have to be.

Power flow simulations have been performed based on the prevailing conditions of a project (Baltic InteGrid) striving to commission roughly 11 GW of offshore wind power joined between Sweden, Poland and Lithuania. Wind data from the area has been obtained in order to create estimated power outputs from the wind power plants as well as appropriate electricity market interactions for the connection points onshore. Due to the electricity market being based on estimated power output from the WPPs, simulations when no forecast error existed as well as when a large forecast error existed were performed. Additionally, due to the electricity intraday market is planned to change from operating on a one-hour-basis to a 15-min-basis, the impact of this has been evaluated. Lastly, due to the DC-system being connected to the AC utility grid, the primary control of the AC-grid is available for use. Both simulations with no AC-grid dependency as well as simulations allowing some AC-grid dependency were performed.

To an existing simulation model of Baltic InteGrid created in OpenModelica, a simplified BESS was implemented. The BESS is performing both short-term energy management (periods of seconds) and long-term energy management (periods of hours). The short term management is utilizing a DC-droop voltage control. To decrease the BESS capacity, the electricity intraday market is utilized in order to sell or buy energy in order to regulate the State of Charge (SOC) of the BESS. For the intraday market, three control strategies were implemented to decide if and to what extent a market interaction was needed. Method 1 utilizes only the current SOC of the BESS. Method 2 utilizes the predicted SOC of the BESS at one time-unit forward and Method 3 utilizes the predicted SOC of the BESS for both one time-unit forward and two time-units forward.

Through extensive simulations, it was found that all methods solved the problem of regulating the DC-grid with little or no AC-grid dependency. It was also found that the intraday market time-basis was of very large importance. Furthermore, both the forecast error and allowing the AC-grid to perform the primary control to some extent led to a much smaller BESS capacity generally. Method 1 was the least complex to implement but was largely outperformed by the more complex Method 2 and Method 3 in all aspects considered. Method 3 was better than Method 2 in terms of lower magnitudes of market interaction as well as a smaller amount of energy being transferred for altering the SOC of the BESS. However, Method 2 gave a slightly better result in terms of AC-grid dependency. The BESS capacity needed was somewhere in the range of 130-4000 MWh for Method 1 depending on the intraday market time-basis, forecast error as well as AC-grid dependency. The

figures for Method 2 and Method 3 were 60-1900 MWh. Ruling in the number of SOC-cycles and thereby evaluating the lifetime of the BESS, initial results suggest a larger BESS capacity would be needed. For Method 2 and 3, allowing AC-grid dependency and a 15 min Elbas time-basis a capacity in the range of 120 - 180 MWh depending on wind power forecast error would be the bare minimum for reaching an acceptable theoretical lifetime.

Through very brief economic calculations it was concluded that implementing a BESS could with high possibility be a superior choice compared to the alternative of upgrading the AC utility grid to handle the large fluctuations. However, regarding if Method 2 or Method 3 should be utilized in order to regulate the BESS, more research with higher resolution is needed.

# Acknowledgements

This thesis is the final step towards my Master's degree in Electrical engineering from the Faculty of Engineering, Lund University. It was carried out at the division of Industrial Electrical Engineering and Automation (IEA).

I would like to express my gratitude to my supervisor Dr. Jörgen Svensson. His deep knowledge in the field, as well as his great experience in modelling and simulations, have been very valuable in this work. But more importantly, his passion and enthusiasm have triggered me to leave no stone unturned and achieve a much better result.

I would also like to send a thank you to the employees at the IEA division for the great coffee room discussions that have not necessarily been about battery storages and mitigating power discrepancies.

Harald Åkesson,
2019-04-01

# Nomenclature

| | |
|---|---|
| $C$ | Capacitance [F] |
| $C_b$ | Battery Energy System capacity [MWh] |
| $E_{01}$ | Predicted energy balance from time t until t+1 [MWh] |
| $E_{12}$ | Predicted energy balance from time t+1 until t+2 [MWh] |
| $E_{23}$ | Predicted energy balance from time t+2 until t+3 [MWh] |
| $n$ | Number of segments |
| $P_{balance}$ | Difference between power input and power output in the DC-system [MW] |
| $P_{charge}$ | Charge power of BESS [MW] |
| $P_{discharge}$ | Discharge power of BESS [MW] |
| $P_{fixed}$ | Power setpoint for charge/discharge of BESS [MW] |
| $P_{MI}$ | Power setpoint for market interaction [MW] |
| $P_{MI_{01}}$ | Power setpoint for market interaction at time t until t+1 [MW] |
| $P_{MI_{12}}$ | Power setpoint for market interaction at time t+1 until t+2 [MW] |
| $P_{MI\_buy}$ | Power setpoint for buying from intraday market [MW] |
| $P_{MI_h}$ | Maximum power setpoint for market interaction [MW] |
| $P_{MI\_sell}$ | Power setpoint for selling to intraday market [MW] |
| $P_{MI_{t2}}$ | Alternative power setpoint for SOC at time t+2 [MW] |
| $P_{MI_{t3}}$ | Alternative power setpoint for SOC at time t+3 [MW] |
| $P_{THRES}$ | Threshold limit when a charging/discharging of BESS should occur [MW] |
| $SOC_b$ | SOC of Battery Energy Storage System |
| $SOC_H$ | Upper SOC-limit of the normal operation band |
| $SOC_{init}$ | Initial SOC of BESS |
| $SOC_L$ | Lower SOC-limit of the normal operation band |
| $SOC_{max}$ | Maximum SOC-limit of the usable capacity |
| $SOC_{max\_hyst}$ | Hysteresis band related to $SOC_{max}$ |
| $SOC_{min}$ | Minimum SOC-limit of the usable capacity |
| $SOC_{min\_hyst}$ | Hysteresis band related to the $SOC_{min}$ |
| $SOC_t$ | SOC-value at time t |
| $SOC_{t+1}$ | SOC-value at time t+1 |
| $SOC_{t+2}$ | SOC-value at time t+2 |
| $SOC_{t+3}$ | SOC-value at time t+3 |
| $SOC_T$ | SOC-target value |
| $SOC_{T\_H}$ | High SOC-target |
| $SOC_{T\_L}$ | Low SOC-target |
| $SOC_{T\_M}$ | SOC-target is the centre of the usable capacity |
| $x_i$ | Time-unit for the midpoint calculations, i=[0,12] |

| | |
|---|---|
| BESS | Battery Energy Storage System |
| BC | Best Case (scenario) |
| DoD | Depth of discharge |
| DSO | Distribution System Operator |
| EMS | Energy Management System |
| ESS | Energy Storage System |
| FC | Forecast |
| LCC | Line-Commutated Converter |
| LIB | Lithium-Ion Battery |
| MI | Market Interaction |
| NOB | Normal Operation Band |
| OCP | Onshore Connection Point |
| $P_{reg}$ | Power regulation |
| PWM | Pulse Width Modulation |
| RES | Renewable Energy Source |
| SOC | State of Charge |
| TSO | Transmission System Operator |
| $V_{reg}$ | Voltage regulation |
| VSC | Voltage Source Converter |
| WC | Worst Case (scenario) |
| WPP | Wind Power Plant |

# Contents

# List of Figures

# List of Tables

# Chapter 1

# Introduction

---

*This first chapter gives an introduction to the subject of the thesis. It formulates the background to the problem as well as the methodology and limitations of this Master thesis. It also gives a short introduction of Baltic InteGrid, which is the project this thesis is based on.*

---

## 1.1 Background and Motivation

The electricity and energy sector contributes to a substantial share of the total global greenhouse gas emissions. With the United Nations recently determined Paris agreement of keeping this century's temperature increase well below 2°C [1], serious measures have to be taken in terms of decreasing this impact. The incentives for substituting the fossil sources in favour of renewable have increased the last decade with the rapid development in the field. Worldwide an extensive development of renewable electricity production plants consisting predominantly of wind and solar are ongoing [2]. Both wind and solar power are weather bounded variable Renewable Energy Sources (RES), thereby in the conventional power grid only connectable if there is sufficient amount of dispatchable electricity production, e.g hydropower, nuclear power etc, to provide the regulation needed to uphold a stable network. This is because the magnitude of the production has to be the same as the magnitude of the usage at all times. Naturally, the electricity consumption cannot follow the fluctuations from the RES, leading to more demand on the regulating units. Related to this, one of the requirements for a stable grid is the frequency of the grid voltage. In certain parts of the world, including Sweden, the frequency has to be close to 50 Hz at all times. When there is a mismatch between electricity generation and consumption the frequency of the grid deviates from its nominal value. It is thereby very important to ensure that the regulation capacity and ancillary services are abundant enough when planning the development of RES in the power grid.

A future global trend is to build very large clusters of Wind Power Plants (WPP) with capacities of far more than 1 GW. An example is Markbygden in Sweden with a total installed capacity of 4 GW [3]. Another, and the one that is going to be central in this Master thesis, is Baltic Integrid. These large clusters of WPPs entail many new challenges. The fluctuation alone from a large cluster of WPP could in the

extreme case easily be large enough to cause a blackout on the grid. Furthermore, the electricity market consists simplified of one day ahead market and one intraday market. With more RES, utilization of the intraday market will increase since the production is hard to predict with accuracy long time ahead. The intraday market operates currently on an hourly basis. The basis is planned to change until 2020 to a 15 minute time-basis [4]. Still, over the time of 15 minutes, the actual production might still differ substantially from what was projected. Due to this, the fluctuations to the grid will be large, especially when RES holds a large share of the total production.

With a larger share of RES, those areas of concern stated above will have to be solved. The Transmission System Operators (TSOs) are developing new grid codes requesting the WPPs to have regulation capacities under steady-state conditions [5]. However, the challenge of performing the balancing of the grid with very large fluctuations have to be solved. One solution to this could be to integrate an Energy Storage System (ESS) in the WPP-system. The ESS could, for instance, consist of Lithium-Ion batteries (LIB) which are seeing an upswing in numbers and downswing in price with the ongoing increase in electric vehicles. The batteries are projected to reach their technical end-of-life for vehicle applications much before the car. This could potentially lead to a large secondary market of batteries in the future. Despite having a slightly lower capacity when substituted from the vehicles, the batteries are still likely to be worthwhile for grid-applications.

## 1.2 Baltic Integrid

The work in this Master thesis is based on the EU project Baltic InteGrid which is in the preliminary investigative phase as of this report. The project is expected to enable the development of offshore WPP clusters of a total of 11.2 GW in the South Baltic Sea. Baltic InteGrid will be joint between Poland, Lithuania and Sweden [6]. The system will consist of various WPP clusters connected internally in a DC-system. The project is planned to commission it's first functioning plants in 2025 and further continue the development until finished in the year 2045. It should be noted that a plan to integrate an energy storage solution in this project does currently not exist.

## 1.3 Objectives

The objective of this Master thesis is to investigate the system characteristics of a DC-system with a large amount of WPP clusters where a Battery Energy Storage System (BESS) is implemented to perform the primary control. The objectives of this thesis are further defined through the following problem statements:

- What are the challenges regarding the system and what does the output data look like in the connection points to shore where the grid codes need to be followed?

- What control strategy should be used to minimize the BESS capacity and still uphold the stability of the DC-grid.
- What different electricity markets exist in Sweden, and how can the BESS affect these. Additionally, how can the primary control of the AC utility grid be combined with the BESS's ability of DC voltage control in minimizing the size of the storage?
- What is the economic difference between an optimized energy storage compared to extensive onshore reinforcements to manage the large power fluctuations?

## 1.4 Methodology

This work has been conducted through two main areas of concern. The first being an extensive literature background study of the conventional power grid, the functioning of a DC-system as well as the functioning, characteristics and applications of the BESS. The background study has been targeting those areas to the extent where enough knowledge is achieved to comprehend the complexity of an RES HVDC-system with a BESS. Thereby, some areas will be described to a deeper degree than others.

The second part is a series of simulations of the system. The simulations has been performed in the software OpenModelica and is based on an existing simulation model of Baltic Integrid. The model has been altered to fit the purpose of this Master thesis. The main alteration is the implementation of the BESS. Different possible scenarios related to the intraday market time-basis as well as the power output prediction have been decided, in which the effect of the BESS will be analyzed.

## 1.5 Scope and Limitations

Considering the broadness of a DC-system with a high amount RES connected to AC-systems and with a BESS as the primary controller, a full study combining all areas of concern have not been a reasonable goal for this master thesis. A model for normal operation has been created with various simplifications. The system has been simplified in the sense that no trans-boundary electricity market has been considered. The only power inputs to the system are the WPPs and the connection points to the AC-grid can thereby only act as a power output. This means that the DC-grid are largely underused. Only cable losses are considered, no conversion losses in the converter units or BESS exist. The measurement data for the WPP have a resolution of 10 min and range a full year.

## 1.6 Outline

Chapter 1 is the introduction of the report, where the background, objectives, methodology, scope and limitations, as well as a short introduction of Baltic InteGrid, is presented. Chapter 2 gives an overview of the different technical fields related to Baltic InteGrid as well as stating the challenges related to it. It continues with the theoretic knowledge needed of the different fields to understand the system integration. Chapter 3 describes the control strategies and methods used to solve the problems related to primary and secondary control in the DC-system. The implementation of the simulation model, as well as the scenario setups, are described in chapter 4. In chapter 5 the different parameter settings are explained as well as the result for the different methods given. An analysis and comparison between the methods are presented in the same chapter. Chapter 6 contains the discussion and conclusion of the report.

# Chapter 2

# System Integration

---

*This chapter will provide the technical background to this work. Initially the large WPP cluster of Baltic InteGrid is presented together with some technical data as well as the challenges related to it. The chapter continues with an overview of the AC utility grid, with the function of the electricity market as well as the functioning of the regulation. The chapter continues with an overview of a DC-system before presenting some basics of wind power. The last part of the chapter presents the technical background related to batteries and Energy Storage Systems.*

---

## 2.1 Baltic InteGrid

Baltic InteGrid consists of offshore WPP clusters of varying size connected to a multi-terminal DC-grid between onshore connection points (OCPs) in Sweden, Poland and Lithuania to the AC utility grid. The information in this report about Baltic InteGrid is prevailing at the time of writing but could be subject to change. Poland will have two connection points, one located in proximity to the city of Słupsk and the other one just west of Gdynia (Żarnowiec). Lithuania will have one connection point close to Klaipėda and in Sweden, the connection points will be north of Karlshamn (Hemsjö) as well as outside of Kalmar (Nybro). The area of Baltic InteGrid stretches between above-stated endpoints in the Baltic Sea, as seen in Figure 2.1. Four WPP clusters will connected directly to the system and take part in transboundary electricity trading. These represent roughly 4.8 GW of the total 11.2 GW of installed capacity planned. Additionally, local WPPs will be built in proximity to each country's land border providing the remaining 7 GW. The majority of these extra WPP clusters will be connected to Poland. These are also the ones that are planned to be commissioned first with the goal to be finished by 2025. The project is complex and comprises many different systems, the key components include:

- HVDC-grid
- AC utility grid
- Wind Power Plants
- The electricity market

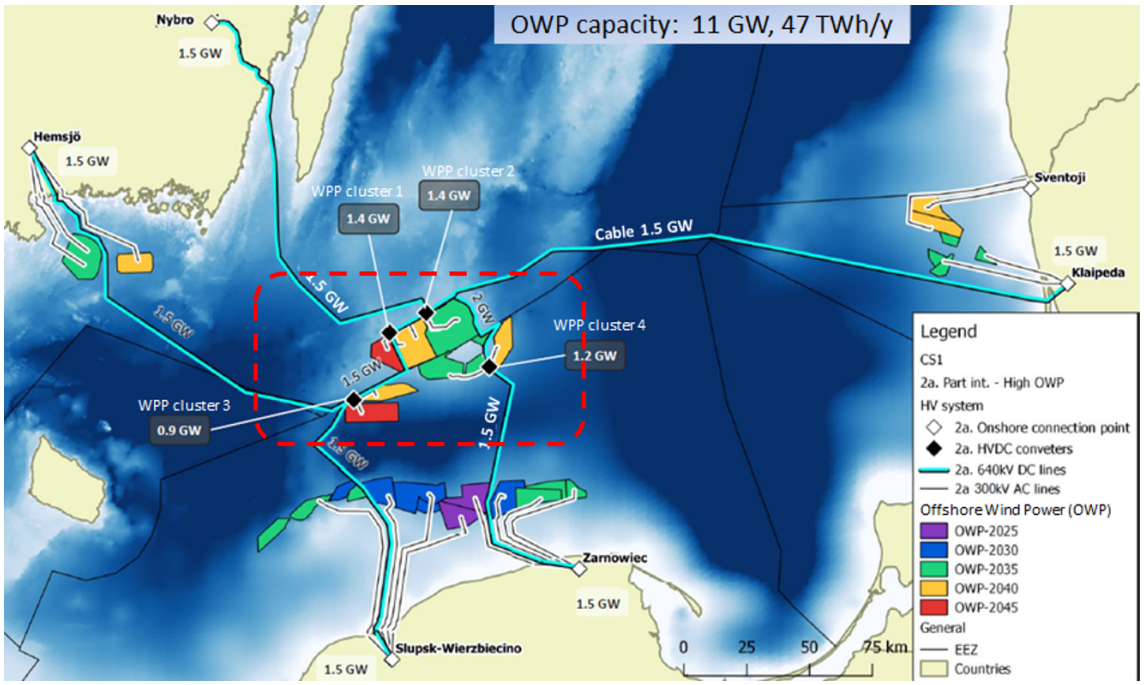


**Figure 2.1:** Overview of Baltic InteGrid [7] - The red dashed area highlights the WPP clusters that are interconnected in the DC-system.

### 2.1.1 Technical data

The four WPP clusters that are connected in the DC-system are the only ones considered in this work. Those have individual capacities of 876 MW, 1440 MW, 1404 MW, 1140 MW providing a total of 4860 MW of installed capacity [7]. The connection points on land are connected by Voltage Source Converters (VSC) to the high voltage AC-grid, 400 kV AC in Sweden and Poland and 330 kV AC in Lithuania. At each OCP, an electricity trade according to the Nordpool Spot and Elbas market (day ahead and intraday market) will be allowed. The intraday is currently working on a 1h time-basis. The transmission technology to be used is bipolar DC transmission lines rated at 1.5 GW and with a nominal voltage of 1 MV. A schematic system overview is presented in Figure 2.2. In the system, the arrows show the direction. Thus, an input to the system is defined as positive and an output is defined as negative. The wind data from the area has been collected from the mast 'FINO2' with one measure point every 10 minutes [8]. Linear interpolation is performed between the measurement points. The power output from the WPP clusters can be seen in figure 2.3a. Figure 2.3b shows a zoom in of the intermittency from the WPP clusters over a 12 day period. As seen in the figures, the maximum power output is roughly 4.8 GW.

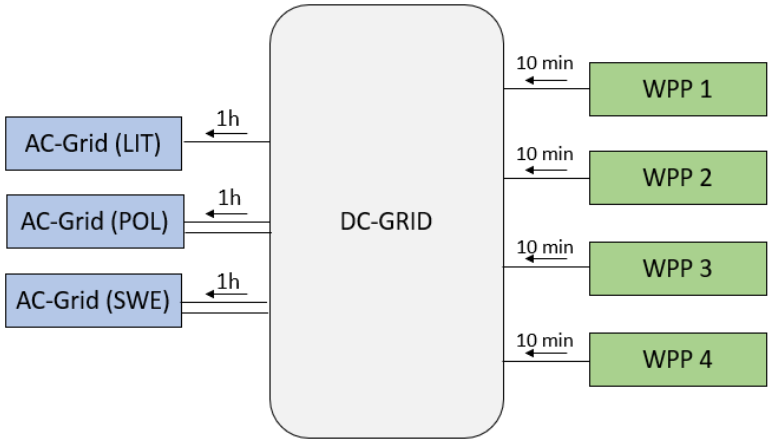


**Figure 2.2:** System overview of Baltic InteGrid - The four WPP clusters are connected to the DC-grid. This, in turn, is connected to three AC-grids. Two connections are in Sweden, two in Poland and one in Lithuania. The intraday market works on an 1 hour time-basis. The AC-grids are continuously balancing the DC-grid..

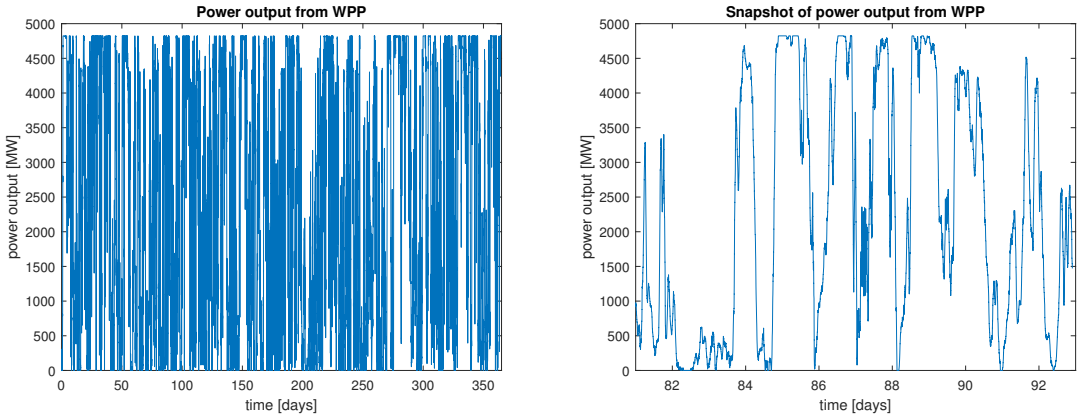


**(a)** **(b)**

**Figure 2.3:** Output data for the WPPs in Baltic InteGrid - (a) shows the fluctuations over the full year and (b) a zoom in for a 12 day period. Very large fluctuations can be spotted, with a maximum power output of 4.8 GW.

### 2.1.2 Challenges

The project contains many challenges that have to be solved before an actual implementation will be accepted by the Transmission System Operators (TSOs) of the countries. Initial analysis suggests that the high power rating of the DC transmission lines (1.5 GW) allows very high fluctuations on the connected AC-grid, which could potentially be larger than the dimensional fault of the AC-grid. This is especially significant for Sweden and Poland where two connections exist, giving a total maximum fluctuation of 3 GW. This will be further explained in section 2.2.2. Furthermore, to sell the electricity, a prediction of how much electric energy will be

generated for the selling period must be determined. While the predicted energy for the time period might be within the margins of error, the power output (energy per second) from the WPP clusters fluctuates constantly and are very rarely corresponding to the average power of the predicted energy output. This is illustrated in Figure 2.4. Since the power in the DC-grid always has to be balanced, the demand on the AC utility grid and its balancing units are increased compared to generation from dispatchable sources. Some initial simulations of the proposed structure relating to this have been performed to further decide the challenges. The results can be seen in Figures 2.5, 2.6 and 2.7. The results are representative of the year the data are collected from. Data from other years might differ.

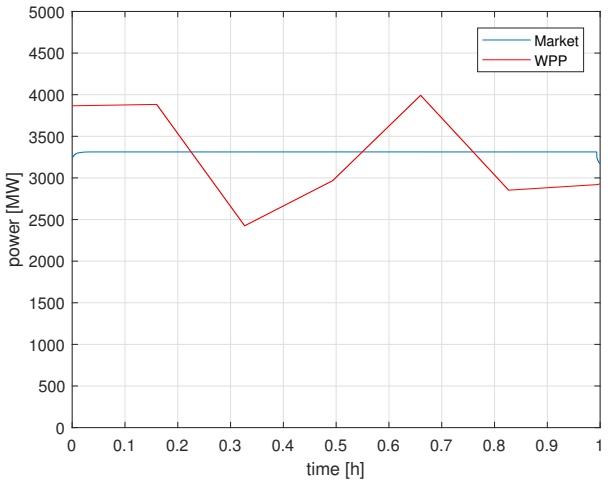


**Figure 2.4:** Power and energy output for one hour - The blue line is the average power output for one hour. The average power output is 3400 MW giving a total energy of 3400 MWh to be sold via the market for the period. The red line is the actual power output from the WPPs at every time. The difference between the two are the power balance in the DC-system

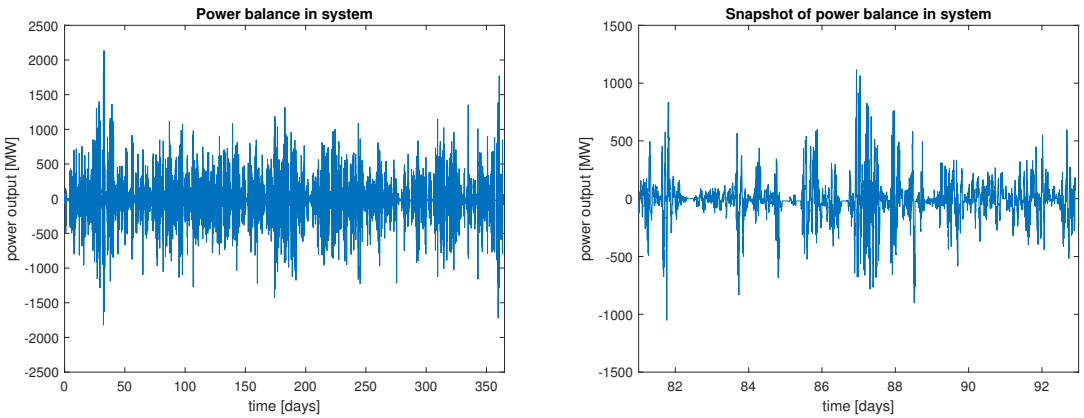


**(a)** **(b)**

**Figure 2.5:** Power balance in the DC-system with no forecast error - The input of power is from the WPPs and the output of power from the connection points to the AC power grid. A positive value is defined as a power surplus and a negative a power deficit.

As seen in Figure 2.5, the fluctuations are very large throughout the year confirming the high requirement on the regulation. The peak power unbalance exceeds the cable rating of 1.5 GW, suggesting that more than one connection point has to act as the regulation unit. Continuing, it is important to understand that the power output in the above figures are estimated when no forecast (FC) error are considered. The FC error will be further discussed in section 4.3 but for now, it is enough to understand that the fixed electricity market values at the OCPs are calculated based on the predicted WPP output. If the WPP output differs from the prediction, the power unbalance naturally gets larger since the electricity market values are set according to a forecast with no error. This is confirmed by Figure 2.6 where a 20 min FC error is used as an example and that the power unbalance more often reaches a larger value. This is clear by comparing the power at time = 30 days, where the power exceeds -2000 MW when a FC error is considered.

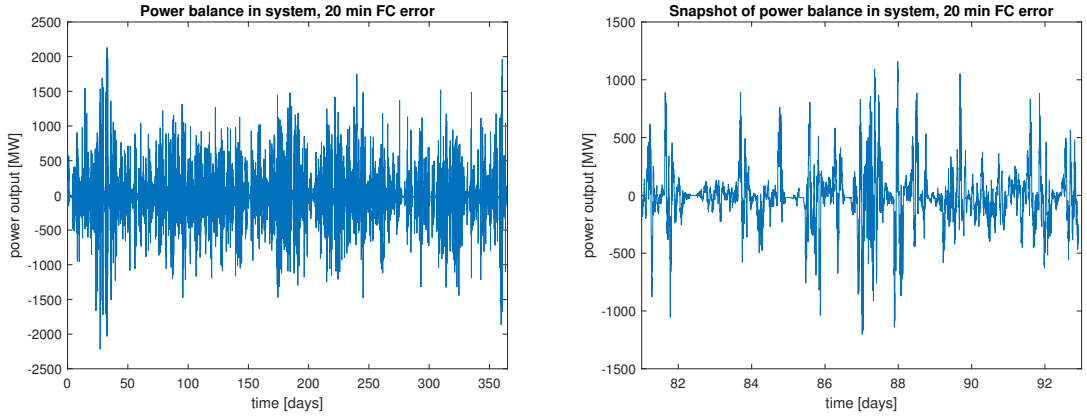


**Figure 2.6:** Power balance in the DC-system with 20 min forecast error

Continuing, just as important as the power balance in the DC-system is the energy balance. Figure 2.7 shows the fluctuations of the energy for the first 60 days of the year for used data and market calculation.

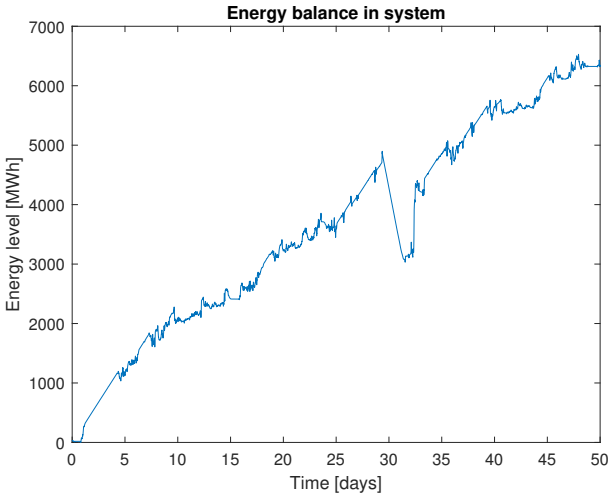


**Figure 2.7:** Energy balance in the DC-system for 50 days

As seen in Figure 2.7, very large ESSs would be needed to both mitigate the short term intermittency as well as mitigating the energy surplus and deficit over longer periods of time.

## 2.2 AC utility grid overview

The AC utility grid, or conventional power grid, is designed for large centralized production facilities. In the north of Sweden there are large hydro plants, and scattered around the southern parts of Sweden there is a handful of nuclear power plants. These types of production cover around 80 % of the total generation in Sweden today [9]. Above stated production types, although seemingly different, both use a turbine of sort for converting the kinetic energy to AC electric energy. The generated electricity is distributed to the AC power grid that typically has a voltage of 400 kV. In substations, the electricity is converted to lower voltages depending on area and intended use. The sub-transmission grid, connecting the areas of Sweden where 400 kV transmission lines have not yet been built, keep a nominal voltage of 220 kV. The medium voltage transmission lines, typically 10 - 70 kV in Sweden and the low voltage transmission lines, typically 400 V in Sweden, are part of the distribution grid. The distribution grid is connected to the end consumer, where 400 V is for private households and 10 - 70 kV for larger costumers, e.g factories. The Transmission System Operator (TSO), Svenska kraftnät in Sweden, is responsible for the maintenance, operation and development of the transmission lines. The Distribution System Operator (DSO) is responsible for corresponding in the distribution grid [10]. Additional to HVAC transmission lines, HVDC lines are also implemented in the system. As of writing the Swedish HVDC link Sydvästlänken, currently being built, will be ready for use in 2019. This will increase the power capacity by 25 % in the south of Sweden (SE4) [11]. Additionally, a line connecting the Swedish island Gotland exist as well as trans-boundary lines with Finland, Denmark, Germany, Poland and Lithuania.

### 2.2.1 Electricity market structure

Most of the generated electricity in the Nordic and Baltic countries are traded on trans-border markets organized by NordPool and Nasdaq OMX Commodities Europe. NordPool Spot is a day-ahead market, where the electricity generation companies leave bids for the electricity they are forecasting to generate for the next day. Elbas, the intraday market, (operated by NordPool) and the financial market governed by Nasdaq commodities are two complementary markets to NordPool Spot [12]. The Elbas intraday market works according to a 60 minute time-basis. This means that on the intraday market the electricity is traded for a full 60 minute period. Additionally, The trading has to be set at least 60 minutes before each new trading hour (so-called powerhours) begin. However, restrictions to this exist, where, e.g, trading within Norway has to be done 120 minutes before the start of the powerhour [13]. Furthermore, Elbas 4 is a newly instituted intraday market handling intraday trade on 15 and 30 minute basis, although, it is currently only available for the German market [14]. However, as earlier mentioned, the time-basis

for the intraday market will be changed to 15 minute in 2020. In 2011 Sweden was divided into price areas where different electricity spot price occurs [15]. The segments were SE1 in north ranging to SE4 in the south. The reason was the north being the main generation area while the south was the main consumption area, leading to bottlenecks in the transition zones. With the new system, the price is regulated by demand and supply leading to typically a higher price in the south and thereby increasing the incentives and profitability in generating electricity there.

### 2.2.2 Grid codes and ancillary services

Grid codes are a number of technical requirements decided for each country and with the role to ensure the stability of the utility grid. The grid codes apply to all customers and producers who want to connect to the utility grid. In Sweden and the Nordic countries a shared grid code, the Nordic grid code, is used for increasing the integration between the countries and enhance the function of the utility grid. The requirements relate to, among others, the frequency and voltage regulation. However, they also relate to preventing faults. The n-1 criteria is especially important. It expresses that the power system can lose one vital component, e.g a production unit, line, transformer etc, and still function [16]. Furthermore, The dimensioning fault is the largest impact the power system can withstand. This is regularly changing, but currently in Sweden, this is 1.4 GW [17]. This means that maximum 1.4 GW interconnectors can be connected. As a comparison, Baltic InteGrid is planned to have two 1.5 GW interconnectors.

#### Frequency regulation

The 36 member countries of the European Network of Transmission System Operators (ENTSO-E) is divided into 6 different synchronous areas [18]. Synchronous relates to the frequency of the grid that is exactly the same at all points in the area at all times. The frequency of the grid is crucial for the stable system. All grid connected appliances produced for the Swedish and European market are dependent on the electricity from the grid being 50 Hz. Generators and transformers are designed to run under nominal frequency. If the frequency deviates enough from nominal values the machinery connected to it might break following overheated internals. The frequency is constantly changing due to the continuous variation in production and consumption. However some variations, as long as they are within certain limits, are accepted. To maintain a frequency of around 50 Hz, frequency regulation is required. In relation to this three main reserves are present. The primary reserve is associated with the primary control. The primary control is fast and responds within seconds to a deviation in frequency. The objective of the primary control is to interrupt the deviation and stabilize the frequency at a steady value. However, this value can be higher or lower compared to the nominal value, which is why the secondary reserve and secondary control is needed. The secondary control is automatically activated within minutes. Thereby restoring the primary reserve in case a new fault would happen. The goal of the secondary control is to bring back the frequency to the nominal value. Lastly, a third reserve which is related to the

tertiary control exist. That is a fully manual response, activated by the operational personnel at the power plants during very large deviations [19].

The primary control in Sweden is regulated by certain hydropower plants in the north of the country. Svenska Kraftnät is responsible for reserving a certain amount of power from various balancing parties in order to handle variations. When it comes to variations of the frequency and the primary control, two different terminologies are used: Frequency containment for normal operation (FCR-N) and frequency containment for disturbances (FCR-D). The first is used for deviations in the normal operation range of 49.9 to 50.1 Hz, and the latter for more severe situations, such as black-outs or fall away of certain loads or generation facilities. A normal strategy For operating the frequency control is through Droop control. Droop control is essentially a way of letting the generators respond to the change in frequency in relation to their production capacity. The difference in power output due to the control can be described according to equation 2.1.

$$\Delta p_m = -\frac{1}{R}\Delta f \tag{2.1}$$

where $\Delta p_m$ is the change in output from the turbine of the machine, R is the regulation constant, denoted in either Hz/MW or p.u/p.u depending on the units of the other components in the formula and $\Delta f$ is the change in frequency of the system related to the nominal value. It is important to notice that active power is what regulates the frequency. When $\Delta p_m$ is negative, downregulation occurs, i.e power is drawn from the grid to lower the frequency. The opposite, when $\Delta p_m$ is positive, is known as upregulation and is done by injecting power to the grid [20]. In Sweden and the Nordic countries, a total $\frac{1}{R}$ of 6000 MW/Hz is required as control power in the system. Since normal operation conditions is within $50 \pm 0.1$Hz, the required power reserves needed are 600 MW [21]. Comparing this to Figure 2.5 from the challenge description, it can be seen that the power unbalances in Baltic InteGrid are far larger than 600 MW. While the DC-system is connected to three AC-systems with primary reserve, meeting this demand is still problematic. Thus, highlighting the challenge of balancing the DC-system.

Since the imbalance between generation and consumption is constantly changing, the additional feature of inertia is important. All generators connected to the system are synchronous with the same frequency. When smaller deviations in frequency occur, the synchronous generators limits the frequency change with their inertial response. Additionally, the mechanical Torque $T_m$ initially remains constant while the electrical torque $T_e$ of each turbine-generating unit increases to handle the increased load. This comes from Newton's second law:

$$J\alpha = T_m - T_e \tag{2.2}$$

Where J is the inertia, $\alpha$ the acceleration and $T_m$ and $T_e$ the mechanical and electrical torque respectively. With the above reasoning, the acceleration $\alpha$ becomes negative. Thereby, deaccelerating the turbine-generators and releasing the kinetic energy as a result of the speed dropping. The electrical frequency of each generator also drops, since it is proportional to the rotor speed of the synchronous machines [20]. With

the same logic as when discussing the potential lack of primary reserve. The inertial response in the AC-systems is likely to be insufficient for the increased intermittency and fast changes in power due to the RES.

### Voltage regulation

The voltage in the AC-system has to be within certain limits at all times. While the active power regulates the frequency, the reactive power regulates the voltage. Active and reactive power are related according to Figure 2.8. Almost all components in the AC-system consume both active and reactive power. Active power is the useful power in terms of work and reactive power maintains the system reliability. By decreasing the reactive power, the voltage falls and vice versa when increasing the reactive power. Reactive power can not be transferred over long distances. Various voltage regulators are thereby needed throughout the system. The reactive power regulation units include various sources or sinks for reactive power (like Static Var Compensators (SVC), synchronous condensers etc.), Line reactance compensators (like series capacitors) and regulating transformers [22]. Exactly how these function is outside the scope of this study, however, it is important to understand that by changing the phase angle between voltage and current the reactive power can be regulated.

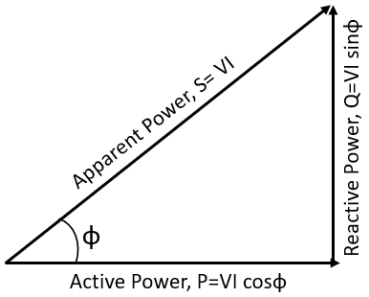


**Figure 2.8:** Relationship between active and reactive power - Φ is the phase angle between the voltage and current.

## 2.3 HVDC-System Overview

DC technology was present already at the beginning of the 20th century. At this time the battle between the AC and DC technologies in being the main one used took part. The DC technology lost, and it wasn't until 1954 that the technology had matured enough to be implemented in the first commercial project. This project was the domestic undersea cable connecting the Swedish island of Gotland with the mainland. Gotland 1, as the project was called, used mercury arc valves as converters. 16 years later thyristor valves were introduced, playing a key role in the commercial development of HVDC-systems globally [23]. Today HVDC is considered an efficient technology which for certain applications are preferred over the more commonly used HVAC. The designated use is for transporting very large quantities

of electrical power over very long distances. This with a smaller loss in energy than the competing technology of HVAC. The drawback, related to the technology still being in the development phase, is the larger cost of converters and filters required in the linking points. However, the fewer and thinner transmission lines, as well as the smaller transmission losses, make the technology competitive, especially for longer distances. According to Siemens, Generally, 30-40 % more power can be transmitted for overhead HVDC compared to HVAC given the same diameter of the cables [24].

The HVDC transmission lines are commonly used in trans-boundary applications. If two areas are part of two different synchronous areas a DC-line is convenient since it is separating the two areas while still being able to provide them with power. In applications like Gotland 1, or other sub-sea or underground related projects, it is almost exclusively the technology used. The reason for this being that due to the capacitance of the HVAC cable a large amount of reactive power needs to be transmitted as well as the active power to the load. This leads to wider cables with higher losses. In cables, the capacitance is higher and the inductance lower compared to overhead lines [20]. With other words, restrictions due to the law of physics are limiting the AC transmission in these kinds of transmission links. According to research in [25] the distance is limiting the active power from around 50 km of cable length. This corresponds with other sources telling the break-even point for economic value regarding HVDC vs. HVAC submarine or underground cables is around the same distance [26]. Furthermore, the transmission losses are typically 30-50% lower for HVDC transmission lines. However, the power electronics in the connection points (terminal stations) are more expensive for HVDC than corresponding for HVAC. The break-even distance cost for overhead line transmission is thereby somewhere in the range of 600-800 km [26]. This figure is decreasing with the developments in the field.

### 2.3.1 Configuration of a DC-grid

Typically the DC transmission links are connected over long ranges, connecting two incompatible AC-systems. The terminal stations include the power electronics making the transition from AC to DC and DC to AC possible. The main power electronics needed are the electronic power converters. Those are commonly bidirectional, thereby functioning in both inversion mode (DC to AC) and rectification mode (AC to DC). The main topologies for HVDC transmission converters today include Line-Commutated Converters (LCC) and Voltage Source Converters (VSC). However, since VSC is the topology used in Baltic Integrid, this is the only one of importance in this work.

#### Voltage Source Converters

VSC uses mainly Insulated Gate Bipolar Transistors (IGBTs) which is a type of controllable switch commonly using Pulse Width Modulation (PWM). PWM is a way of switching between ON and OFF-state in order to imitate a sinusoidal output signal. The VSC-technology is implemented in Sydvästlänken in Sweden. The main advantages of the technology are that it can rapidly and independently control the

reactive and active power. It contains the ability to black-start since no short-circuit power from the connected AC-grid is required. Although not being commonly used, it does provide the possibility to use multilevel topologies which are desirable due to the lower switching losses. Multilevel meaning that more than two voltage levels can be achieved in one phase leg, improving the harmonic distortion of the sinusoidal output voltage wave. Typically, the main drawbacks of VSC are the losses due to the high switching frequency. However, those are decreasing with the current development of the technology [27].

### Multi-terminal HVDC

Typically HVDC-systems are connected point to point in a two-terminal system (interconnectors) with converter stations at each end. In systems where many point to point connections are needed, for example in Baltic InteGrid where large offshore WPP clusters are spread out, the traditional two-terminal system could be replaced by a multi-terminal system. In this kind of system, multi-terminal could decrease the cost due to the fewer number of converters and length of cables needed. However, the technology is very much in the development phase, with only a handful of implemented projects. With the increased integration of many connection points, the sensitivity to a fault on one of the lines or nodes become an increasing risk. Fault protection is thereby a very important aspect. Without the protection, the whole system would cease to work causing large consequences to the surrounding systems dependant on it. Since more systems are connected to a multi-terminal system, the consequences would be larger than for the standard two-terminal system. A solution to this is implementing HVDC circuit breakers at strategic places in the system to isolate the faults and thereby avoiding a complete collapse of the system. It should be noted that those are very expensive and thereby only used at a few very strategic places in the system. However, with the development in the field the prices are likely to decrease and the usage to increase [28].

### HVDC Transmission technologies

The HVDC transmission systems can be configured in a few different ways depending on conditions and requirements. The most basic is the monopole, with bipolar being more advanced and expensive but also gives higher security. Monopolar links in its basic form consist of two converters and a single insulated high-voltage cable, thereby being the simplest form of HVDC transmission lines. A simple local ground connection in the DC circuit is used for potential reference. The earth or sea is typically used as return path of the current, making it a cost-effective way of transferring power for offshore applications. However, this type of link is not widely used today [29].

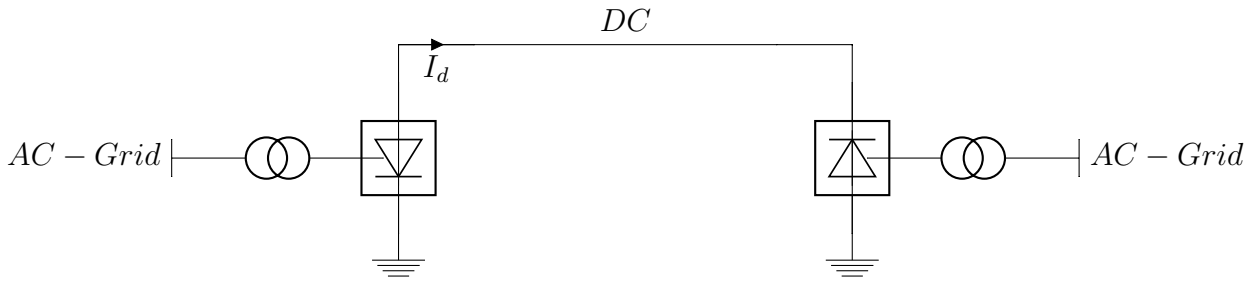


**Figure 2.9:** Monopolar configuration

The Bipolar link is the most widely used configuration. It uses two converter units at each end that are grounded in between, giving two independent DC lines. The two DC lines have opposite polarity related to each other. In case of a fault on one of the lines, the other can still function as a monopolar link, transmitting half of the power. Thereby giving a more reliable system [30].

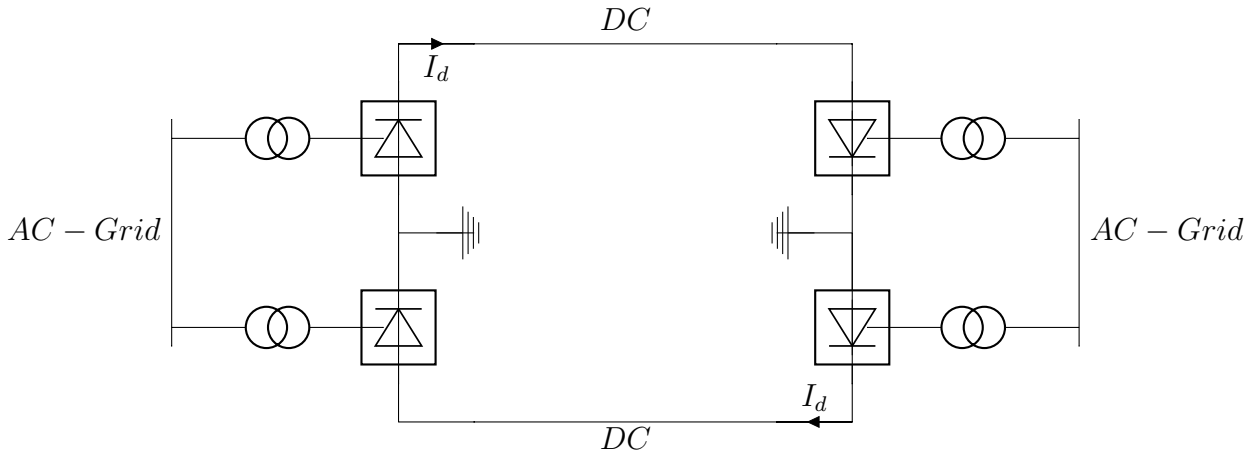


**Figure 2.10:** Bipolar configuration

### 2.3.2 Ancillary services in the DC-system

In an AC-system, reactive and active power have a vital role in providing grid stability. However, the operation of a DC-system differs from the way an AC-system is managed. No reactive current, reactive power or phase angle exist in the DC-system. The most important measure point is thereby the DC node voltages. Frequency regulation in the AC-system is closely related to maintaining the power equilibrium in the system. Voltage regulation is the equivalent for the DC-system, which in turn maintains the power balance from the production, storage and consumption. In a system like Baltic InteGrid, the three connected AC-systems would share the responsibility of regulating the DC-system by injecting and withdrawing active power. This could of course also be done by only one AC-system, but as seen in the challenges, the power unbalances are exceeding the power limits of 1.5 GW making

this impossible. Furthermore, as discussed in section 2.2.2, the primary reserve in Sweden is also too small for it to be possible.

### DC Droop control

Normally the regulation of the voltage in a DC-system is not done by only one converter unit. Because of this DC droop control is needed to share the contribution between the units. Figure 2.11 illustrates the DC droop control. Mathematically the droop can be expressed as:

$$(u_{dc} - u_{dcref}) = k(I_{dc} - I_{dcref}) \tag{2.3}$$

where $U_{dcmax}$ and $I_{dcmax}$ are the maximum limits for the DC voltage and current, $U_{dcref}$ and $I_{dcref}$ are the reference values for the dc voltage and current of the converter side and k is the droop coefficient. Consequently increasing or decreasing the current in the system, will control the voltage proportionally [31].

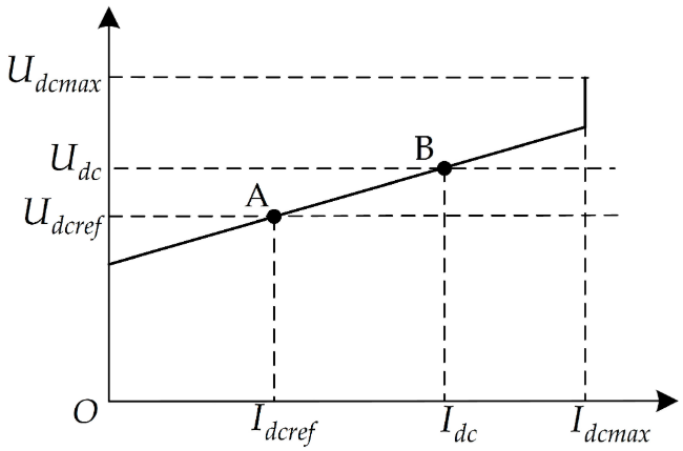


**Figure 2.11:** DC droop characteristics [32]

## 2.4 Wind power basics

Wind power turbines utilize the energy in the wind to spin its rotor and generate electricity. Modern turbines being installed today have normally a rated output of 4 to 6 MW, however as much as 9.5 MW currently exist [33]. This figure is expected to rise in the future with more development. A wind power turbine consists of the following main components:

- Foundation and tower
- Nacelle with the drive train and power electronics
- Rotor with a number of blades

The foundation used is highly dependent on the characteristics of the location. For offshore locations monopile or gravity-based foundations is usual for shallow

waters and smaller turbines. Jacket foundation is typically used for larger turbines installed at a depth of 25-50m while very large turbines on deep ocean require floating foundations. The height of the tower is important since the wind speed is typically higher at higher altitude. This follows from equation 2.4.

$$v_2 = v_1 * ln(\frac{h_2}{z})/ln(\frac{h_1}{z}) \tag{2.4}$$

where $v_2$ is the velocity at the upper height, $v_1$ is the velocity at the lower height, $h_2$ is the upper height, $h_1$ is the lower height and z is the terrain description constant. Additionally, equation 2.5 expresses the power output from one wind power turbine.

$$P_w = 0.5\rho A v^3 C_p \eta \tag{2.5}$$

where $\rho$ is the air density, A the swept rotor area, v the wind speed, $C_p$ the coefficient of performance and $\eta$ the efficiency of the wind turbine. It is important to notice that the power output depends on the cube of the velocity of the wind, thereby highlighting the importance of the height. It can be shown that the terrain description (surface roughness) also play an important role in the total output from the power plant. It should also be noted that due to the wind energy being converted when hitting the rotor of the wind turbine, the wind speeds behind it are lower. Thus, the power output from one wind power turbine as calculated above cannot be expected from all turbines in a WPP. The losses are called array-losses and are one reason why proper dimensioning and sizing of WPPs are important.

The nacelle contains the drive train and for some models, the power electronics converting the kinetic energy from the spinning rotors to electric energy. The rotor is connected to the main shaft on the nacelle side that is sometimes connected to a gearbox. However, nowadays most turbines use direct drive and a slightly larger generator. The electricity produced from the turbine is converted to DC in the rectifier and then further converted back to AC in an inverter to the AC utility grid. The nacelle also includes the yaw system. The yaw is a mechanism that allows the rotors to always be properly aligned towards the wind. The last main component is the rotors and the blades. Typically three blades are mounted on a horizontal axis. However, development on turbines that have more or less than two blades as well as being mounted on a vertical axis is ongoing. The aerodynamics of the rotors are very important, as is the length of them. As seen in equation 2.5 the larger swept area, the more power can be generated. Furthermore, pitch control of the rotor blades allows the aerodynamics of the blades to change. This can be done to lower the power coefficient ($C_p$) and with that keep the rotational speed of the rotor constant once the rated power has been reached.

A turbine cannot produce electricity at all wind speeds. Typically the cut-in speed is around 3-4 m/s with an exponential increase until it reaches its rated power at around 11-14m/s. At low to mid 20 m/s the wind speed reaches the turbines cut-out velocity and stops the rotors to prevent high stress. A typical power curve from a wind power turbine can be seen in Figure 2.12 [34].

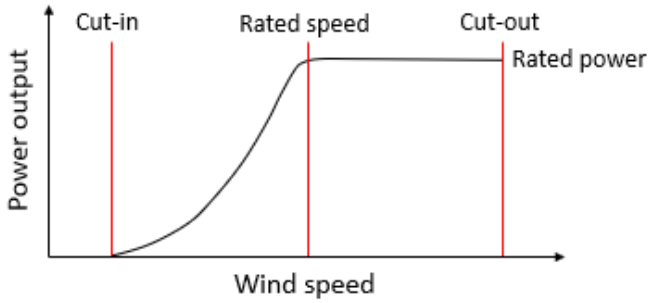


**Figure 2.12:** Wind turbine power output characteristics with steady wind speed

### 2.4.1 Wind power plant cluster

A wind power plant cluster is two or more WPPs connected in an internal system. The reason for separating the WPPs could be due to the economic reasons like better power output due to less array losses. It could also be due to environmental, biodiversity reasons etc. The electricity from the WPPs are not directly connectable to the grid. Normally, each and every one of the WPPs would need to be connected to a converter to be connectable to the main grid. By connecting the WPPs together in one internal system the total number of converters can be reduced since fewer connection points are needed. A figure illustrating a WPP cluster is presented in Figure 2.13.

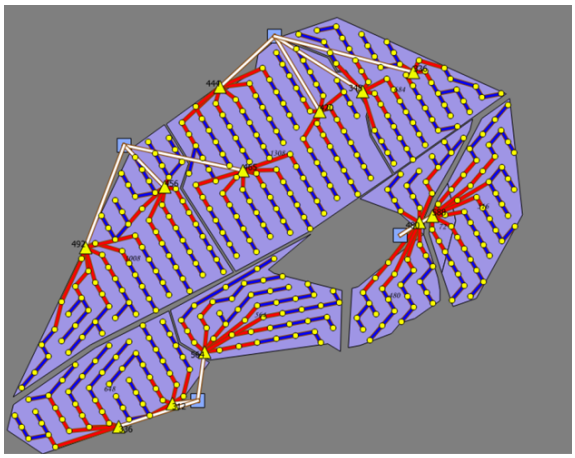

**Figure 2.13:** Overview of the wind power plant clusters connected in Baltic InteGrid - The yellow dots indicates the wind turbines. All wind turbines are connected to 14 local transformer stations. The local transformer stations are connected to four converter stations connecting them to the DC-grid.

### 2.4.2 Wind power plant controllability

Modern wind power turbines have the ability to provide some grid services. For instance, by tilting the blades the wind turbines can regulate their power output. When a power surplus in the system occurs, a down-production can be performed to

regulate down the power in the system. However, this can only be done if the wind is correct and is thereby an unreliable option. When connected to an AC-grid, since the WPP contain power electronics the ability to provide reactive power to the AC-grid exist. Additionally, modern wind turbines can detect frequency deviation and counteract this by using so called synthetic inertia [35]. This is done by extracting extra electricity from the kinetic energy stored in the rotating masses.

### 2.4.3 Wind power plant output forecasting

Forecasting of the WPP power output is very important. While the forecasts for the upcoming 2-3 hours can be predicted relatively accurate, the predictions one day ahead are not. A figure illustrating the forecast error over time is presented in Figure 2.14. The difference between the prediction error and the actual production have to be balanced by other components in the grid. According to an empirical Finnish study, a prediction error of 4-6% can be expected for the first hour while the same figure for 24 hours ahead is closer to 7-14% [36]. Because of the fact that the accuracy is higher for a shorter time span, the importance of the day ahead market increases.

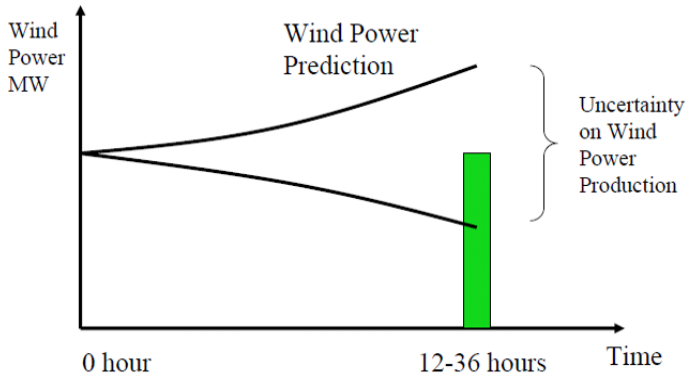


**Figure 2.14:** Prediction of WPP production over time - With predictions further ahead of time the accuracy is significantly lower.

## 2.5 Energy storage system overview

Energy Storage Systems (ESS) are typically used to move the energy output from the generation sources from a time when there is a surplus in the system to a time when there is a deficit. This need becomes especially apparent for solar power in the winter, when the sun hours does not correlate with the common hours of energy use. Furthermore, an increased intermittency in the electricity production is inevitable with the increasing share of renewable energy sources. This will give rise to a higher frequency of occurrences with energy surplus or deficit in the power system. The range of ESS-technologies is large, and extensive research on the subject is ongoing.

### 2.5.1 Energy storage technologies

Energy storages exist in many different shapes and forms. When talking about storage three main characteristics is important. Energy and power, reliability and durability and finally cost efficiency and value generation [37]. While Lithium-Ion batteries, as this work is based on, might be very good as short-term storage with high power output, it does not necessarily answer very well to the other aspects. Therefore is it important to consider alternative storage solutions, either as a substitute or as a compliment. The typical technologies used as energy storage are electrochemical batteries, such as Lithium-Ion, redox or fuel cells, chemical like hydrogen cells or even mechanically pumped-storage hydroelectricity to name a few [38].

#### Electrochemical and redox technologies

Batteries are typically suitable for applications that require short-term storage. They have a very large power output under a relatively short time and answers well to instant fluctuations. However, they have a relatively low energy storage density and have the negative attribute of self-discharging over time, making it very poor as long-term storage. Additionally, the battery storage has a lifetime of around 8-10 years, depending on use. Apart from the Lithium-Ion batteries that will be discussed in section 2.5.2, Vanadium is an interesting element for grid energy storage applications. Vanadium has gained more attention since it subject to its first commercial installation in 2001 [39]. It is a redox flow battery that shows great potential. The main feature is its long cycle life and deep Depth of Discharge (DOD). It has a fast response time and high energy efficiency, although slightly lower than the Lithium-Ion battery. The drawback at the time of writing, just like most other energy storage technologies, is the price. However, this is subject to change until 2030 according to predictions [40]

#### Chemical energy technology

With the future prospected increase in hydrogen applications, such as fuel cells for cars and ships, using hydrogen as storage is a very promising option. Hydrogen is created through electrolysis, e.g using electricity to split water into hydrogen and oxygen. While the efficiency only being around 65-70%, the energy density is very high. The hydrogen is stored in gaseous, liquid or metal hydrides depending on the storage space and prospected use. The hydrogen could as well be part of the short-term regulation in the system, however, the conversion of hydrogen back to electricity in a fuel cell is at best 50%. Pressurizing the hydrogen for storage is very energy-intensive. On the other hand, storing it in liquid form is very space-demanding. Creating hydrogen with the excess electricity might thereby be a very effective application especially for offshore wind power where space is not a restriction [40].

**Kinetic Energy technology**

In Sweden, by far the largest today existing energy storage is the dams connected to the hydropower in the north. While those dams are naturally encapsulating the water in the rivers, the option of using excess electricity to pump up the water in similar dams exist. This is a proven technology used in, for instance, Kruonis pumped storage plant in Lithuania, as well as being implemented in certain models of new wind power turbines from General Electrics. The main feature of this technique is the long lifetime as well as being superior for long-term storage [40].

### 2.5.2 Battery energy storage systems (BESS)

Battery energy storage systems (BESS) using Lithium-ion Batteries (LIBs) is the technology that is most matured and used in most projects to date [41]. This is partly thanks to the vehicular industry using Lithium-Ion battery packs as the energy storage and because of that has been forcing up the production volume which has lead to lower prices. The price decline is a development expected to further continue in the future [42]. Another reason for the use of Lithium-Ion batteries is the characteristics of the technology. This will be discussed later on in the section. Once the battery packs of the vehicles have reached their end-of-life for vehicular applications, they could be recovered and reused as energy storage units in future "smart-grids" [43]. This can be compared to swapping a dead battery from a flashlight to a remote controller and see it spring back to life for additionally some time. Battery packs consist of many battery cells connected together as Figure 2.15 illustrates. This will be further explained in section 2.5.3. However, it should be added that modern battery packs for vehicle applications have reached a capacity of 100 kWh [44].

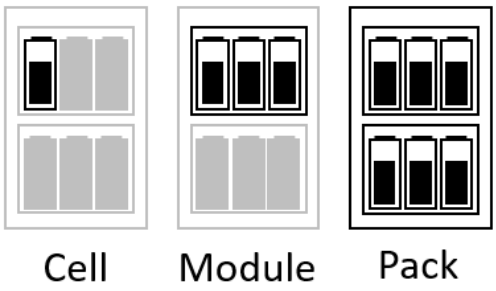


**Figure 2.15:** Build-up of a battery pack

### 2.5.3 Operation of a Lithium-Ion battery cell

A LIB is an example of an electrochemical cell. Electrochemical cells consist of a positive and a negative electrode with a separating electrolyte in between. The basic concept of an electrochemical cell is that a reaction between the electrolytes of the cell takes place. This reaction is known as a redox-reaction since an electrochemical reduction takes place in the cathode (positive electrode) and an oxidation takes place

in the anode (negative electrode). The electrons are transferred via an external circuit from one electrode to the other, whilst ions are transferred through the electrolyte to upheld the cell balance. A cell that can repeat this cycle in reverse, i.e both charge and discharge, is known as a secondary cell. A battery pack consisting of these cells is better known as a rechargeable battery pack.

The material of the electrodes, as well as the electrolyte, decides the characteristics of the battery cell. Electrodes determine the capacity, cell voltage and energy of the cell. The electrolyte determines for instance at what rate the energy can be released from the cell. The negative electrode of the today used batteries are typically an insertion material like graphite. Graphite is preferred due to its low potential and its ability to insert and extract large amounts of lithium ions [45]. The positive electrode side is more varied, with Lithium Cobalt Oxide, Lithium Manganese Oxide and Lithium Iron Phosphate being common. However, extensive research on electrode materials is conducted in order to optimize the characteristics of the battery.

The cell voltage, i.e the potential between the electrodes, is 3-4 V for a Li-Ion cell depending on what materials are used. By connecting multiple cells in series the voltage capacity is increased. If the cells are connected in parallel instead, the total capacity of the battery would increase. Hence, for a battery pack with a voltage rating of 100 V and capacity of 3000 mAh, a total number of roughly 28 3.6 V Li-Ion 3000 mAh cells series coupled would be needed. Consequently, if the cells where parallel coupled, the capacity would increase to 84 Ah with the voltage rating remaining at 3.6 V. With the above reasoning, it is possible to create a battery pack according to the specifications needed either by connecting multiple cells or connecting multiple battery packs. A picture showing what a BESS for grid use can look like is shown in Figure 2.16.

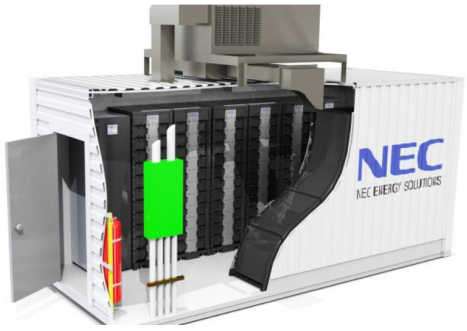


**Figure 2.16:** Picture of a battery pack being built in a container [46]

Another property to consider is the discharge and charge rate of the battery, commonly known as the C-rate. This is defined as the current to discharge the capacity in one hour [45]. Assuming a battery with a capacity of 3000 mAh being discharged with a C-rate of 1. This means that the discharge current of the battery is 3000 mA. Using a higher C-rate usually incur on the lifetime of the battery. The lifetime is also related to the Depth of Discharge (DOD) of the battery. DOD relates to how deep the battery is being discharged where 0% indicates a full battery and 100% indicates an empty battery. A higher DOD decreases the lifetime of the battery drastically as seen in Figure 2.17. Lifetime, in this case, is related to the number

of cycles the battery can be charged and discharged. State of charge (SOC) is an alternative form av the same measurement as DOD and will be highly important in this work. It relates to the current energy in the battery much like the works of a normal gauge where, e.g, 40% means that the battery is 40% full. This means that for a battery pack with a capacity of 100 MWh with 40% SOC, 40 MWh of energy is stored. However, as earlier mentioned, discharging the battery pack to deep will impact the lifetime. In reality, the usable energy stored in the battery pack is thereby below 40 MWh.

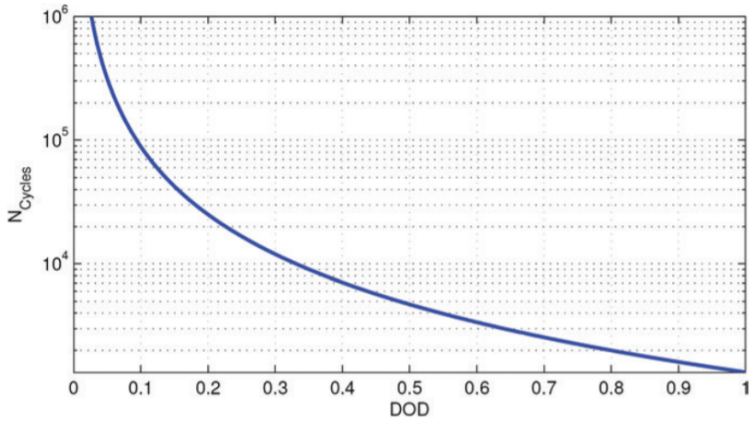


**Figure 2.17:** Estimated Lithium-Ion Battery lifetime in cycles, as a function of the depth of discharge [47]

### 2.5.4 BESS application scope

In this work, the main objective for the BESS is to perform the primary control in the DC-system by balancing the voltage in the grid at nominal level. Because of the fast response times of LIBs active power can be provided to uphold the voltage level. However, depending on the system the BESS is integrated into, its implementation and management, the BESS can be used for various applications. These include technical applications related to performing grid services, as well as purely economic, used to improve the profitability of the system.

#### Ancillary services in the AC-grid

Similar to the application for the DC-grid, the LIB can with very short response time provide active power to the system. As mentioned before, providing active power to an AC-system regulates the frequency. When the load is either decreased or increased, leading to the frequency deviating from the nominal value of 50 Hz as discussed, the BESS can provide the lacking power very fast. Today the hydropower in Sweden is the sole frequency regulating unit, giving a very large dependency on it. With the introduction of BESS, this dependency could be shared. However, as previously described, the inertial response of the synchronous generators, in for instance the turbines of the hydropower, are still important since they provide a force that opposes the change [40]. The LIB can only provide active power and

therefore by itself not provide any voltage regulation in the AC-system. However, when connected to an inverter, reactive power can be provided to the AC-system and with that the voltage to be regulated.

#### Peak shaving

The electricity demand varies from day to day and from hour to hour. The energy demand is especially high in the morning and evening. Peak shaving relates to reducing these peaks. This is a common challenge today and one that will be even more significant with a larger share of RES. The reason for this is because RES are intermittent as previously described and does typically not correlate very well with the demand from the consumer-side. By installing a BESS, peak shaving can be performed by storing the electricity when the demand is lower than the production and vice versa. Thereby giving a more even distribution of the load level on the grid without the peaks, hence the name. Additionally, there is an economic incentive for the consumer since the electricity price correlates with the electricity balance of the system [40].

#### Power smoothing

Power smoothing refers to the smoothing of the direct power output from the production source. Typically the output from, for instance, a wind power plant is highly intermittent, creating large stress on the grid. Power smoothing typically already exists in the pitch control of the turbines. However, this could cause large mechanical stress and damages to the blades if fast changes in pitch angle occur in order to mitigate those short-term fluctuations [48]. An alternative way of doing this could be with the use of a BESS.

### 2.5.5 Implementation of BESS in a DC-system

The BESS is built up by a battery pack, a DC/DC converter and a controller. The battery pack and DC/DC converter need to be dimensioned accordingly. The converter need a high enough power rating to handle to loads. In this work the cable rating is 1.5 GW and the power unbalances the same. That means that the converter has to be rated for 1.5 GW to be able to deal with this. Continuing, the battery pack needs to have both a high enough energy rating and a high enough power rating to diminish the power unbalances. In this work, the battery pack has been somewhat simplified in the sense that it is assumed it can handle 1.5 GW regardless of its capacity.

The battery pack can either be voltage or power regulated. When power regulated the controller is regulating the power setpoint from the battery pack by utilizing a PI-controller. If voltage regulated, the controller is measuring the voltage on the DC-grid and then with a P-controller utilizing DC-droop control to regulate the power output. The system coupling to the DC-system is as in Figure 2.18.

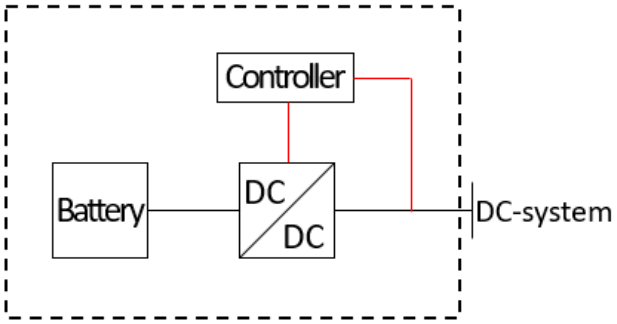


**Figure 2.18:** BESS connection to the DC-system - The dashed line indicates the components included in the BESS. The system comprise a battery pack, a converter and a controller. The black lines indicates power lines and the red lines the communication lines for the controller.

### 2.5.6 Battery energy management system

The battery Energy Management System (EMS) is key to the working power system. The main target and objective for the EMS are to ensure that the system maintains its core characteristics and with that upholds the stability at every moment. It does so by assigning appropriate power references to the regulating units. In an AC-system, both the active power and the reactive power has to be balanced. In the DC-system however, only the active power is of importance [49]. While many EMS with different tasks exists in a power system, only the EMS related to the BESS is considered in this report. Generally, energy management can be divided into two parts. Short-term management for interval of milliseconds to seconds and minutes depending on the application and long-term management for longer periods of times stretching from minutes to hours, days or months [50]. In this report, since the storage unit used is batteries, the short term management only relates to the instantaneous power balancing of the system. As being discussed before, this is commonly done with droop control equally sharing the power distribution from each regulating unit. The short-term power balancing is crucial both for the stability of the grid but also from a safety and stress point of view. The long term management, on the other hand, is more related to forecasting what the future outcomes will be and storing energy over longer period of times. In a power system, the forecasting could be related to anticipating the production from the generation units (Power prediction) as well as the consumption from the consumers (Load forecasting) but could also include other applications like load sharing and electricity market interactions [51]. Since the required response times are lower for this storage, another type than LIBs that fits the purpose better can be used. A schematic figure of the cooperation of the short-term and long-term management in the EMS is presented in Figure 2.19.

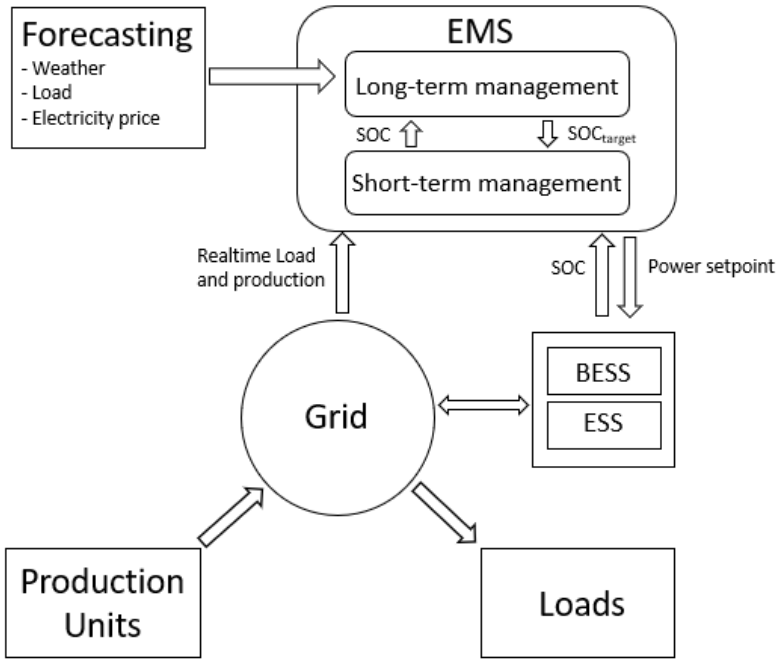


**Figure 2.19:** Overview of the role of the EMS - The figure shows the key role of the EMS. Depending on the system characteristics and predictions, different power setpoints for the BESS are determined. The BESS is the primary storage used for instantaneous power balancing. The ESS is the secondary storage used for long-term management.

# Chapter 3

# Operation Strategy and Control Method

---

*In this chapter, the short-term and long-term control strategies used in this report are presented. In the first section, the short-term management as well as the system functions related to the BESS is described. In the section 2 the strategy of using the intraday market for long-term management is described. In section 3 the different control methods related to the intraday market interaction is presented.*

---

## 3.1 Management logic and objective

With no BESS implemented in the DC-system, the connected AC-systems would have to use their regulation units to balance the power from the DC-system as well. This would not be an optimal solution according to various reasons previously discussed. By implementing the BESS to the DC-system as in Figure 3.1, it should act as the main regulating unit but with the AC-system as a back-up. The main target for the BESS in this project is for the DC-system to function properly and to a large extent with no AC-grid dependency from a regulating perspective. The basic concept is to let the BESS utilize its storage capacity to either behave as a load to store energy when there is a surplus (overproduction) in the DC-system or act as a power supply and provide energy when there is a deficit (underproduction).

The objectives of the control management are to find what strategy minimizes the time the AC-grid is performing the primary control, as well as finding a sufficient BESS capacity and parameter settings for the strategy. Minimizing the BESS capacity is important from an economic standpoint as well as from an environmental. Certain general algorithms related to the system functions are implemented to create a working model. Additionally, different methods with different complexity are created with the goal to decrease the AC-grid dependency as well as decreasing the BESS capacity. The system functions created to make a working model are described below with the different specific control methods described in Section 3.3.

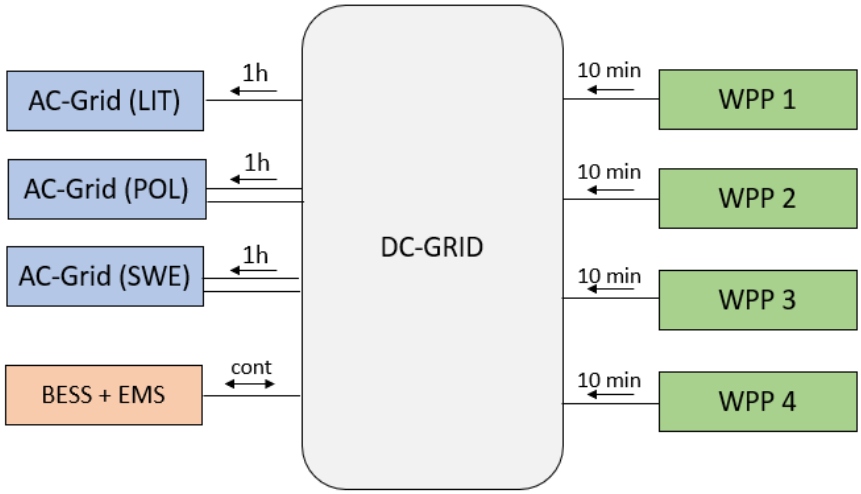


**Figure 3.1:** Extended system overview of Baltic InteGrid - The same conditions as in Figure 2.2 applies but with the addition of the BESS. The BESS is main the regulating unit of the DC-grid, and the AC-grid only withdraws power due to the market interaction.

### 3.1.1 Regulation strategy of BESS

The most critical point of concern is the task of performing primary control in the DC-system. The primary control is the regulation of the voltage at nominal level. Previous work in [52] suggests using the BESS as a voltage controller employing DC droop control. The BESS is then autonomously performing instantaneous power balancing based on the voltage level in the system. From here on after the primary control will be referred to as the 'Voltage regulation' or $V_{reg}$ in short. Furthermore, [53], [54] and [55] suggests that the SOC of the BESS ($SOC_b$) can be used as a control parameter to adjust whether charging or discharging of energy is desirable. However, due to battery characteristics being discussed in Section 2.5.3 the lifetime of a battery is heavily decreased if depleted too deep or charged to full. An upper ($SOC_{max}$) and lower limit ($SOC_{min}$) of the usable storage range is defined as in Figure 3.2a. $SOC_{min}$ is set to 0.2 (20%) and $SOC_{max}$ to 0.9 (90%) due to Lithium-Ion battery characteristics [56]. A strict limit is implemented, restricting the BESS from working above $SOC_{max}$ and below $SOC_{min}$. A study by [57] suggests dividing the operation area of the battery into different bands as in Figure 3.2a to increase the controllability of it. A hysteresis control strategy, as in Figure 3.2b, related to the $SOC_{max}$ ($SOC_{max\_hyst}$) and $SOC_{min}$ ($SOC_{min\_hyst}$) is utilized. The strategy is used since the BESS cannot be guaranteed to contain a sufficient amount of energy to perform the voltage regulation satisfactorily for a longer period of time within this band.

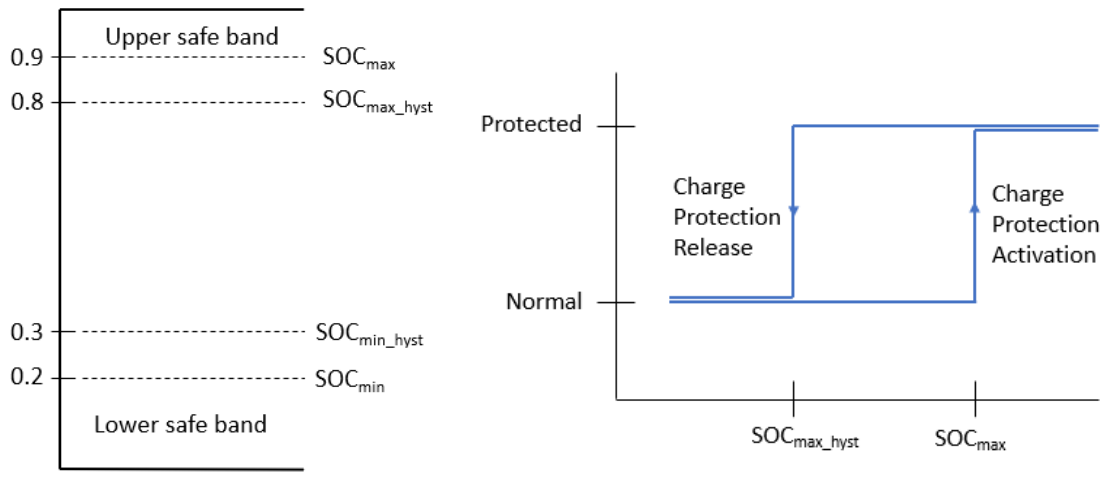


**(a)** SOC-limits of the battery **(b)** Function of the hysteresis

**Figure 3.2:** BESS hysteresis function - The BESS are allowed to charge and discharge freely in normal mode. When in protected mode, only discharge is allowed until $SOC_{max\_hyst}$ is reached. The logic is the same for the opposite case with $SOC_{min\_hyst}$ when the BESS is depleted.

When the SOC-level of the BESS is reaching $SOC_{max}$ or $SOC_{min}$, the BESS no longer possess the capability to perform the internal voltage regulation. However, without the voltage regulation, the DC-system shuts down. Instead, the EMS of the AC-grid, from here on after only referred to as the AC-grid since seen as one unit, overtakes the role of voltage regulating unit for the DC-system at this time. The DC-system thereby changes from utilizing an internal voltage regulation to utilizing an external voltage regulation from the AC-grid. When the switch of voltage regulating unit between the BESS and the AC-grid is performed a short overlapping period exist when both units perform the voltage regulation by droop control. This is done in order to prevent a voltage dip at this time. Since the BESS no longer is responsible for the power balance in the system when the AC-grid performs the voltage regulation, its new objective is to bring back $SOC_b$ to a secure SOC-level. In the model, this has been implemented by using power regulation, $P_{reg}$, where the setpoint is the charging or discharging power. This is described in greater depth in the section 3.1.2. When $SOC_b$ once again is greater than $SOC_{min\_hyst}$ or lower than $SOC_{max\_hyst}$, the BESS regain the task of voltage regulator. Again, a small overlapping period exists as discussed before. In the band between $SOC_{min\_hyst}$ and $SOC_{max\_hyst}$ the BESS is free to discharge or charge according to what is required from the system. The control scheme for the above-described strategy of switching the task between the voltage regulating units is illustrated in Figure 3.3.

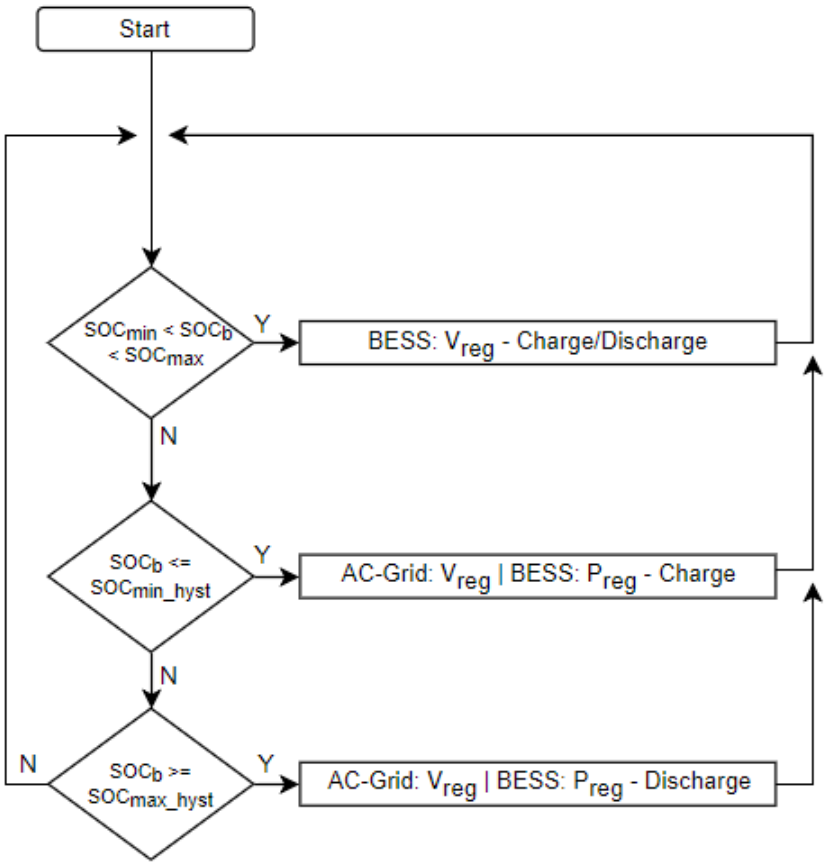


**Figure 3.3:** Flow-chart describing the voltage regulation scheme of the DC-system - If $SOC_b$ is inside the NOB, the BESS performs the voltage regulation occurs without restriction. When reaching $SOC_{min}$ or $SOC_{max}$, the BESS is charging or discharging until reaching $SOC_{min\_hyst}$ or $SOC_{max\_hyst}$, respectively. The AC-grid is performing the voltage regulation at this time.

### 3.1.2 Charge and discharge strategy for BESS when power regulated

When the SOC of the BESS has reached $SOC_{max}$ or $SOC_{min}$ and because of that is not performing the voltage control a charge and discharge strategy is needed to bring back $SOC_b$ to a desirable level. Logically the BESS would charge if the SOC is low and there is a power surplus in the DC-system and discharge if the SOC is high and there is a power deficit in the DC-system. However, allowing the BESS to charge even though there is a small power deficit in the system and discharge even though there is a small power surplus in the system could improve the system without significant consequences. A threshold limit, $P_{THRES}$, on either side of 0 W related to the real-time power balance of the DC-system ($P_{balance}$) is implemented as in Figure 3.4. The BESS is charging and discharging according to fixed values, $P_{fixed}$, depending on the power balance of the system as in Figures 3.4a and 3.4b. This is further explained with the relationships in Equation 3.1 and 3.2.

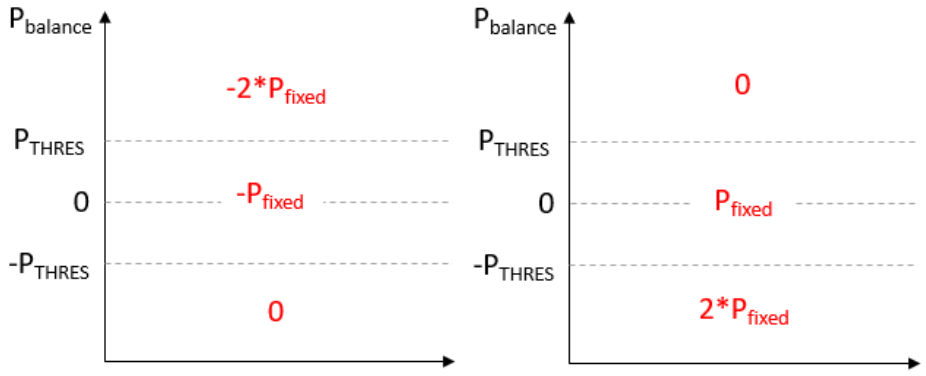


**(a)** Charging schedule **(b)** Discharging schedule

**Figure 3.4:** Charging and discharging schedule for BESS when power regulated

$$P_{charge} = \begin{cases} -2 * P_{fixed}, & P_{balance} > P_{THRES} \\ -P_{fixed}, & -P_{THRES} < P_{balance} < P_{THRES} \\ 0, & P_{balance} < -P_{THRES} \end{cases} \tag{3.1}$$

$$P_{discharge} = \begin{cases} 2 * P_{fixed}, & P_{balance} < -P_{THRES} \\ P_{fixed}, & -P_{THRES} < P_{balance} < P_{THRES} \\ 0, & P_{balance} > P_{THRES} \end{cases} \tag{3.2}$$

Where $P_{charge}$ is the charge power, $P_{discharge}$ is the discharge power. Due to the definition of the direction of the system, the discharge power is positive since seen as an input to the DC-system and the charge power negative since seen as an output from the DC-system. $P_{fixed}$ is the charging/discharging power, $P_{THRES}$ is the power deficit or surplus threshold, and $P_{balance}$ is the real-time power balance of the DC-system from the WPP input and market output.

## 3.2 Utilizing the Elbas market as a secondary storage

Just as identified in the challenge description and as Figure 2.7 highlights the need for a very large ESS to handle both the long-time energy unbalances and the short-time power unbalances would be needed. A very large BESS could be implemented as illustrated in Figure 3.5a. However, it is not a very beneficial solution, neither from an economic or technical standpoint. A solution that is answering more to the specific need of fast instantaneous power balancing, as well as mitigating energy unbalances over long times, is needed. This could be realized by implementing a smaller BESS unit that mitigates the instantaneous power unbalances and a larger secondary storage with a high energy density that charges and discharges according to long term energy surpluses and deficits. This storage unit could, for example, be a hydrogen storage. Figure 3.5b illustrates this example. A completely different

approach, and the one that is used in this work, is to utilize the conventional AC utility grid as a fictive secondary storage. Since the Elbas intraday market allows market interactions up to 1 hour before the powerhour starts as described in section 2.2.1, it can be seen as a slow secondary storage with response times of one intraday market time-basis. The size of the BESS would thereby need to be slightly larger than if a slower physical ESS would be implemented. However, implementing a large physical ESS is a much larger economic investment. This strategy is illustrated in Figure 3.5c. It should also be noted that, since the DC-system is connected to an AC-system with regulation features, at certain high demanding scenarios this can be utilized. By allowing the DC-system to use those regulating features, the BESS capacity could theoretically be minimized.

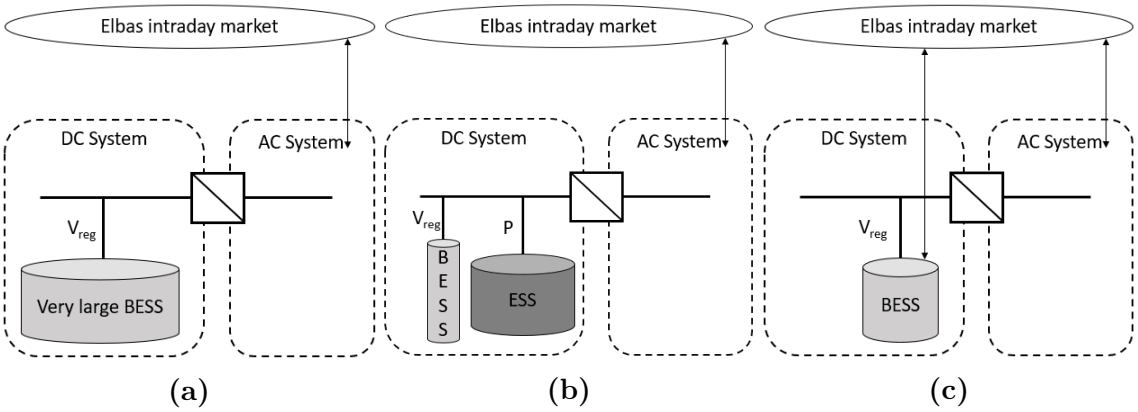


**Figure 3.5:** System structure with different ESS-strategies

As the figures illustrate, in Figure 3.5a the BESS is regulating the instantaneous power unbalance as well as storing all energy surplus in the DC-system. In Figure 3.5b a slower ESS is complementing the fast BESS. The ESS is storing energy over long times while the BESS is regulating the instantaneous power unbalances. Because of this, a much smaller BESS is needed, however, an ESS of a large capacity is needed instead. In Figure 3.5c the large ESS is removed and a possibility to sell and buy energy from the market based on the SOC of the BESS is added. Because of this, only the BESS is needed as a physical energy storage. However, the capacity needs to be slightly larger than in Figure 3.5b since the response time of the market is slower than a physical secondary storage.

### 3.2.1 Market interaction strategy

By utilizing the Elbas electricity intraday market in a beneficial way, $SOC_b$ can be regulated to have a more desirable value by selling or buying extra energy depending on this level. In the most simple case, when $SOC_b$ is high, it's beneficial to sell extra energy and vice versa when $SOC_b$ is low. The intraday market is presently working on an hourly basis but will be changed to a 15 min time-basis in the near future, as described in section 2.2.1. To simulate this scenario the proposed market interaction (MI) can only be realized one time-unit after the decision if an MI is desired or not. Consequently, the MI is realized for the full time-unit. The strategy is illustrated in Figure 3.6. At each time 't' a decision based on whether an MI is desirable or not

takes place. The limits $SOC_H$ and $SOC_L$ are introduced and acts as the selling and buying MI trigger levels.

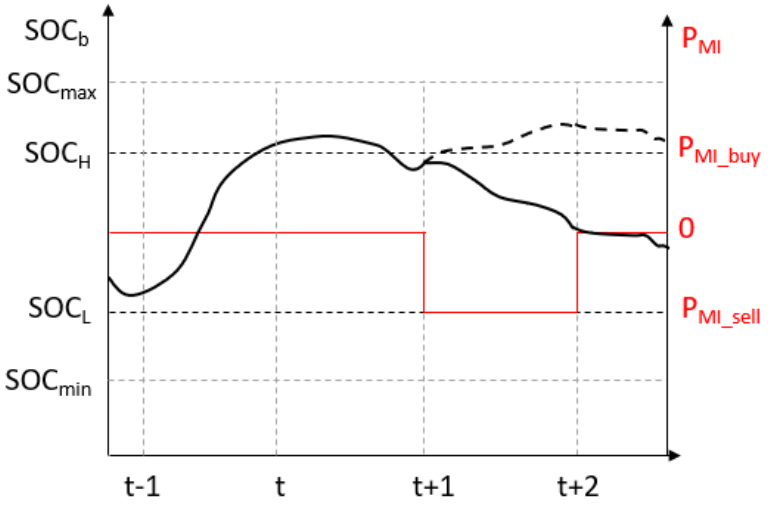


**Figure 3.6:** Illustration of the market interaction - $t$ is the time parameter, $P_{MI\_sell}$ is the power output of the energy sold to the market, $P_{MI\_buy}$ is the power output of the energy bought from the market, $SOC_H$ is the upper MI trigger value for selling extra energy, $SOC_L$ is the lower MI trigger value for buying energy. The dashed line is the SOC-curve if no MI was made, and the full black line is the resulting SOC-curve when a MI is made.

As seen in Figure 3.6, at time 't-1': $SOC_b$ is within the MI trigger limits, thereby no MI is desirable. At time 't': $SOC_b$ is higher than the positive MI trigger. In this case, an extra selling of energy is desirable to keep the SOC of the BESS at an optimal level. At time 't+1': The MI takes place for one full time-unit. At time 't+2': The MI has been performed, the full line represents $SOC_b$ when this MI strategy is used. $SOC_b$ is operating within the desirable band at this time. The dashed line represents $SOC_b$ if no MI would take place. $SOC_b$ is operating at a non-desirable level very close to $SOC_{max}$.

## 3.3 Method descriptions

To realize the objective of minimizing the AC-grid dependency related to voltage regulation, control methods of different complexity have been created. In this section three control methods are presented utilizing the system features above and the MI with varying complexity. The method in section 3.3.1 utilizes a very simple strategy to control the SOC while the methods in section 3.3.2 and 3.3.3 are using more complex strategies. The method in section 3.3.3 is a further development of the method in 3.3.2.

### 3.3.1 Market interaction based on fixed limits (Method 1)

The objective of Method 1 is to handle the MI in the simplest possible way. It does so purely based on the current SOC level ($SOC_t$) and two fixed MI-triggers. Just like described in Section 3.2.1, when the SOC level of the BESS is reaching a certain level, $SOC_H$ or $SOC_L$, a constant amount of power to be withdrawn from or injected to the AC-grid for the next time-unit is demanded. Figure 3.7 illustrates this. The reason for introducing the market interaction is to be able to regulate the energy in the BESS to keep within the Normal Operation Band (NOB). The NOB is from now on defined as the band between $SOC_L$ and $SOC_H$. The width of the NOB can be varied depending on how aggressive the energy control of the BESS is desired to be. Limits farther apart give a larger NOB with a more lenient energy control, however with a larger risk of reaching the outer BESS limits $SOC_{max}$ and $SOC_{min}$. A picture of the BESS limits used for Method 1 can be seen in Figure 3.8. The flow chart for the method is presented in 3.9.

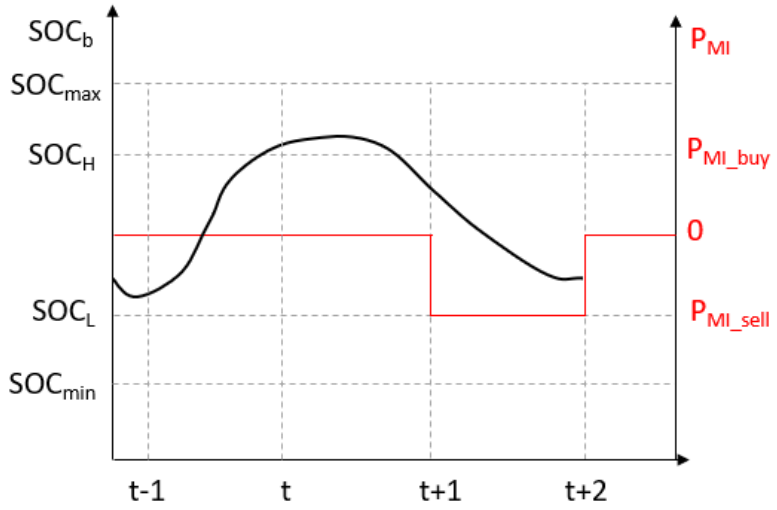


**Figure 3.7:** Market interaction according to Method 1 - In the figure $SOC_b$ at time t ($SOC_t$) is higher than the MI trigger value for selling energy, $SOC_H$. Due to the one time-unit delay for MIs, the selling is realized from time t+1 until t+2.

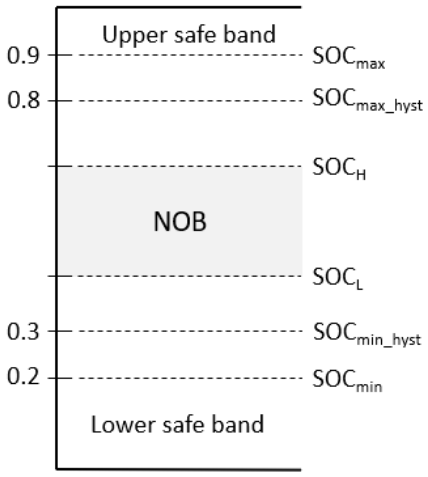


**Figure 3.8:** Limits for the BESS in Method 1 - The grey area represents the Normal Operation Band (NOB).

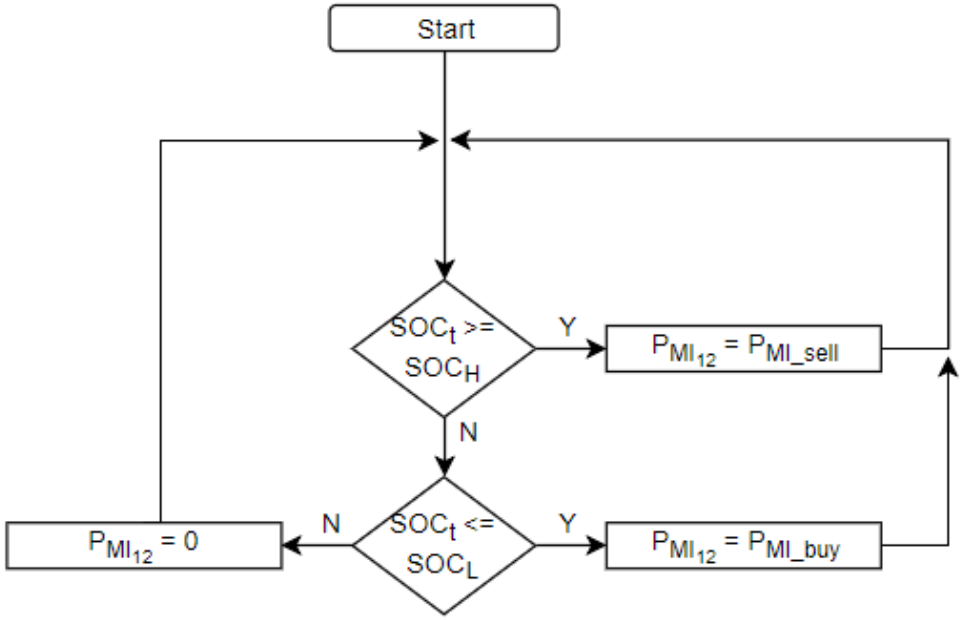


**Figure 3.9:** Flow chart for Method 1 with fixed market interaction power setpoints - If $SOC_t$ is higher than the high MI-trigger ($SOC_H$) an MI for selling energy is desired. If $SOC_t$ instead is lower than the low MI-trigger ($SOC_L$) an MI for buying energy is desired. If $SOC_t$ is within the NOB, no MI is desired.

The disadvantage of Method 1 is that no consideration of the power curve between the time t and t+1 is taken. Because of that, there is an imminent risk that the MI that has been decided is no longer beneficial at the time of realization.

### 3.3.2 Market interaction based on two time-units (Method 2)

By relying only on the current SOC-level of the BESS like in Method 1, a scenario where an MI related to buying or selling extra energy, despite not being beneficial, is likely to happen. The objective for Method 2 is to make a more qualified MI by predicting the future energy balance in the DC-system for one time-unit forward and based on that calculating the future SOC-level of the BESS. Because of the way the MIs are allowed to take place, i.e one time-unit after the calculations are being made. Both the predicted energy balance for the current time-unit (time t until t+1), as well as the predicted energy balance for the next time-unit (time t+1 until t+2), have to be considered. Hence, the energy output from the DC-system for each of the upcoming two time-units ($E_{01}$ and $E_{12}$) are calculated numerically using the midpoint rule according to equation 3.3 and 3.4. Four segments are considered for each estimation as in Figure 3.10. The forecasted power balance, $P_{balance}$ at each point represents the power unbalance between the generated power from the WPP and the output from the electricity market. In this work, the power unbalance is known to a full extent because of previous simulations. Thereby, the chance of predicting the energy balance in the system with no forecast error exists. However, to speed up the simulations only four segments have been chosen which entails an error.

$$E_{01} = \frac{\Delta t}{n} \sum_{x=1}^{4} \frac{P_{balance}(x_i) + P_{balance}(x_{i-1})}{2} \tag{3.3}$$

$$E_{12} = \frac{\Delta t}{n} \sum_{x=5}^{8} \frac{P_{balance}(x_i) + P_{balance}(x_{i-1})}{2} \tag{3.4}$$

Where $x$ is the time parameter, $P_{balance}$ is the forecasted power balance in the DC-system at time $x$, $n$ is the number of segments evaluated, in this case, n = 4 and $\Delta t$ is the time-basis for the Elbas intraday market (15 or 60 min).

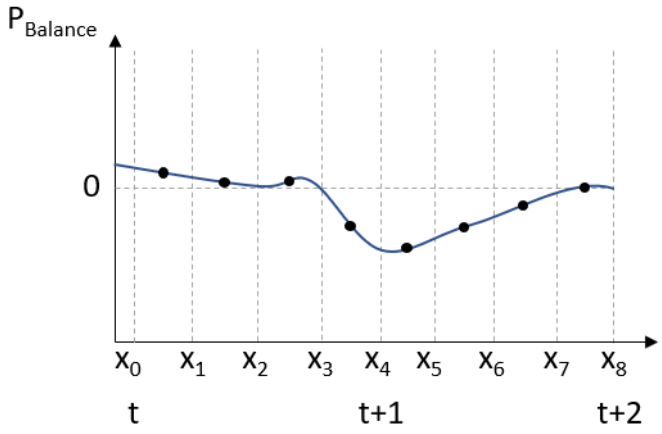


**Figure 3.10:** Illustration of the predicted energy balance calculation for Method 2 - $x_0$ equals the start of the first time-unit ($t$), $x_4$ equals the end of the first time-unit as well as the start of the second time-unit ($t+1$), $x_8$ equals the end of the second time-unit ($t+2$). A positive balance equals a power surplus and a negative value a power deficit as earlier mentioned. The black dots are the evaluation points related to the Midpoint rule.

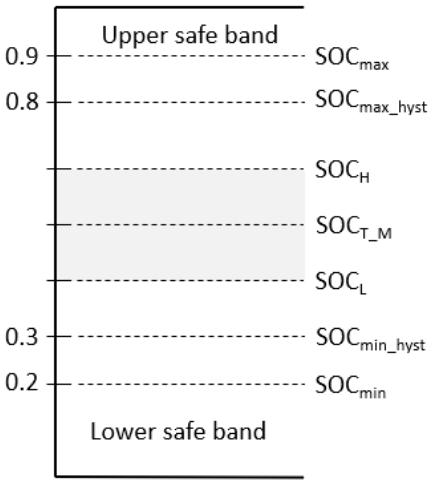


**Figure 3.11:** SOC-limits for the BESS in Method 2 - The grey area is the NOB.

Method 2 considers the same two NOB-limits $SOC_H$ and $SOC_L$ as Method 1. The full range of SOC-limits are as in Figure 3.11. By predicting the SOC-value for time t+2 ($SOC_{t+2}$) and compare this to the NOB, a decision whether an MI is needed or not can be made. However, to calculate $SOC_{t+2}$, the SOC-value at time t+1 ($SOC_{t+1}$) is needed. $SOC_{t+1}$ is calculated according to equation 3.5.

$$SOC_{t+1} = SOC_t + \frac{E_{01} + P_{MI_{01}} * \Delta t}{C_b} \tag{3.5}$$

Where $SOC_t$ is the current SOC-value, $E_{01}$ is the predicted energy balance for the time-unit t to t+1 as calculated in equation 3.3, $P_{MI_{01}}$ is the power setpoint of the

MI calculated from the previous time-unit and $\Delta t$ is the time-basis (15 min or 60 min).

No consideration to the value of $SOC_{t+1}$ is taken since $P_{MI_{01}}$ is already decided. Thus, $SOC_{t+1}$ can not be modified. However, the value of $SOC_{t+1}$ is needed since $SOC_{t+2}$ is a further prediction based on it, as in equation 3.6

$$SOC_{t+2} = SOC_{t+1} + \frac{E_{12} + P_{MI_{12}} * \Delta t}{C_b} \tag{3.6}$$

Where $SOC_{t+1}$ is the predicted SOC-value at time t+1 as in equation 3.5, $E_{12}$ is the predicted energy balance for the next time-unit as calculated in equation 3.4, $P_{MI_{12}}$ is the power setpoint of the MI for the next time-unit and $\Delta t$ is the time-basis (15 min or 60 min).

By first assuming that no MI is needed ($P_{MI_{12}} = 0$), $SOC_{t+2}$ can be predicted. If the value of $SOC_{t+2}$ is within the NOB when this is assumed, it is confirmed that no MI is needed. However, if $SOC_{t+2}$ is higher or lower than the NOB-limits, an MI related to bringing it inside the NOB is desired. The SOC-target for Method 2 is always the centre of the usable range ($SOC_{T\_M} = 0.55$) since this gives the highest possibility of staying within the NOB the upcoming time-unit. By rearranging equation 3.6 the MI ($P_{MI_{12}}$) that realizes this is found as in equation 3.7.

$$P_{MI_{12}} = \frac{(SOC_{T\_M} - SOC_{t+1}) * C_b - E_{12}}{\Delta t} \tag{3.7}$$

Where $SOC_{T\_M}$ is the target value for $SOC_{t+2}$, $SOC_{t+1}$ the predicted SOC-value at time t+1, $C_b$ the BESS capacity, $E_{12}$ the predicted energy balance between time t+1 and t+2 and $\Delta t$ the time-basis (15 min or 60 min). Furthermore, A negative $P_{MI_{12}}$ represents a selling of energy and a positive a buying of energy. The strategy is illustrated in Figure 3.12.

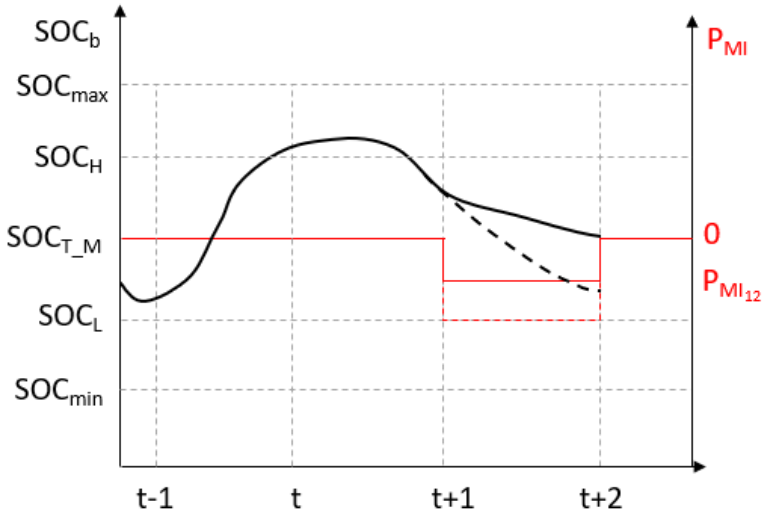


**Figure 3.12:** Market interaction according to Method 2 - The full line represents the $SOC_b$ behaviour when Method 2 is used for calculating the MI. The dashed line is the corresponding when Method 1 is used for calculating the MI. A negative value of $P_{MI}$ equals a selling of energy and a positive value a buying of energy.

The illustration in Figure 3.12 is a made up scenario based on the power balance in Figure 3.10. As seen, the method gives a calculated MI-value that corresponds to $SOC_b$ returning to the desired SOC-value. The dashed line is a comparison with Method 1 that gives a fixed MI-value. In this made-up scenario, the fixed MI is higher than desired leading to $SOC_b$ depleting more than necessary. The full flow-chart of this control method is described in Figure 3.13.

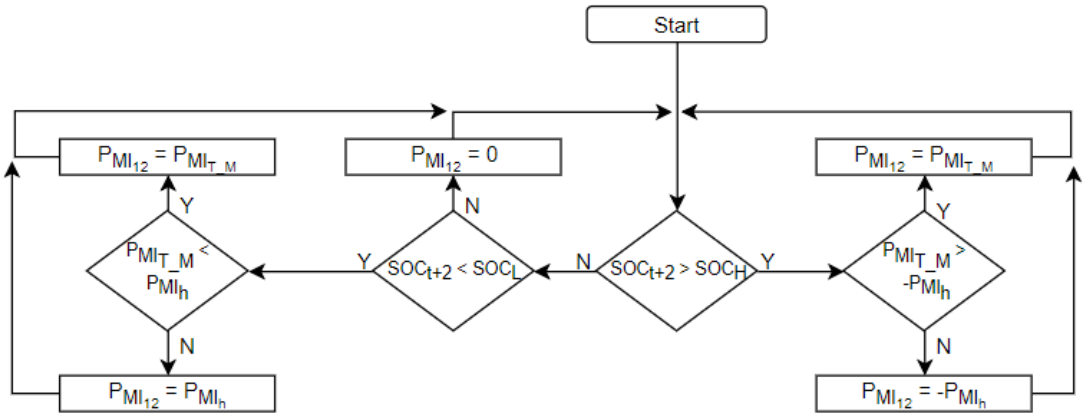


**Figure 3.13:** Flow-chart for Method 2 with market interaction based on two time-units - if $SOC_{t+2}$ is within the NOB, no MI is needed. However, if lower than $SOC_L$ or higher than $SOC_H$ an MI bringing it back to the NOB are desired. The power setpoint of the MI is based on calculations, but with the maximum value of $P_{MI_h}$.

### 3.3.3 Market interaction based on three time-units (Method 3)

The objective for Method 3 is to make an even more qualified MI than Method 2. This is done by enhancing the strategy in Method 2 by considering one more time-unit (time t+2 until t+3) in addition to the two already used in Method 2. In Method 2 it is always beneficial for the SOC-target to be the centre of the usable SOC-capacity as previously discussed. However, by predicting the energy balance and the SOC-level for one time-unit further the SOC-target can be altered in a beneficial way. For instance, when an overproduction is predicted, a lower SOC-target is desirable, and when an underproduction is predicted a higher SOC-target is desirable. This gives a higher chance of staying within the NOB the next time-unit as well as potentially giving a smoother MI. The energy balance for the extra time-unit ($E_{23}$) is calculated with the midpoint rule the same way as earlier, as shown in equation 3.8 and illustrated in Figure 3.14.

$$E_{23} = \frac{\Delta t}{n} \sum_{x=9}^{12} P_{balance} \frac{(x_i + x_{i-1})}{2} \tag{3.8}$$

Where $x$ is the time parameter, $P_{balance}$ is the forecasted power balance in the system at time $x$, $n$ is the number of segments evaluated, in this case, n = 4 and $\Delta t$ is the time-basis for the Elbas intraday market (15 or 60 min).

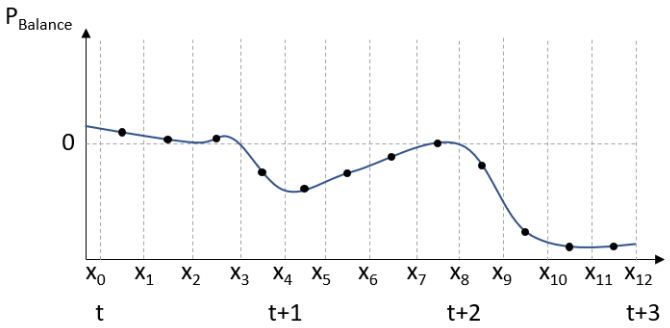


**Figure 3.14:** Illustration of the predicted energy balance calculation for Method 3 - $x_8$ equals the start of the third time-unit $(t + 2)$ and $x_{12}$ equals the end of the third time-unit $(t + 3)$. A positive value equals a power surplus and a negative value a power deficit. The black dots are the evaluation points related to the Midpoint rule.

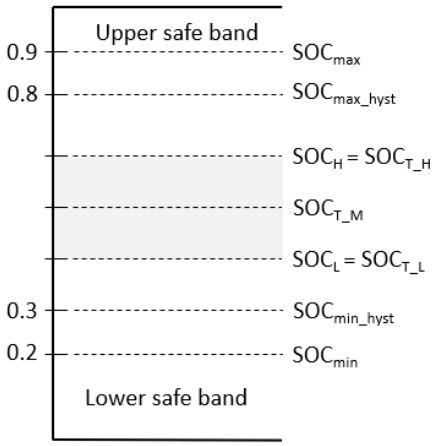


**Figure 3.15:** SOC-limits for the BESS in Method 3 - The grey area illustrates the NOB

The same SOC-limits as in Method 2 are used, however with the two additional SOC-targets ($SOC_{T\_L}$ and $SOC_{T\_H}$), as seen in Figure 3.15. By predicting $SOC_{t+2}$ and $SOC_{t+3}$ and comparing this to the NOB a decision whether an MI is needed or not can be made. Again, $SOC_{t+1}$ can not be modified due to the MI related to this time-unit being set at a previous time. However, $SOC_{t+1}$ is still needed for calculating both $SOC_{t+2}$ and $SOC_{t+3}$. $SOC_{t+1}$ and $SOC_{t+2}$ are calculated as earlier (see equation 3.5 and 3.6). $SOC_{t+3}$ is calculated as in Equation 3.9. $P_{MI_{t3}}$ is the MI related to $SOC_{t+3}$ which will be described deeper later on in the calculations. When predicting the value of $SOC_{t+3}$, $P_{MI_{t3}}$ is assumed to be 0.

$$SOC_{t+3} = SOC_{t+2} + \frac{E_{23} + P_{MI_{t3}} * \Delta t}{C_b} \tag{3.9}$$

Where $SOC_{t+2}$ is the predicted SOC-value at time t+2 as in equation 3.6, $E_{23}$ is the predicted energy balance for third time-unit (time t+2 until t+3) as calculated in equation 3.8, $P_{MI_{t3}}$ is the MI related to the third time-unit, $\Delta t$ is the time-basis (15 min or 60 min) and $C_b$ is the BESS capacity.

Depending on the values of $SOC_{t+3}$ and $SOC_{t+2}$ different MIs are desired. The scenarios to consider are shown in the list below accompanied with an illustration in Figure 3.16. To clarify, "<>" means "within" and "><" "outside".

- **Scenario 1** - $SOC_{t+3}$ <> NOB and $SOC_{t+2}$ <> NOB: No MI is needed. An illustrated of the scenario is presented in Figure 3.16a
- **Scenario 2** - $SOC_{t+3}$ < NOB and $SOC_{t+2}$ <> NOB: Two alternative $P_{MI_{12}}$ are calculated to decide which one is more beneficial. One MI that increases $SOC_{t+3}$ to $SOC_{T\_M}$ and one that increases $SOC_{t+2}$ to $SOC_{T\_H}$. The MI to reach those targets are calculated according to equation 3.10 and 3.11, respectively.

$$P_{MI_{t3}} = (SOC_{T\_M} - SOC_{t+3}) * C_b \tag{3.10}$$

$$P_{MI_{t2}} = (SOC_{T\_H} - SOC_{t+2}) * C_b \tag{3.11}$$

If $P_{MI_{t3}}$ is of lower magnitude than $P_{MI_{t2}}$, $P_{MI_{12}} = P_{MI_{t3}}$. Thereby, $SOC_{t+3}$ will reach its target while $SOC_{t+2}$ is still within the NOB. However, if $P_{MI_{t3}}$ is of larger magnitude than $P_{MI_{t2}}$, $P_{MI_{12}} = P_{MI_{t2}}$. Thereby, $SOC_{t+2}$ will reach the maximum limit of the NOB while $SOC_{t+3}$ still has not reached $SOC_{T\_M}$. However, the best possible chance of $SOC_{t+3}$ staying within the NOB without further MIs at the calculations at time t+1 has been given. An illustration of the scenario is presented in Figure 3.16b.

- **Scenario 3** - $SOC_{t+3} >$ NOB and $SOC_{t+2} <>$ NOB: Similarly, one MI that decreases $SOC_{t+3}$ until it has reached $SOC_{T\_M}$ or until $SOC_{t+2}$ has reached $SOC_{T\_L}$ is calculated. The MI to reach these targets are as in equations 3.12 and 3.13, respectively.

$$P_{MI_{t3}} = (SOC_{T\_M} - SOC_{t+3}) * C_b \tag{3.12}$$

$$P_{MI_{t2}} = (SOC_{T\_L} - SOC_{t+2}) * C_b \tag{3.13}$$

If the magnitude of $P_{MI_{t3}}$ is larger than $P_{MI_{t2}}$, $P_{MI_{12}} = P_{MI_{t3}}$. Thereby, $SOC_{t+3}$ will reach its target while $SOC_{t+2}$ is still within the NOB. If the magnitude of $P_{MI_{t3}}$ is less than $P_{MI_{t2}}$, $P_{MI_{12}} = P_{MI_{t2}}$. Thereby, $SOC_{t+2}$ will reach the minimum limit of the NOB while $SOC_{t+3}$ still has not reached $SOC_{T\_M}$. Again, the best possible conditions for the upcoming calculations have been given. An illustrated of the scenario is presented in Figure 3.16c.

For the upcoming scenarios, an MI directing $SOC_{t+2}$ to a desirable value is of priority. All MIs are calculated as in equation 3.14 with the appropriate SOC-target ($SOC_T = SOC_{T\_L}$, $SOC_{T\_M}$ or $SOC_{T\_H}$) for each scenario.

$$P_{MI_{12}} = (SOC_T - SOC_{t+2}) * C_b \tag{3.14}$$

- **Scenario 4** - $SOC_{t+3} <>$ NOB and $SOC_{t+2} <$ NOB: an MI to increase $SOC_{t+2}$ to $SOC_{T\_L}$ is desired. This will give the highest chance of $SOC_{t+3}$ staying within the NOB. An illustration of the scenario is presented in Figure 3.16d.
- **Scenario 5** - $SOC_{t+3} <>$ NOB and $SOC_{t+2} >$ NOB: an MI to decrease $SOC_{t+2}$ to $SOC_{T\_H}$. This will give the highest chance of $SOC_{t+3}$ staying within the NOB. An illustration of the scenario is presented in in Figure 3.16e.
- **Scenario 6** - $SOC_{t+3} ><$ NOB and $SOC_{t+2} ><$ NOB: an MI to bring $SOC_{t+2}$ to $SOC_{T\_M}$ is desired. An illustration of the scenario is presented in in Figure 3.16f.

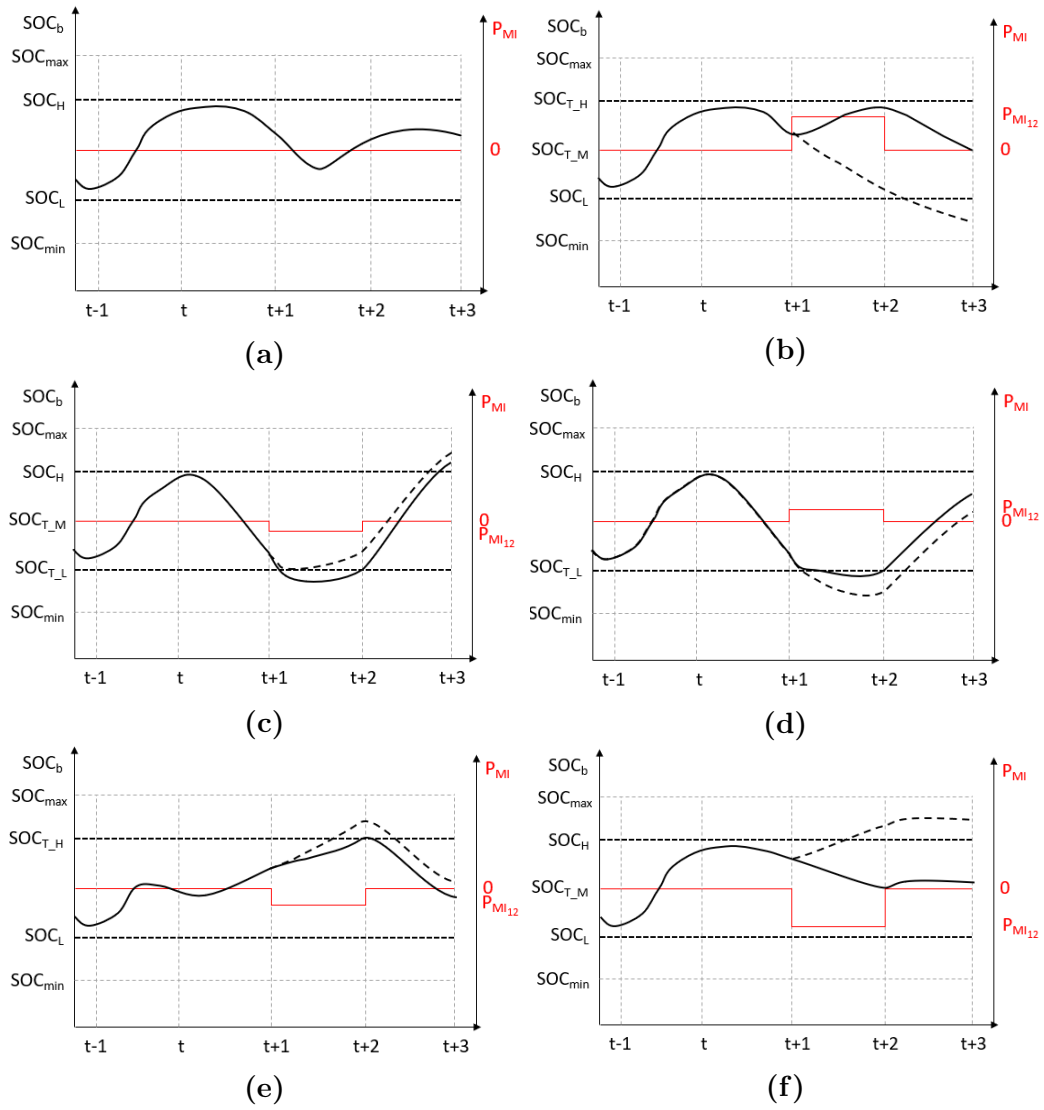


**Figure 3.16:** Possible scenarios for Method 3 - The dashed line represents $SOC_b$ if no MI was made and the full line represents the $SOC_b$ when the MI as described in the scenarios above are realized. The red line indicates the power setpoint of the MI. A positive MI means a buying of energy and a negative a selling of energy. In the examples, the high and low SOC-targets are equal to the high and low NOB-limits.

As can be seen, in Figure 3.16a no MI is needed. In Figure 3.16b the SOC-target for $SOC_{t+3}$ is reached while $SOC_{t+2}$ stays below the maximum NOB limit. In Figure 3.16c $SOC_{t+2}$ reaches the minimum NOB-limit thereby not managing to make $SOC_{t+3}$ reach its SOC-target as well. In this specific case, $SOC_{t+3}$ is predicted to be outside the NOB meaning another MI need to be made for the upcoming time-unit. However, since $SOC_{t+3}$ is closer to the limit, a smaller MI can be made. In Figures 3.16d and 3.16e, $SOC_{t+2}$ is on either side of the NOB-limits while $SOC_{t+3}$ is within the NOB. MIs bringing $SOC_{t+2}$ to the closest NOB-limit is therefore made. Lastly, in Figure 3.16f both $SOC_{t+2}$ and $SOC_{t+3}$ is outside of the NOB. $SOC_{t+2}$ is prioritized and thus brought back to the center of the usable SOC range.

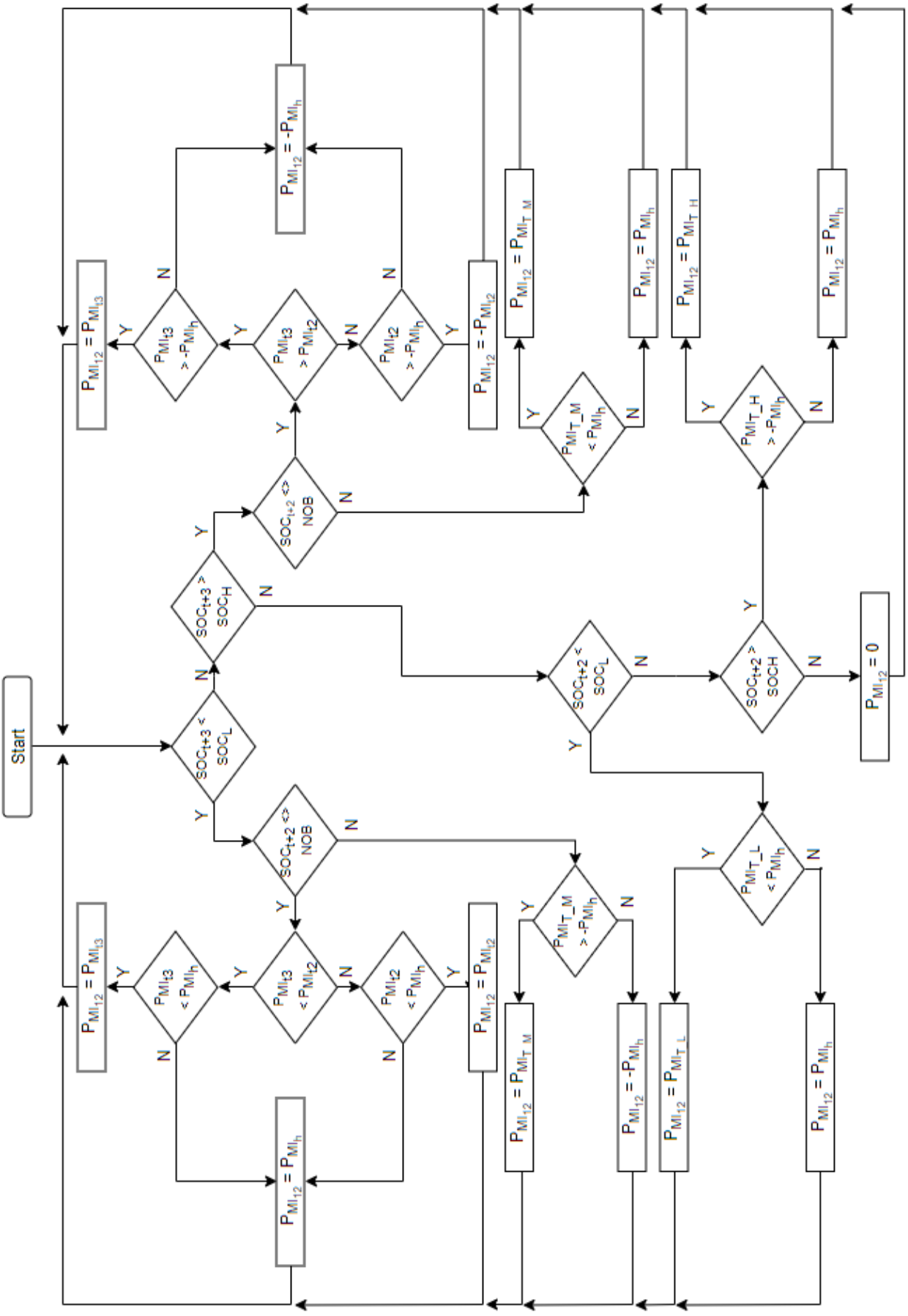


**Figure 3.17:** Flow-chart for the algorithm in Method 3 - If both $SOC_{t+2}$ and $SOC_{t+3}$ is within the NOB, no MI is needed. However, if outside, an MI bringing both $SOC_{t+2}$ and $SOC_{t+3}$ is desired. If that is not possible, $SOC_{t+2}$ is always prioritized.

## 3.4 Market interaction with two or more BESSs

When using two or more BESSs in the DC-system the MI needs to be divided into sub-MIs for each BESS. This is because the power setpoint of the MI is based on the local SOC-value and SOC-target for each BESS. The logic is the same for all methods, but assuming the DC-system are using "N" number of BESSs and Method 2 is chosen. Then the following applies. First and foremost, each BESS is responsible for regulating, storing and dissipating a certain part of the predicted future energy balance. In this thesis an equal droop coefficient is applied, thereby giving a close to equal share for each BESS. The local SOC at time t+1 and time t+2 for each individual BESS is thereby calculated as in equation 3.15 and 3.16.

$$SOC_{t+1_z} = SOC_{t_z} + \frac{\frac{E_{01}}{N} + P_{MI_{01_z}} * \Delta t}{C_{b_z}} \tag{3.15}$$

$$SOC_{t+2_z} = SOC_{t+1_z} + \frac{\frac{E_{12}}{N} + P_{MI_{12_z}} * \Delta t}{C_{b_z}} \tag{3.16}$$

Where the subscript $z$ indicates the BESS considered and $N$ equals the number of BESSs used.

Continuing, the MI requested from each BESS is thereby calculated as in equation 3.17.

$$P_{MI_{12_z}} = \frac{(SOC_{T_z} - SOC_{t+1_z}) * C_{b_z} - \frac{E_{12}}{N}}{\Delta t} \tag{3.17}$$

The total MI ($P_{MI_{12}}$) is calculated as the sum of all individual MIs ($P_{MI_{12_z}}$), as in equation 3.18.

$$P_{MI_{12}} = \sum_{z=1}^{N} P_{MI_{12_z}} \tag{3.18}$$

Consequently, assuming a system where two BESSs are implemented. If equal MIs with opposite signs are requested from the two BESS, e.g one is above the SOC-target and the other below, the resultant MI is zero.

# Chapter 4

# Modelling and Scenario setups

---

*This chapter shows how the models and methods have been implemented in the modelling tool. It will give a brief insight into some of the key components. In the last part, the different scenarios that will be considered in the simulations are described.*

---

## 4.1 Simulation tools

To implement the methods as well as run the simulations the simulation tool OpenModelica has been used. OpenModelica is an open source software based on the Modelica environment. It contains a standard library with various blocks for different applications [58]. Some of them have been used when implementing the simulations model. It also contains the option to create custom blocks which has been used extensively throughout the modelling. The software creates data files containing the output data. MatLab has been used for saving and processing this data.

## 4.2 Modelling

The BESS and the control blocks have been implemented to an existing model of Baltic InteGrid. Both the base model and the extended model are described in this section.

### 4.2.1 Base model

The model is based on the prevailing specifications of the WPP cluster Baltic InteGrid as described in section 2.1. The DC-system consist of four WPP inputs and five outputs representing the Onshore Connection Points (OCPs) to the AC-grid, as seen in Figure 4.1. To simulate the distance in between the WPP clusters and the time it takes for the wind to pass the area an arbitrary delay of 1000 s is implemented between each cluster. In reality this time would change depending on the

wind speed, but for this work this simplification is enough. The data for the WPP input is from a table value, based on wind data for the region as previously mentioned. The data is updated every 10 minutes with linear interpolation in between the measured values. The total time of the data is 3153600 s which is the same as a full year (365 days). Four of the OCPs are power regulated by a PI controller to a fixed table value representing the current market share from the DC-system. The table values are calculated as the average of the WPP output for the specific time-basis. Although being made up, they act as a realistic market output for each OCP based on the generated electricity in the DC-system. The market is updated hourly or every 15 minutes based on the time-basis of the intraday market ($\Delta t$), which is also the frequency of the change in data value from the table. The fifth and last OCP represents the slack bus. The slack bus is compulsory and very important for the grid model since this allows the balance in the DC-system to be upheld. The slack bus is regulated by a PID-controller regulating the voltage at nominal value, as opposed to the other four connection points. In reality, the DC-grid is connected to an AC-grid. The importance of this work is to balance the internal characteristics of the DC-grid. The model is simplified in this sense and sees the surrounding AC-grid as a DC-grid, meaning no frequency characteristics is available. Another simplification is that the transmission lines are modelled as monopolar links instead of bipolar links as the technical description in section 2.1.1 describes. One OCP is described in Figure 4.2. The full system as modelled in OpenModelica can be seen in Figure A.1 in Appendix A.

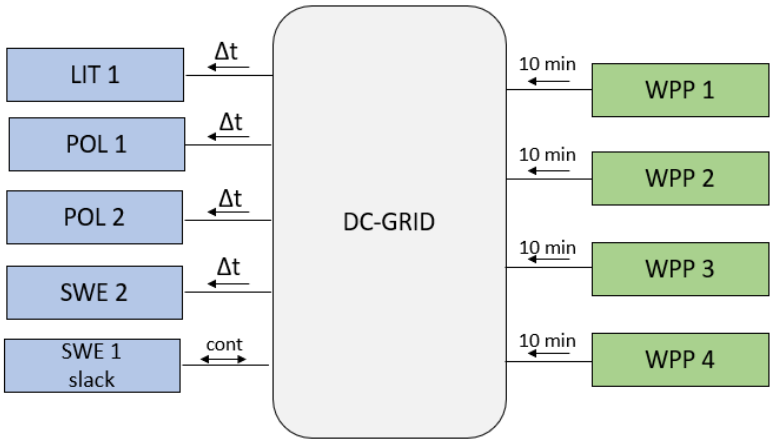


**Figure 4.1:** Schematic overview of Baltic InteGrid model - $\Delta t$ = 15 min or 60 min based on the time-basis of the Elbas intraday market.

In Figure 4.1, SWE indicates that the onshore connection point is in Sweden, POL that the onshore connection point is in Poland and LIT that the onshore connection point is in Lithuania. The direction of the power is defined as positive when going into the DC-grid and negative when going out from the grid, i.e a positive balance in the DC-grid is defined as a surplus and a negative balance a deficit. SWE 1 acts as the slack bus in the base model and is thereby continuously voltage regulating the DC-grid.

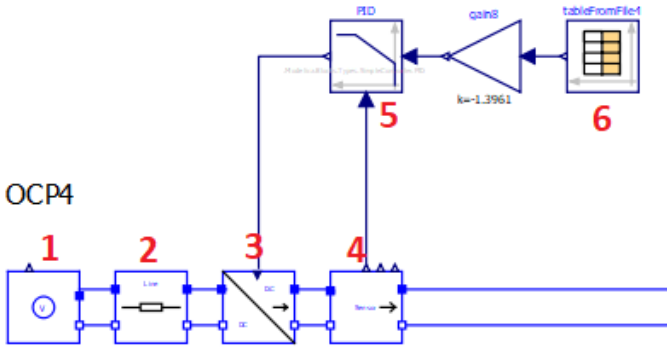


**Figure 4.2:** Model of one Onshore Connection Point in the base model - The OCP is connected to the DC-grid. (1) represents the 400 kV (Sweden) AC-grid onshore, however, modelled as a continuous DC voltage source, (2) the DC-transmission line resistance, (3) the 0.4/1 MV converter, (4) the voltage, power and current measuring unit, (5) the power controller for the electricity market value in the table in (6).

### 4.2.2 Extended model

The base model has been updated and extended by implementing two BESSs as well as an EMS controlling each BESS. The BESS acts as the slack buses regulating the voltage with an equal droop coefficient. These are continuously regulating the system in the normal case. However, when applicable SWE 1 and SWE 2 have the ability to voltage regulate while BESS (1) and BESS (2) are power regulated as described in section 3.1.1. All other OCPs are as earlier described. The additions are described in the sections below. An overview of the extended model from Figure 4.1 are presented in Figure 4.3.

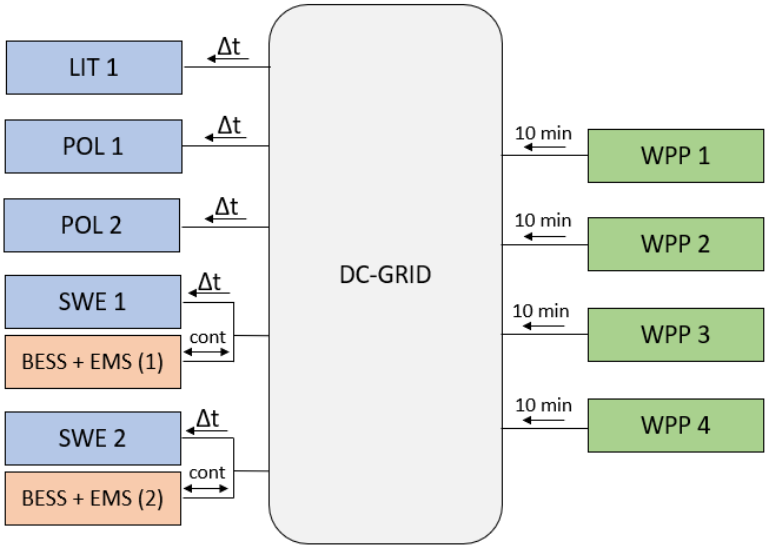


**Figure 4.3:** Schematic overview of extended Baltic InteGrid model - $\Delta t = 15$ min or 60 min based on the time-basis of the Elbas intraday market. Two BESS have been added.

The extension of the base model, with the OCP and BESS, as modelled in OpenModelica is highlighted in Figure 4.4. It should be noted that the OCP has been simplified in the sense that it has two branches. One branch is power regulated with the market value as the setpoint and the other branch is voltage regulating the system when needed. The full extended model can be seen in Figure A.2 in Appendix A.

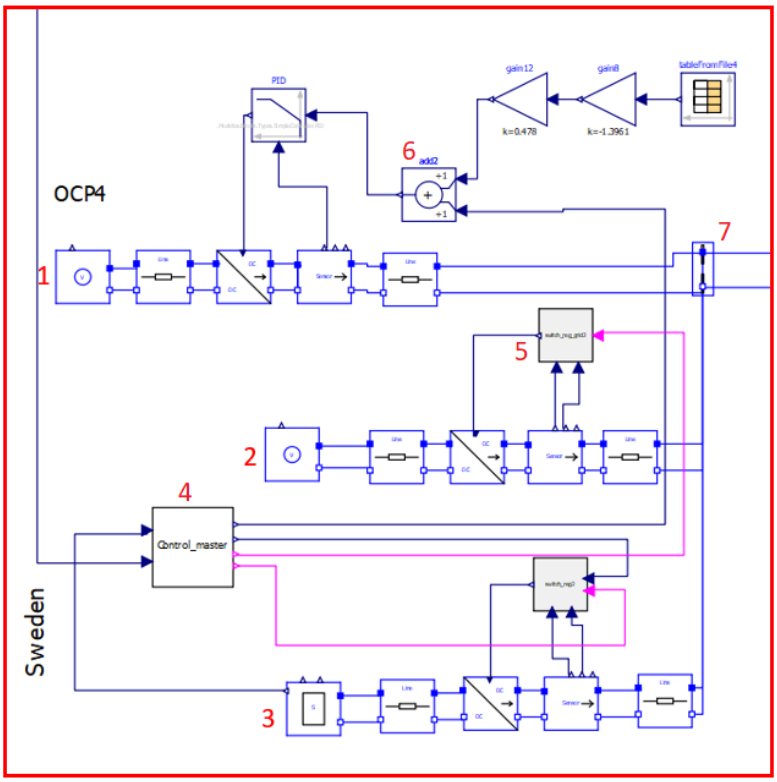


**Figure 4.4:** Extension of the base model - The OCP is branched into two parts. Branch (1) is power regulated with the market value as the power setpoint and branch (2) is regulating the voltage in the DC-system when needed. Branch (3) is the BESS. (4) is the BESS EMS block that will be discussed later on in this chapter, (5) is a block consisting of one P regulator for the voltage control and one PI regulator for the power control. When the BESS is the voltage regulating unit, the AC-grid is power regulated with zero as setpoint. (6) is the addition of the MI setpoint due to the SOC-regulation, (7) is the bus where the branches are connected.

### BESS block

The BESS ((3) in Figure 4.4) is simplified in the sense that it consists of a capacitance and the SOC is represented by the voltage. The model is illustrated in Figure 4.5. In reality, a Lithium-Ion battery has a somewhat exponential voltage discharge curve at the very edges of the SOC-range while being an almost constant value in between. Since the function of the BESS in the model is very similar to a battery, this has been an acceptable simplification. The BESS includes a parameter for changing the maximum capacity as well as deciding the initial SOC level. By knowing the voltage level of the capacitance, the energy stored in the capacitance can be calculated as

in equation 4.1.

$$E = \frac{C * u^2}{2 * 3600} \tag{4.1}$$

Where C is the size of the capacitance in Farads and u the voltage level. The division by 3600 gives the energy in Watthours instead of joules. With this information, the SOC-level can be calculated as in equation 4.2.

$$SOC_b = \frac{E_b}{E_{max}} \tag{4.2}$$

Where $E_b$ is the current energy level of the BESS and $E_{max}$ is the maximum BESS capacity decided by the user. Furthermore, with 4.1 it is possible to set the initial SOC of the BESS by setting the voltage to the value that corresponds to the desirable SOC-value. This is done by rewriting equation 4.1 as in equation 4.3.

$$u_{init} = \sqrt{\frac{SOC_{init} * C_b * 2 * 3600}{C}} \tag{4.3}$$

Where $SOC_{init}$ is the initial SOC-level and is represented by a value between 0 and 1, $C_b$ the BESS capacity and $C$ the capacitance in Farads.

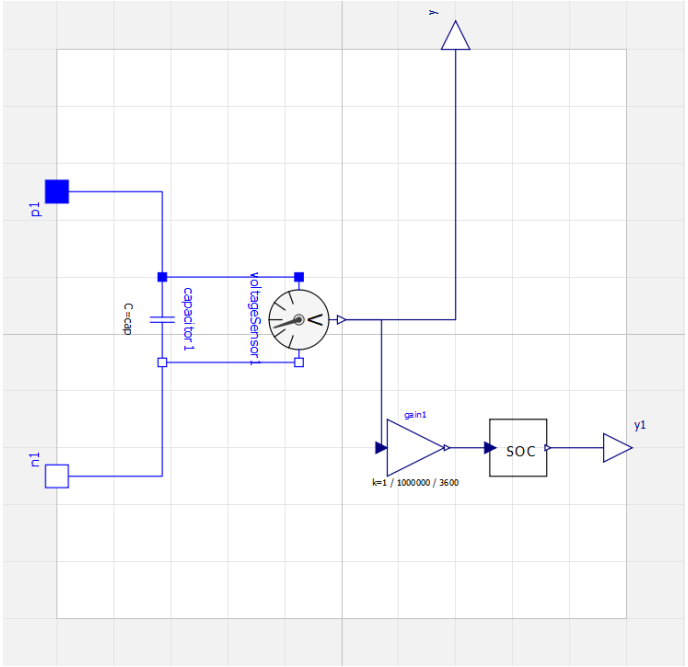


**Figure 4.5:** BESS as modelled in the simulation tool - The BESS consist of a capacitance and a voltage sensor. From the value of the voltage sensor, the energy is calculated and the SOC can be determined.

### BESS EMS block

The EMS of the BESS ((4) in Figure 4.4) possesses the intelligence of the system. Implementation wise the EMS is dependent on the current SOC level of the BESS ($SOC_b$), the current power balance of the input and output from the WPPs and OCPs ($P_{balance}$). Additionally, a pre-simulated data file of the power unbalance is needed to determine the future energy balance in the system. The EMS perform calculations continuously to determine if a market interaction is needed in order to regulate the SOC level of the BESS. If a market interaction is needed the EMS decide the power setpoint. The block also decided if the BESS or AC-grid should perform the voltage regulation. Lastly, the EMS also sets the power setpoint for the charging/discharging of the BESS when power regulated. Additionally, two blocks creating pulses are implemented. During the first pulse, the condition of the current state is measured and the needed calculations according to Method 1, 2 or 3 is calculated. During the second pulse, the output signal determined from the calculations is realized. The period between these two pulses represents the basis for the intraday market and is either 3600 s (60 min) or 900 s (15 min). Figure 4.6 shows the implementation of the EMS block.

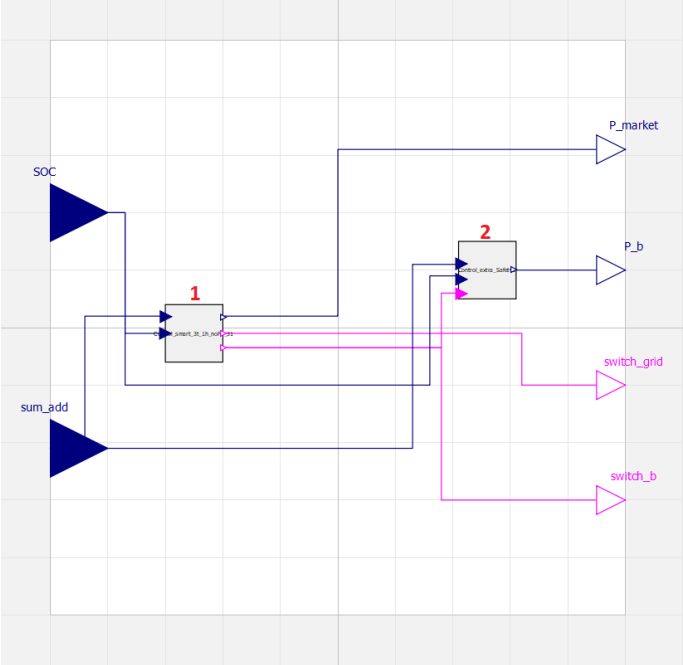


**Figure 4.6:** EMS as modelled in the simulation tool - (1) is the main control block where the future energy balance is calculated, the MI determined and voltage regulating unit decided. (2) includes the specific power setpoint to the BESS and are only used when the BESS is power regulated, i.e when the BESS has reached the outer SOC-limits.

Figure 4.7 shows the build-up of the main block ((1) in Figure 4.6). The top block does all the calculations regarding energy balance predictions and MI setpoints as described in section 3.3. A short part of the MI code according to Method 3 is presented in Appendix B. The two blocks below are the switching algorithms related to if the BESS or AC-grid is performing the voltage control. The reason for using two blocks are due to the short overlap in time when both units are performing the voltage control. These two blocks are modelled as in Figure 4.8 with a slight offset for the one connected to the AC-grid. That means that when the SOC is slightly below $SOC_{max}$ the AC-grid starts performing the voltage regulation and stops performing the regulation when SOC is slightly below $SOC_{max\_hyst}$. The equivalent applies for $SOC_{min}$ and $SOC_{min\_hyst}$.

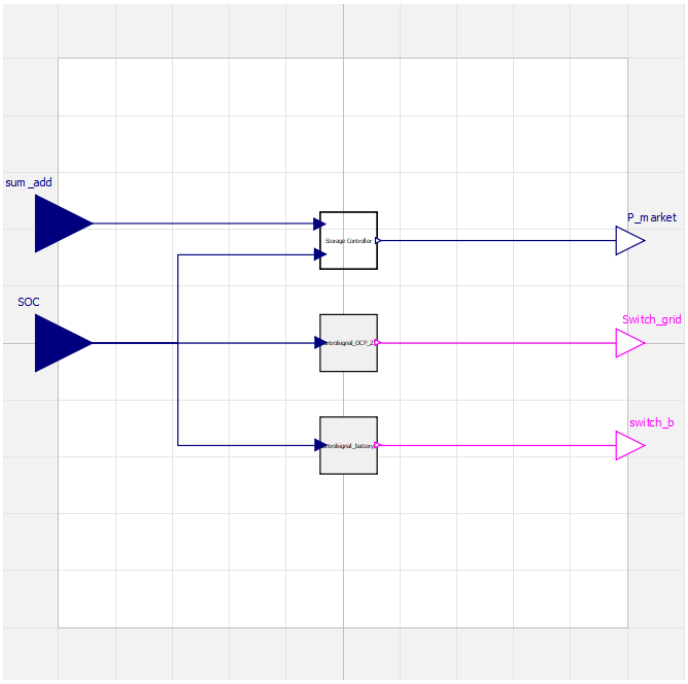


**Figure 4.7:** Main control block as modelled in the simulation tool - The top block includes the code for the methods and the two below include the switch algorithm to determine the voltage regulating unit.

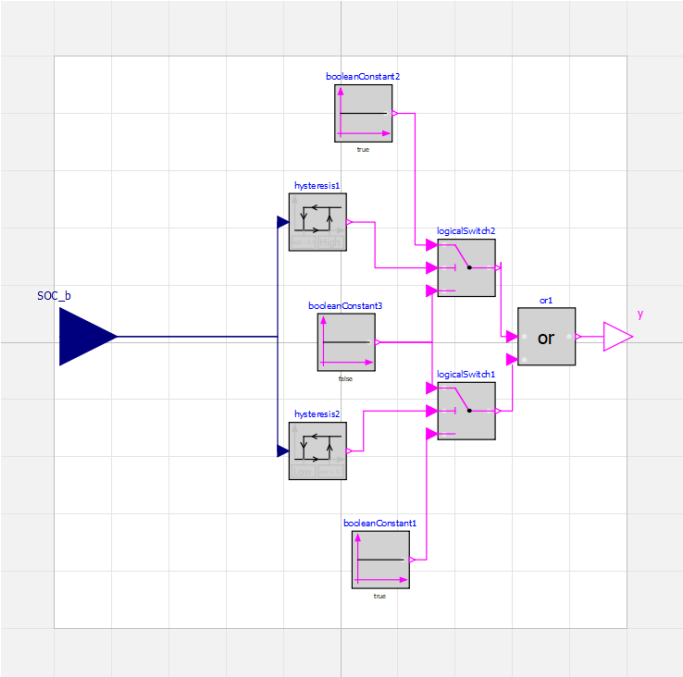


**Figure 4.8:** Switching of voltage regulating unit as modelled in the simulation tool - Depending on the SOC-value the algorithms are determining different logical values to decide if the BESS or AC-grid should perform the voltage regulation.

## 4.3 Scenario description

For the simulations, two different scenarios will be evaluated. First, a set of simulations when the Elbas intraday market is on a 60 min basis ($\Delta t$ = 60). Since this basis is going to change in the near future, the impact of using 15 min $\Delta t$ is also of importance. Furthermore, predicting the wind power output is not possible with a 100% confidence as has been mentioned. According to a study by [36] based on Finnish conditions, a forecast error of between 6 and 10% is to be expected for forecasts 3 hours forward in time. In the simulations in this work, a best case (BC) scenario of no forecast error will be used as well as a worst case scenario (WC) with a forecast error of 5 min for the 15 min time-basis and 20 min for the 60 min time-basis. The WC scenario is slightly more conservative than the result of their study. The initial simulations of the energy balance for the different scenarios are presented in Figure 4.9. Figures 4.9a and 4.9b shows the energy balance when $\Delta t$ = 60 min are used with the best case scenario of no forecast error and the worst case scenario of 20 min forecast error, respectively. Figures 4.9c and 4.9d shows the corresponding scenarios when $\Delta t$ = 15 min, the best case scenario again has no forecast error while the worst case contain 5 min forecast error. In the figures it can be seen that the power unbalances are generally much larger when the FC error increases. This is especially significant by comparing the magnitude at time = 30 days. For 60 min time-basis and 20 min FC error (Figure 4.9b) the magnitude is larger than 2000 MW and additionally has a few more spikes reaching above 1500 MW than when no FC error is used (Figure 4.9a). For the two scenarios with the 15 min time-basis, when a FC error is used (Figure 4.9d) is reaching 1500 MW at

multiple occasions as opposed to when no FC error is used (Figure 4.9c). Due to the power balance in the system exceeding the rated cable capacity of 1.5 GW for all scenarios, two BESS units are the bare minimum to be able to mitigate those peaks.

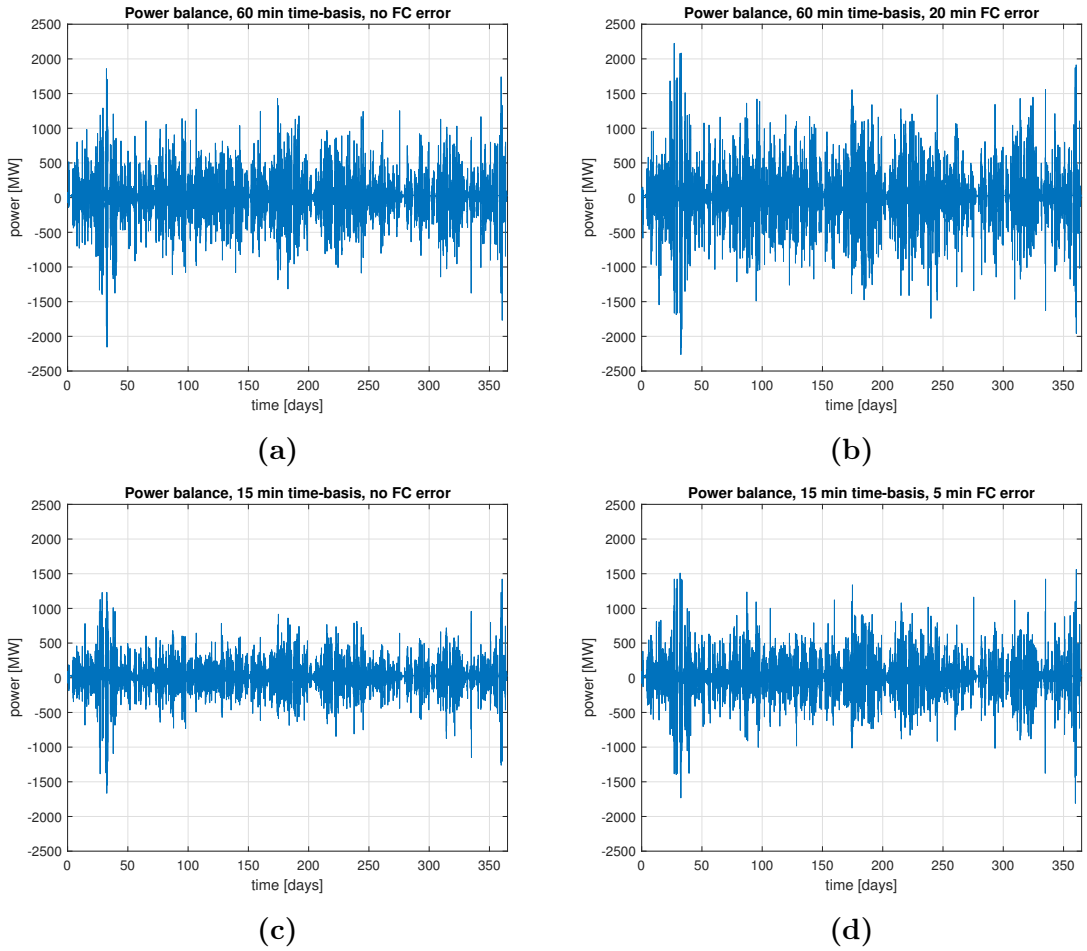


**Figure 4.9:** Power balance in the system over the full year for different $\Delta t$ and scenarios - A positive power balance means an overproduction and a negative power balance an underproduction. The unbalance are larger with more forecast error.

# Chapter 5

# Simulations and Analysis

---

*This chapter will showcase the different features in the simulation models and what impact the different parameters has to the result. In section 2 the results from the simulations are presented and then further analyzed and compared in section 3*

---

## 5.1 Verification of the simulation model

The updated and extended model with a BESS contains two important concepts that are vital for the rest of the functions. The first is the switching between voltage regulating unit and the second is the prediction of the future SOC-value.

### 5.1.1 Switching between voltage regulation resources

The most crucial component in the DC-system is the voltage regulation that upholds the stability at all times. As described previously, when a power deficit in the system occurs, the voltage drops and vice versa when a power surplus occurs. The voltage regulating unit mitigates the power unbalance by providing or withdrawing power. Since the BESS and AC-grid will both be able to regulate the voltage in the DC-system, the switch between them are of high priority when implementing the BESS to the original model. As described in Section 3.1.1 the switch between voltage regulating unit occurs when $SOC_b$ hits the upper or lower limit of the usable BESS capacity, $SOC_{max}$ and $SOC_{min}$ respectively. Figure 5.1 illustrates an example of when this function is used in the simulations. Figure 5.1a shows the power output from the BESS (blue) as well as the AC-grid (orange). Figure 5.1b shows the SOC-level, with the red lines as the outer SOC-limits and the green lines the hysteresis connected to it. Figure 5.1c shows the voltage level in the system.

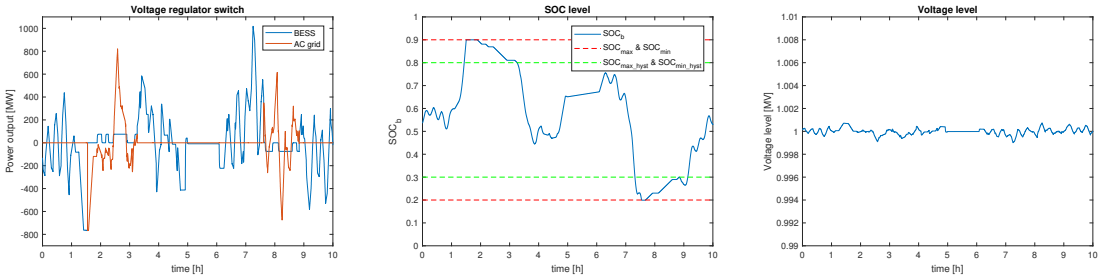


**(a)** **(b)** **(c)**

**Figure 5.1:** Example of the Voltage regulation switch mechanism - (a) is the power output from the BESS and AC-grid, (b) the $SOC_b$-graph and (c) the voltage level in the system.

As can be seen in Figures 5.1a and 5.1b, The SOC of the BESS is increasing rapidly at time = 1.5 h when the BESS is charging (withdrawing energy from the system, thereby seen as negative) and decreasing at time = 3.5 h when the BESS is discharging (injecting energy to the system, thereby seen as positive). Additionally, when the SOC of the BESS reaches $SOC_{max}$ or $SOC_{min}$, the AC-grid starts performing the voltage regulation (orange graph). At all other times, the power output from the AC-grid is stable at close to zero, which is as expected. The opposite is not true since the BESS is performing power regulation in order for $SOC_b$ to return to $SOC_{max\_hyst}$ or $SOC_{min\_hyst}$ and with that bring back the ability to perform to voltage regulation. It is important to notice that the voltage (Figure 5.1c), although fluctuating, is kept well within an arbitrary safety margin of 1% around the nominal voltage at all times. This indicates that the voltage regulation are working well both in normal operation and when the switch occurs.

### 5.1.2 Prediction performance

#### Average power output of time-basis

The predicted energy balance for the upcoming time-units, $E_{01}$ and $E_{12}$, are crucial for the algorithms in Method 2 and Method 3. Since the energy is calculated numerically based on only a few forecasted power output points this becomes an uncertainty for the functioning of the algorithms. Figure 5.2 shows the average power output for the current time-basis for both 60 min (Figure 5.2a) and 15 min basis (Figure 5.2b). It can be noted that there are much less variation within one time-unit when a 15 min time-basis is used.

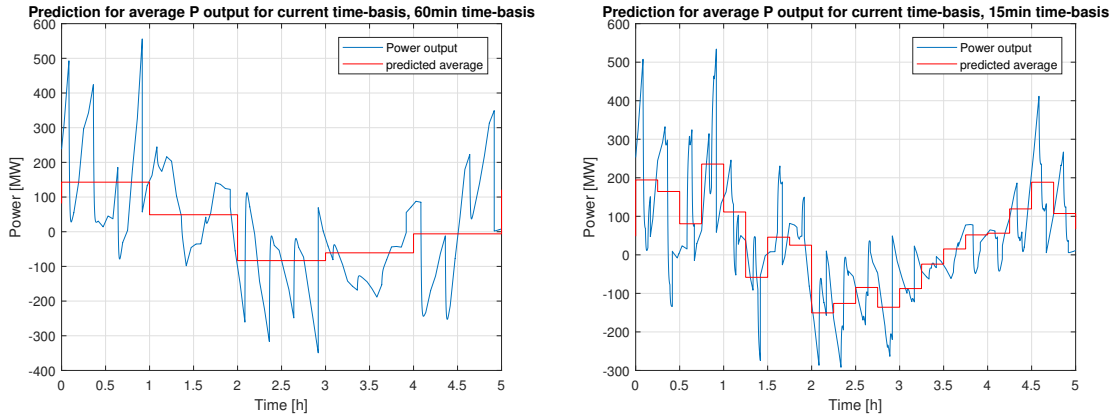


**(a)** **(b)**

**Figure 5.2:** Predicted average power compared to $P_{balance}$ - (a) show the result when the Elbas intraday market is working on a 60 min time-basis and (b) when the time-basis is 15 min.

### Prediction of $SOC_{t+1}$

The predicted SOC at the start of the next time-basis ($SOC_{t+1}$) is calculated based on the predicted energy balance for the current time-unit. Figures illustrating the actual SOC-value as well as the predicted SOC-value at time t+1 for a 300 MWh BESS is presented in 5.3a and 5.4a for the two different time-basis. The figures illustrate a scenario when there is no FC error. The prediction error is thereby only due to the fault when calculating the predicted energy balance in the system with the midpoint rule.

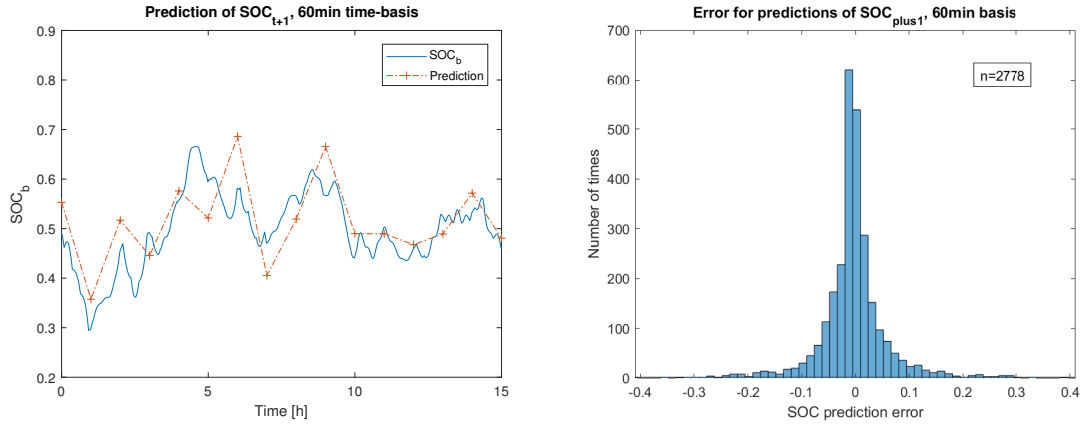


**(a)** **(b)**

**Figure 5.3:** Prediction of $SOC_{t+1}$ and the prediction error when $\Delta t = 60$ min - In the simulation, a 300 MWh BESS is used, consequently a 0.1 deviation represents 30 MWh error.

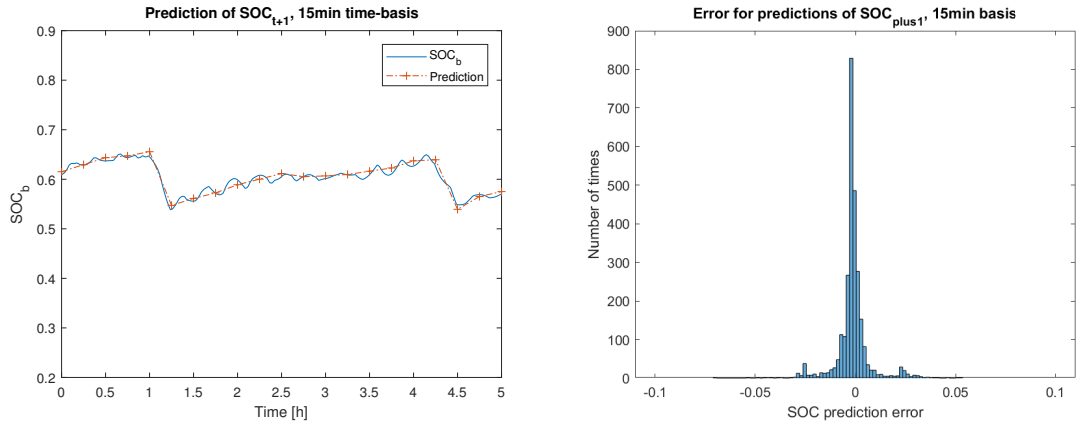


**(a)** **(b)**

**Figure 5.4:** Prediction of $SOC_{t+1}$ and the prediction error when $\Delta t = 15$ min - In the simulation, a 300 MWh BESS is used, consequently a 0.01 deviation represents 3 MWh error.

As can be seen in Figures 5.3 and 5.4, the prediction is much better for the shorter time-basis, as confirmed by Figures 5.3b and 5.4b. The BESS capacities used are identical for both simulations. By minimizing the BESS capacity for the 15 min basis by four times to 75 MWh the results are as in Figure 5.5

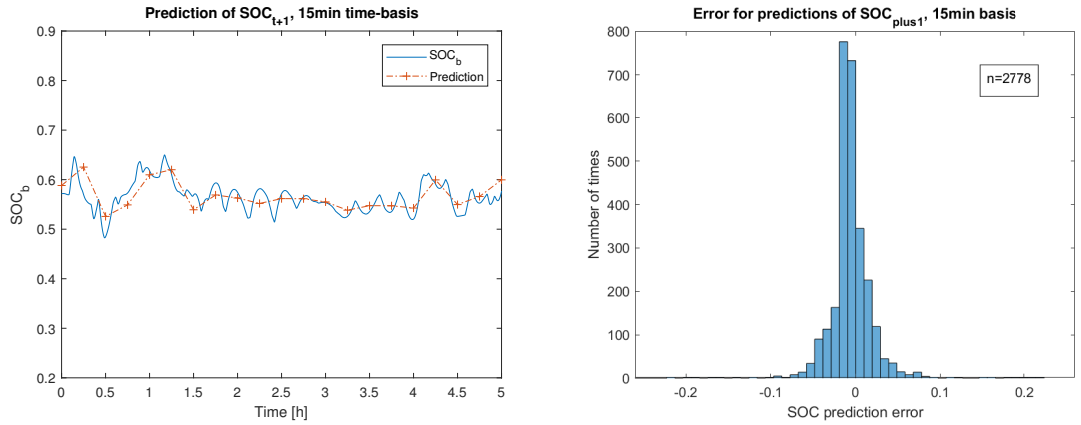


**(a)** **(b)**

**Figure 5.5:** Prediction of $SOC_{t+1}$ and the prediction error when $\Delta t = 15$ min for a smaller BESS - In the simulation the BESS capacity is 75 MWh.

Although the BESS capacity is four times smaller, the prediction of $SOC_{t+1}$ seems to be better than corresponding for 60 min time-basis in Figure 5.3. However, comparing Figure 5.4 and 5.5 it can be seen that the errors are much more significant. With better calculation methods than the midpoint rule with only 4 segments, the predicted $SOC_{t+1}$ should correlate with the actual SOC-value to a higher degree. This will prove to be an important factor to consider in the results.

## 5.2 Model parameter settings

This part will highlight the impact of the different parameters used in the models. The parameters to alter in the simulations are the width of the NOB, the SOC-targets, the fixed power setpoints related to the MI for Method 1 as well as the discharge and charge power when the BESS is power regulated. Multiple simulations with varied parameters have been performed in order to find the significance of them. From these simulations, a set of parameters has been chosen for the individual cases and methods for finding the minimum capacity of the BESS units while the performance requirements are still met.

### 5.2.1 Varying the normal operation band

The NOB decides the area in which the BESS are allowed to operate without any MI. A comparison between a wider and a more narrow area can be seen in Figures 5.6 and 5.7. The algorithm used in this example is the algorithm for Method 2, however, the function and consequence is the same for all algorithms.

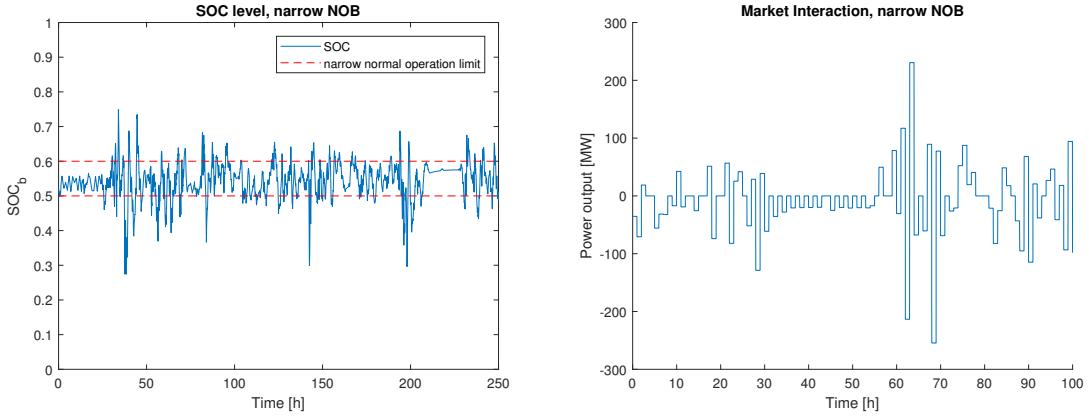


**(a)** **(b)**

**Figure 5.6:** SOC-behaviour and market interaction when a narrow NOB is used - In (b), a large amount of MIs made since the NOB is very narrow. In (a), $SOC_b$ is kept within safe distance of the outer SOC-limits except for a few times.

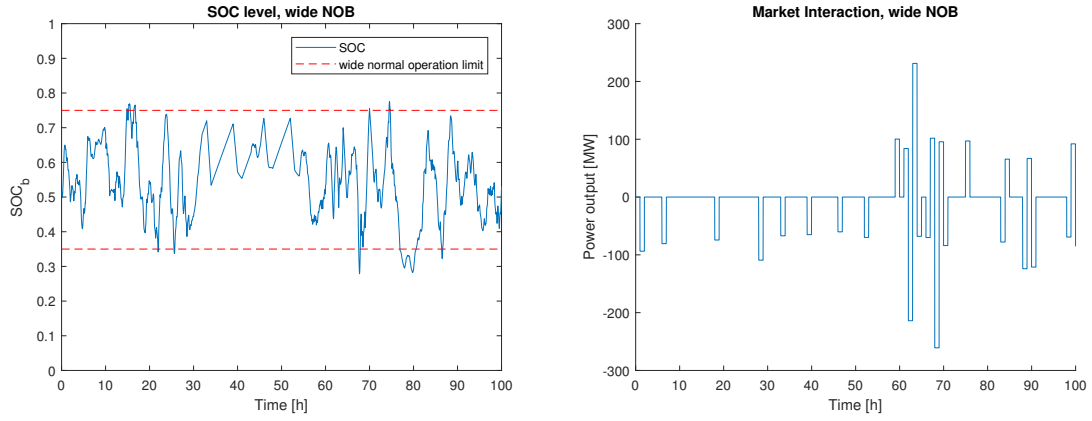


**(a)** **(b)**

**Figure 5.7:** SOC-behaviour and market interaction when a wide NOB is used - $SOC_b$ in (a) is allowed to be closer to the outer limits of the SOC-range since the NOB is wider. Because of this, the risk of reaching the limits are increased. (b) shows the MIs.

As seen, by decreasing the NOB the BESS operates in a much more refined area. Fewer deep cycles can be spotted in Figure 5.6a than Figure 5.7a, which is good from a BESS lifetime point of view. However, the MI becomes much more frequent as a consequence as Figures 5.6b and 5.7b suggests. After multiple simulations with various widths of the NOB, $SOC_H$ and $SOC_L$ have been set to 0.65 (65%) and 0.4 (40%) respectively here on after for all models. This setting has shown to be a good trade-off between performance and number and magnitude of the MI.

### 5.2.2 Regulation of Market interaction

The MI for the different methods works the same way even though the strategy for deciding the magnitude of the MI is different. In Method 1 the magnitude of the MI is simply a fixed power setpoint. By increasing this value, the regulation becomes more aggressive. Consequently, decreasing the value makes the regulation less aggressive. Figures 5.8 and 5.9 show this. In Method 2 and Method 3 the value is decided based on SOC-targets. While the targets for Method 3 can be altered in order to regulate the magnitude of the MI, in Method 2 this is not possible since the target is always the centre of the usable BESS capacity. However, as discussed in section 5.2.1 the MI can still be somewhat regulated by varying the NOB. For Method 3 the MI can be regulated either by creating an extended NOB for $SOC_{t+2}$ that stretches the NOB further apart. This would allow $SOC_{t+2}$ to reach a higher or lower value, as long as $SOC_{t+3}$ is predicted to stay within the NOB. It could also be regulated by increasing or decreasing the SOC-targets. By decreasing the SOC-targets the method would act more like Method 2. The targets are desirable to be as close to the outer limits of the usable SOC-range as possible to gain the most benefits regarding the MI. However, since no consideration of the power distribution within one time-unit is taken, the risk of reaching $SOC_{max}$ and $SOC_{min}$ are increased. In the simulations, $SOC_{T\_L} = SOC_L$ and $SOC_{T\_H} = SOC_H$ have been chosen since this highlights the benefits to a sufficient degree without demanding full knowledge

of the power distribution at each time. In this section, it should also be noted that a cap related to the maximum power setpoint for the MI for all simulations using Method 2 and Method 3 has been implemented. In reality, the DC-cables in the system will be used to a much higher extent, leaving less utilization range for the MIs. The maximum power setpoint has been set to 300 MW per BESS. Since two BESSs are used in the DC-system, the maximum magnitude of the MI from the DC-system is 600 MW.

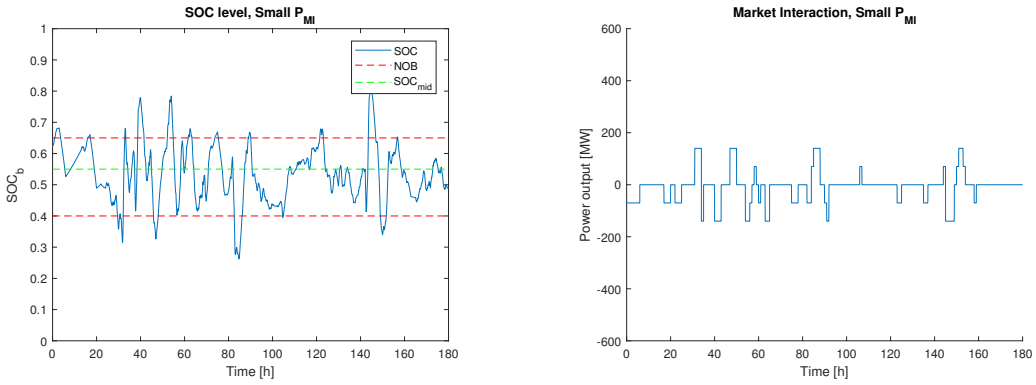


**(a)** **(b)**

**Figure 5.8:** Market interaction with a 70 MW fixed power setpoint - The figure shows the behaviour of $SOC_b$ when Method 1 is used with a fixed power setpoint for the market interaction of 70 MW.

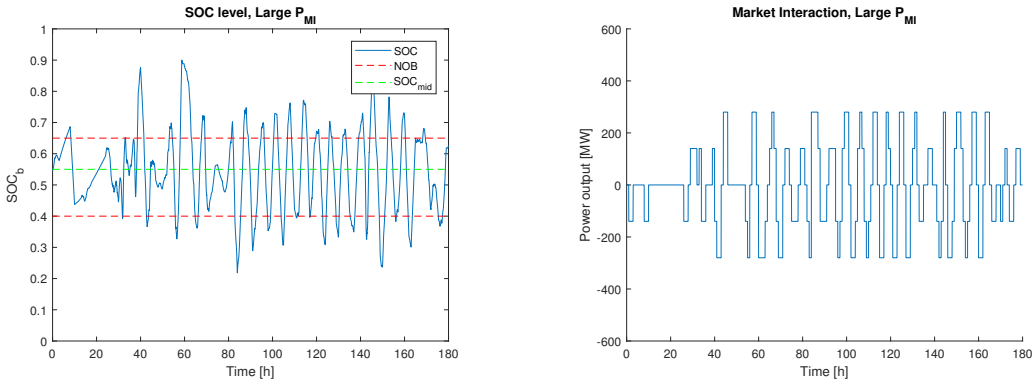


**(a)** **(b)**

**Figure 5.9:** Market interaction with a 140 MW fixed power setpoint - The figure shows the behaviour of $SOC_b$ when Method 1 is used with a fixed power setpoint for the market interaction of 140 MW. The setpoint is larger than desired, leading to oscillations.

As seen in Figure 5.8, when the fixed power output related to the MI is set to an appropriate value, $SOC_b$ is staying within the NOB reasonably well. However, a too small value would not be able to counteract the power surplus or power deficit. On the other hand, a too high value could make the system oscillating due to $SOC_b$ being regulated too aggressively. This is shown in Figure 5.9.

### 5.2.3 Varying the fixed charge and discharge power

A larger charge or discharge power ($P_{fixed}$) combined with a larger threshold value, ($P_{THRES}$), will allow the BESS to return faster to a sufficient SOC-level for performing the voltage regulation. However, This is only beneficial if the power surplus or power deficit that filled up or depleted the BESS has been mitigated. If not, the BESS will return to voltage regulation just to be filled up or depleted shortly after. The power output for the different simulations has been decided for each individual case. However, a base setting of $P_{fixed} = 75$ MW has been set.

## 5.3 Simulation performance

In this section, the parameters to evaluate the methods are presented as well as the results from the simulations. It should be noted that two BESSs have been used in this work. The capacity stated in the result is per unit. The total capacity needed is thereby the double of this.

### 5.3.1 Evaluation parameters

The evaluation of the performances for the different models is very important. No standard procedure for evaluating the performance exist today, but [59] suggests considering the percentage of unmet demand. In this report, this will be measured as the total energy the AC-grid need to inject or withdraw from the system to uphold the stability, $E_{grid}$. The same source also recommends measuring the percentage of unused energy from renewables. In this report, however, no surplus energy is discarded. The range of performance evaluating parameters is described below.

- $T_{grid}$ [%] - This is the main evaluation parameter. It is used for deciding the optimal sets of parameters as well as the minimum BESS capacity. For each model the minimal size of the BESS when $T_{grid} = 0$ and when $T_{grid} = 3$ % will be decided. 3 % is an arbitrary limit, allowing some dependency on the AC-grid. The parameter shows the total amount of time the AC-grid is performing the voltage control. The parameter is calculated by dividing the total time the AC-grid is performing the voltage control with the time of the simulation period, in this case the full year. The reason why evaluating this is important is mainly to evaluate to what extent the DC-system is non-dependent on the AC-system. Future demands for implementing very large intermittent production plants might require a certain extent of self-sufficiency.
- $E_{grid}$ [%] - Amount of energy withdrawn from or injected to the DC-grid while the AC-grid is performing the voltage control ($Vreg = AC - grid$). This is calculated by dividing the regulation energy from the AC-grid by the total regulation energy needed. This parameter will help justify the significance of $T_{grid}$
- $T_{mean}$ [s] - Mean time of interval the AC-grid is performing the voltage regulation. Since more than one BESS is implemented, the parameter considers the

time from when the first BESS has reached $SOC_{max}$ or $SOC_{min}$ until the last BESS has reached $SOC_{max\_hyst}$ or $SOC_{min\_hyst}$ respectively.

- $Vreg_{nbr}$ - Number of times the AC-grid is performing the voltage control. The parameter helps justify the significance of $T_{grid}$ and $E_{grid}$. A lesser number of $V_{reg}$-switches are desirable.
- $P_{MI_{nbr}}$ - The total number of market interactions. A lower number of market interactions are desired. The parameter is split into $P_{MI\_sell_{nbr}}$ and $P_{MI\_buy_{nbr}}$.
- $P_{MI_{mean}}$ [MW] - The mean magnitude of the market interactions. To justify the number of market interactions. This parameter is split up into $P_{MI\_buy_{mean}}$ and $P_{MI\_sell_{mean}}$.
- $SOC_{nbr}$ - The total Number of SOC-cycles. Due to the complexity of computing cycles in a Lithium-Ion battery, this is implemented in a very simplified way considering a number of fixed ranges on the SOC scale. The ranges are: 0.25 - 0.55, 0.35 - 0.65 and 0.45 - 0.75. One SOC-cycle is calculated when the SOC of the BESS is reaching the lower trigger point of the range and thereafter the higher trigger point. The parameter is used as a way of hinting towards how many cycles the BESS is run through over a year than showing the actual fact.

### 5.3.2 Results when BESS is sole voltage regulating unit

In this section, the results from the different simulations are presented. Method 1 and 2 have been optimized in terms of finding the smallest BESS for the parameter setting when $T_{grid} = 0\%$, i.e the AC-grid is never performing voltage control. Method 3, since being a further development of Method 2, is simulated with the same BESS capacity as Method 2 to improve the comparison. The simulations and optimization are done both for the best case (BC) scenario and the worst case (WC) scenario. Again, the BESS capacities presented in the tables are the capacity per BESS unit. For all methods two BESS units are used, i.e the total BESS capacity needed is double. It should be noted that the results are representative for the one data set that has been used in this work. For data sets with more or less intermittency, the results may differ.

#### Method 1

The specific parameters possible to alter in this model are the fixed power setpoint of the MI requested per BESS, $P_{MI}$ and the NOB limits, $SOC_H$ and $SOC_L$. The parameters are as in Table 5.1, where $Ref$ marks the parameter settings and scenario for the simulations. Table 5.2 shows the results.

**Table 5.1:** Method 1, Simulation parameters - The table shows the parameter settings that have been used for the simulations. The scenarios include varying the Elbas time-basis ($\Delta t$) as well as the forecast error (BC and WC).

| **Ref** | $\Delta t$ [min] | Scenario | $SOC_H$ | $SOC_L$ | $P_{MI}$ [MW] |
|---|---|---|---|---|---|
| **1** | 60 | BC | 0.65 | 0.4 | 60 |
| **2** | 60 | WC | 0.65 | 0.4 | 60 |
| **3** | 15 | BC | 0.65 | 0.4 | 50 |
| **4** | 15 | WC | 0.65 | 0.4 | 50 |

**Table 5.2:** Method 1, Results when $T_{grid} = 0\%$ - The table shows the result of the simulation scenarios.

| **Ref** | $C_b$/unit [MWh] | $P_{MI\_sell_{nbr}}$ | $P_{MI\_sell_{mean}}$ | $P_{MI\_buy_{nbr}}$ | $P_{MI\_buy_{mean}}$ | $SOC_{nbr}$ |
|---|---|---|---|---|---|---|
| **1** | 1200 | 1505 | 77 | 255 | 78 | 38 |
| **2** | 2000 | 1570 | 91 | 544 | 93 | 137 |
| **3** | 200 | 6649 | 58 | 6 | 75 | 17 |
| **4** | 600 | 6170 | 66 | 341 | 64 | 156 |

Because of the energy surplus for the input data used for the simulations, there is a considerable majority of MIs related to selling energy. A roughly four times increase in number of MIs is noticed for the 15 min time-basis. However, comparing the two simulations for BC, the figure when $\Delta t = 15$ min is closer to 4.4 times larger than when $\Delta t = 60$ min. The number of buying is on the other hand much lower making up for this figure. The total BESS capacity needed, i.e two units, each with the capacity in Table 5.2, is in the range of 2400 - 4000 MWh for a 60 min time-basis and 400 - 1200 MWh for a 15 min time-basis when method 1 is used and the BESS is sole voltage regulating unit.

### Method 2

Method 2 contains the following parameters to be varied. The limits for the NOB, $SOC_H$ and $SOC_L$ and the $P_{MI_{max}}$. The set of parameters and simulation cases are found in Table 5.3. The results are presented in Table 5.4.

**Table 5.3:** Method 2, Simulation parameters - The table shows the parameter settings that have been used for the simulations. The scenarios include varying the Elbas time-basis ($\Delta t$) as well as the forecast error (BC and WC).

| **Ref** | $\Delta t$ [min] | Scenario | $SOC_H$ | $SOC_L$ | $P_{MI_{max}}$ [MW] |
|---|---|---|---|---|---|
| **1** | 60 | BC | 0.65 | 0.4 | 300 |
| **2** | 60 | WC | 0.65 | 0.4 | 300 |
| **3** | 15 | BC | 0.65 | 0.4 | 300 |
| **4** | 15 | WC | 0.65 | 0.4 | 300 |

**Table 5.4:** Method 2, Results when $T_{grid} = 0\%$ - The table shows the result of the simulation scenarios.

| **Ref** | $C_b$/unit [MWh] | $P_{MI\_sell_{nbr}}$ | $P_{MI\_sell_{mean}}$ | $P_{MI\_buy_{nbr}}$ | $P_{MI\_buy_{mean}}$ | $SOC_{nbr}$ |
|---|---|---|---|---|---|---|
| **1** | 600 | 1459 | 153 | 545 | 234 | 48 |
| **2** | 950 | 1343 | 230 | 635 | 337 | 27 |
| **3** | 120 | 5149 | 78 | 133 | 154 | 52 |
| **4** | 240 | 4349 | 160 | 1265 | 247 | 9 |

The BESS capacity is much lower than for Method 1. A higher magnitude of the MIs can be noticed compared to Method 1. Some correlation between BESS capacity and magnitude of MI is also found. This follows for the upcoming results as well. For Method 2, the number of MIs are roughly 3 times more when a 15 min time-basis are used. The total BESS capacity needed is in the range of 1200 - 1900 MWh for a 60 min time-basis and 240 - 480 MWh for a 15 min time-basis when method 2 is used and the BESS is sole voltage regulating unit.

### Method 3

Apart from the parameters in Method 2, $SOC_H$, $SOC_L$, Method 3 also contains the high and low SOC-target, $SOC_{T\_L}$ and $SOC_{T\_H}$ respectively. As earlier mentioned, they have both been set to the same levels as the NOB limits. The sets of parameters used are as stated in Table 5.5. Table 5.6 shows the results.

**Table 5.5:** Method 3, Simulation parameters - The table shows the parameter settings that have been used for the simulations. The scenarios include varying the Elbas time-basis ($\Delta t$) as well as the forecast error (BC and WC).

| **Ref** | $\Delta t$ [min] | Scenario | $SOC_H$ | $SOC_L$ | $SOC_{T\_H}$ | $SOC_{T\_L}$ | $P_{MI_{max}}$ [MW] |
|---|---|---|---|---|---|---|---|
| **1** | 60 | BC | 0.65 | 0.4 | 0.65 | 0.4 | 300 |
| **2** | 60 | WC | 0.65 | 0.4 | 0.65 | 0.4 | 300 |
| **3** | 15 | BC | 0.65 | 0.4 | 0.65 | 0.4 | 300 |
| **4** | 15 | WC | 0.65 | 0.4 | 0.65 | 0.4 | 300 |

**Table 5.6:** Method 3, Results when $T_{grid} = 0\%$ - The table shows the result of the simulation scenarios.

| **Ref** | $C_b$/unit [MWh] | $P_{MI\_sell_{nbr}}$ | $P_{MI\_sell_{mean}}$ | $P_{MI\_buy_{nbr}}$ | $P_{MI\_buy_{mean}}$ | $SOC_{nbr}$ |
|---|---|---|---|---|---|---|
| **1** | 600 | 1616 | 128 | 718 | 156 | 78 |
| **2** | 950 | 1458 | 194 | 770 | 246 | 57 |
| **3** | 120 | 5531 | 73 | 196 | 119 | 81 |
| **4** | 240 | 4450 | 157 | 1395 | 225 | 42 |

When Method 3 is used a higher number of MI can be noticed compared to Method 2. However, the average magnitude is lower.

### 5.3.3 Results when the AC-grid supports with voltage regulation

In this section, the BESS capacity for Method 1 and Method 2 have been minimized when $T_{grid} \approx 3$ %, i.e the AC-grid is performing voltage control 3% of the year. 3 % is an arbitrary percentage giving a high enough self-sufficiency in terms of voltage regulation without completely isolating the DC-system. Method 3 has again been simulated with the same BESS capacity as Method 2.

The parameters are as stated above with the addition of the fixed discharge and charge rate ($P_{fixed}$). The parameter is decided based on the BESS capacity in each case. The normal setting is 75 MW but is larger for very large BESS and smaller for very small BESS. Since the results in this part will include both data related to MI and data related to voltage regulation, the results have been divided into two tables.

#### Method 1

Table 5.7 states the reference, $ref$ for each set of parameters and scenarios as well as the discharge and charge power, $P_{fixed}$. Table 5.8 shows the results related to the voltage regulation and Table 5.9 shows the results related to the MI.

**Table 5.7:** Method 1, Additional simulation parameters when $T_{grid} \approx 3$ % - The table shows the parameter settings that have been used for the simulations. The parameter settings are the same as in previous tables, however with the addition of the discharge and charge power $P_{fixed}$.

| **Ref** | $C_b$/unit [MWh] | $P_{fixed}$ [MW] |
|---|---|---|
| **1** | 575 | 75 |
| **2** | 1125 | 150 |
| **3** | 65 | 40 |
| **4** | 225 | 75 |

**Table 5.8:** Method 1, Part 1 of the results when $T_{grid} \approx 3\%$ - The table shows the results related to the voltage regulation as well as the number of SOC-cycles.

| **Ref** | $C_b$/unit [MWh] | $T_{grid}$ [%] | $E_{grid}$ [%] | $T_{mean}$ [h] | $Vreg_{nbr}$ | $SOC_{nbr}$ |
|---|---|---|---|---|---|---|
| **1** | 575 | 2.9 | 6.5 | 1.6 | 158 | 654 |
| **2** | 1125 | 3.1 | 7.8 | 1.7 | 164 | 495 |
| **3** | 65 | 2.9 | 6.9 | 0.6 | 381 | 1822 |
| **4** | 225 | 3.1 | 7.5 | 0.8 | 363 | 1096 |

As seen, when the time-basis is shorter the average time the AC-grid is performing the voltage regulation becomes shorter, however with a higher number of occurrences. The total BESS capacity needed is in the range of 1150 - 2250 MWh for a 60 min time-basis and 130 - 450 MWh for a 15 min time-basis when method 1 is used and the AC-grid supports with voltage regulation.

**Table 5.9:** Method 1, Part 2 of the results when $T_{grid} \approx 3\%$ - The table shows the results related to the MI.

| **Ref** | $C_b$/unit [MWh] | $P_{MI\_sell_{nbr}}$ | $P_{MI\_sell_{mean}}$ | $P_{MI\_buy_{nbr}}$ | $P_{MI\_buy_{mean}}$ |
|---|---|---|---|---|---|
| **1** | 575 | 2247 | 91 | 1178 | 96 |
| **2** | 1125 | 2171 | 97 | 1131 | 105 |
| **3** | 65 | 7874 | 65 | 1974 | 72 |
| **4** | 225 | 7960 | 75 | 2481 | 84 |

### Method 2

Table 5.10 states the reference case, BESS capacity and the charge and discharge power ($P_{fixed}$), as earlier described. The results related to the Voltage regulation are presented in Table 5.11 and the results related to the MI in Table 5.12.

**Table 5.10:** Method 2, Parameters when $T_{grid} \approx 3\%$ - The table shows the parameter settings that have been used for the simulations. The parameter settings are the same as in previous tables, however with the addition of the discharge and charge power $P_{fixed}$.

| **Ref** | $C_b$/unit [MWh] | $P_{fixed}$ [MW] |
|---|---|---|
| **1** | 180 | 75 |
| **2** | 240 | 75 |
| **3** | 30 | 40 |
| **4** | 45 | 40 |

**Table 5.11:** Method 2, Part 1 of the results when $T_{grid} \approx 3\%$ - The table shows the results related to the voltage regulation as well as the number of SOC-cycles.

| **Ref** | $C_b$/unit [MWh] | $T_{grid}$ [%] | $E_{grid}$ [%] | $T_{mean}$ [h] | $Vreg_{nbr}$ | $SOC_{nbr}$ |
|---|---|---|---|---|---|---|
| **1** | 180 | 3.0 | 6.2 | 0.9 | 286 | 945 |
| **2** | 240 | 2.9 | 5.9 | 1.3 | 194 | 650 |
| **3** | 30 | 3.1 | 9.5 | 0.5 | 533 | 1808 |
| **4** | 45 | 3.0 | 6.2 | 0.8 | 340 | 1089 |

The total BESS capacity needed is in the range 360 - 480 MWh for a 60 min time-basis and 60 - 90 MWh for a 15 min time-basis when method 2 is used and the AC-grid supports with voltage regulation.

**Table 5.12:** Method 2, Part 2 of the results when $T_{grid} \approx 3\%$ - The table shows the results related to the MI.

| **Ref** | $C_b$/unit [MWh] | $P_{MI\_sell_{nbr}}$ | $P_{MI\_sell_{mean}}$ | $P_{MI\_buy_{nbr}}$ | $P_{MI\_buy_{mean}}$ |
|---|---|---|---|---|---|
| **1** | 180 | 3254 | 96 | 1672 | 131 |
| **2** | 240 | 3280 | 128 | 1838 | 179 |
| **3** | 30 | 12866 | 36 | 1527 | 56 |
| **4** | 45 | 13769 | 66 | 5498 | 95 |

**Method 3**

The discharge and charge power is the same as for Method 2. Table 5.13 shows the results related to the voltage regulation and Table 5.14 shows the results related to the MI.

**Table 5.13:** Method 3, Part 1 of the results when $T_{grid} \approx 3\%$ - The table shows the results related to the voltage regulation as well as the number of SOC-cycles.

| **Ref** | $C_b$/unit [MWh] | $T_{grid}$ [%] | $E_{grid}$ [%] | $T_{mean}$ [h] | $Vreg_{nbr}$ | $SOC_{nbr}$ |
|---|---|---|---|---|---|---|
| **1** | 180 | 3.8 | 7 | 1.0 | 329 | 1167 |
| **2** | 240 | 3.3 | 6.2 | 1.4 | 212 | 926 |
| **3** | 30 | 3.9 | 10.9 | 0.5 | 659 | 2063 |
| **4** | 45 | 3.3 | 6.5 | 0.7 | 397 | 1429 |

**Table 5.14:** Method 3, Part 2 of the results when $T_{grid} \approx 3\%$ - The table shows the results related to the MI.

| **Ref** | $C_b$/unit [MWh] | $P_{MI\_sell_{nbr}}$ | $P_{MI\_sell_{mean}}$ | $P_{MI\_buy_{nbr}}$ | $P_{MI\_buy_{mean}}$ |
|---|---|---|---|---|---|
| **1** | 180 | 3822 | 76 | 2027 | 97 |
| **2** | 240 | 3720 | 106 | 2233 | 137 |
| **3** | 30 | 14394 | 32 | 2189 | 38 |
| **4** | 45 | 14851 | 59 | 6458 | 78 |

Similar to the result when $T_{grid} = 0$, a larger number of MIs but with a lower magnitude is noticed compared to Method 2.

## 5.4 Analysis of performance

### 5.4.1 Elbas time-basis dependency

The first thing to be noticed is the major reduction in BESS capacity when the 15 min time-basis is introduced. This follows for all methods. For Method 1 the BESS capacity is roughly 3-10 times less depending on the scenario and if the AC-grid is allowed to voltage regulate or not. This figure for Method 2 and 3 are roughly 4-6 times. The result is somewhat expected since the calculated market values for each OCP as described in section 4.2.1 give a much smaller power unbalance as seen in Figure 4.9. The number of MI get substantially more when a shorter time-basis is used. However, the figure is roughly 4 times as many compared to the 60 min time-basis. This corresponds to an equal share of the powerhours used over the year. Furthermore, the result for 15 min time-basis with no FC error gives an outstanding result for all simulations. This has been found to be due to symmetry in the power unbalance. The power unbalance generally consists of one positive and one negative spike of similar magnitude for each time-basis, as can be noticed in Figure 5.2.

### 5.4.2 AC-grid dependency

By comparing the results from section 5.3.2 to section 5.3.3, it can be found that the BESS capacity can be heavily reduced. Sizing the BESS after the top requirement is shown to require very large units. By allowing the AC-grid to perform the voltage regulation 3 % of the time, the total BESS capacity can be reduced by 2-4 times for Method 1 depending on the scenario and time-basis and 3-6 times for Method 2 and 3. This utilization of the AC-grid can be compared to when an ESS is utilized to perform peak shaving. As discussed in section 2.5.4, peak shaving is when an ESS is used to reduce the peak energy use at certain high demanding hours in the AC-grid. With that, the system does not have to have a rated max capacity according to some few high demanding situations.

**Table 5.15:** Rough estimate on how the BESS capacity depend on the AC-grid dependency

| $C_b$/unit [MWh] | $T_{grid}$ % |
|---|---|
| 30 | 3.9 |
| 45 | 1.4 |
| 60 | 0.7 |
| 75 | 0.3 |
| 120 | 0 |

When considering the dependency on the AC-grid it is also important to consider the evaluation parameter deciding the total amount of regulation energy that the AC-grid is using ($E_{grid}$). For all methods and scenarios, this percentage is roughly two or three times larger (6-11 %) than the corresponding $T_{grid}$ percentage. This highlights the high demanding situations when the AC-grid has to voltage regulate the system. Furthermore, by evaluating the $V_{reg}$-parameter it can be seen that the number of times for the full year that the AC-grid voltage regulates the system are between 158-328 times when a 60 min-basis are used and 340-552 times when a 15min time-basis are used. That is equivalent to roughly 0.5-2 times a day at an average of 30-100 minutes per occasion. No further analysis about at what time of the day this usually occurs have been performed.

### 5.4.3 SOC-cycles

The number of SOC-cycles are very roughly estimated and can thereby only hint towards the actual truth. The BESS capacity for Method 1 when $T_{grid} \approx 3$ % and Method 2 and 3 when $_{grid} = 0$ is fairly similar. By comparing the number of SOC-cycles it can be seen that Method 2 and 3 performs much better than Method 1. Additionally, Method 2 performs better than Method 3 for all scenarios. This is most likely due to Method 3 using higher SOC-targets and is thereby more inclined to reach a SOC-cycle trigger. Generally, the number of SOC-cycles corresponds to the BESS capacity, where a smaller capacity gives a higher number of SOC-cycles. Since the number of SOC-cycles in the result are very high the predicted lifetime of the BESS gets shorter according to Figure 2.17. Further simulations to estimate

the dependency on the BESS size have been made for the worst performing scenario and method. This is Method 3 when a 15 min time-basis has been used with no FC error. The result is as in table 5.16.

**Table 5.16:** Rough estimate on how the number of SOC-cycles depend on BESS capacity

| $C_b$/unit [MWh] | $SOC_{nbr}$ |
|---|---|
| 30 | 2063 |
| 45 | 1035 |
| 60 | 392 |
| 75 | 305 |
| 120 | 81 |

As the table indicates the number of SOC-cycles has an exponential relationship to the capacity in BESS.

### 5.4.4 Comparing Method 1 to Method 2 and 3

Method 1 and Method 2 and 3 differ vastly in the complexity of the implementation. While Method 1 is very easy to implement, it does non-beneficial decisions frequently. Method 2 and 3 are far superior than Method 1 both when the evaluation parameter $T_{grid}$ is 0% and 3%. The BESS capacity for Method 1 when 3% AC-grid voltage regulation is allowed is fairly similar to the BESS capacity for Method 2 and 3 when no AC-grid voltage regulation is allowed. This result is as expected. However, the method does solve the initial problem stated in Figure 2.7 where the energy surplus and deficit over long times are mitigated. No further analyses have been made since the Method performs very poorly compared to Method 2 and 3.

### 5.4.5 Comparing Method 2 to Method 3

The results for the two methods are very similar at first sight. The main difference in implementation between the methods is that Method 3 is using the predicted SOC-value for one extra time-basis forward to decide whether it is desirable to regulate SOC to a higher or lower value, while the target for Method 2 is always the centre of the usable capacity. This difference is illustrated with an example in Figure 5.10.

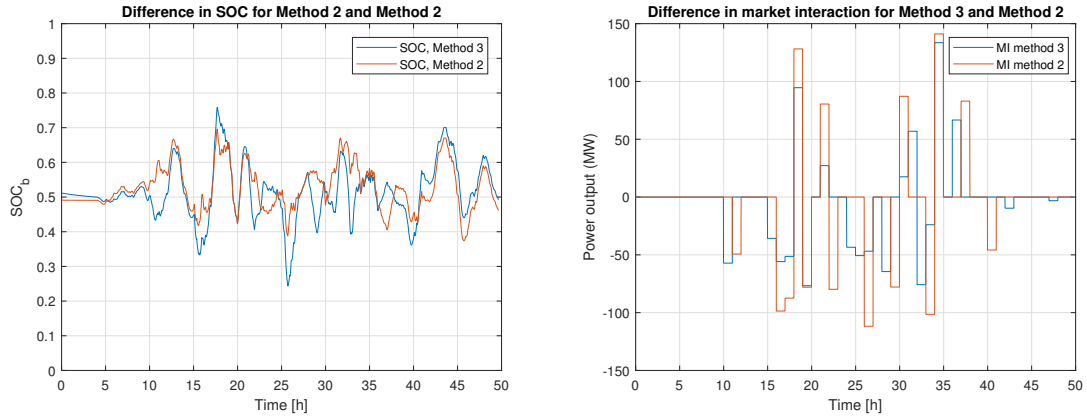


**(a)** **(b)**

**Figure 5.10:** Difference in functioning of Method 2 and Method 3

At t = 10-11: Method 3 decides at an earlier time that an MI bringing down the SOC is desirable. The outcome from this scenario is similar, however with a slightly lower MI from Method 2. This scenario is repeated at t = 36-37. At t = 15-19: Method 3 decides one time-unit earlier that an MI that decreases the SOC is beneficial. Because of this, lower magnitudes are needed for the rest of the period. However, it can be seen that the SOC-value are closer to the outer limits of the usable capacity. This case repeats at t = 24-26. At time 21-22: A smaller positive MI with $SOC_{T\_L}$ as the target for Method 3 leads to no MI is needed at time t = 22. Method 2 is, in this case, counteracting the change in both cases leading to larger MIs. A similar scenario happens at t = 30-35.

### AC-grid dependancy

The $T_{grid}$-parameter from the results indicates that a slightly higher BESS capacity would be needed for Method 3 to reach the target of 3 %. In relation to that, the AC-grid has to perform the voltage regulation a higher number of times for Method 3 compared to Method 2. Logically Method 3 should be less AC-grid dependent since it directs the SOC-towards a higher value when an underproduction is predicted and vice versa. This has not been the case. One reason for this is due to no consideration of the power balance within the measurement points are taken. Simulations have shown that the number of times Method 3 prevents $SOC_b$, for instance, from reaching $SOC_{min}$ due to a higher SOC-target than Method 2 have been far fewer than the number of times $SOC_b$ have reached $SOC_{max}$ due to the higher SOC-target. Figure 5.10 indicates this behaviour.

### Market interaction

The main difference between the methods is the number of MIs, with Method 3 having a larger amount. The higher number has to do with the extra condition that has to be met at time t+2. While $SOC_b$ only has to be within the NOB at time t+1 for Method 2, it has to be within the NOB both at time t+1 and t+2 for Method

3. However, the distribution of the magnitude of the MIs differs vastly between the methods. A histogram showing this for the two methods both when the time-basis is 60 min and 15 min is presented in Figure 5.11a and 5.11b, respectively.

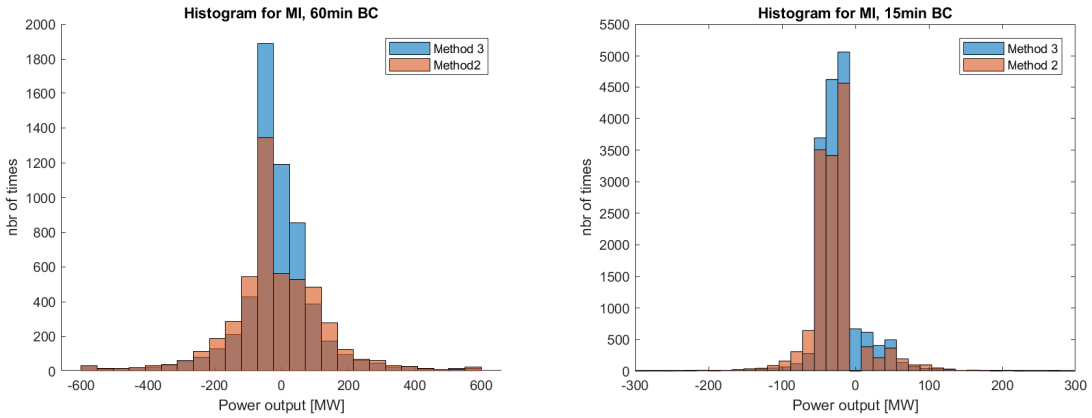


**(a)** **(b)**

**Figure 5.11:** Histogram of magnitude of market interaction for Method 2 and 3 - A negative value equals a selling of energy and a positive a buying of energy. The darker orange bars indicate the same number and magnitudes of the MI. The blue colours indicate MI for Method 3 and the brighter orange the MIs for Method 2.

As seen in the figures, Method 3 requires a higher number of MIs but with a smaller magnitude than Method 2. This is true regardless of time-basis. From a regulation point of view, this indicates a more conservative strategy, and are a desired feature. For the very large magnitudes, the number of times seems to be equal for both methods. Another interesting figure is that of the total energy being transferred due to the MI for the two methods. A breakdown of the MI for the two methods when $T_{grid} \approx 3\%$ are presented in table 5.17.

**Table 5.17:** Energy sold and bought from the intraday market

| Scenario | $E_{sold}$ [GWh] | $E_{bought}$ [GWh] | $E_{diff}$ [GWh] | $E_{sum}$ [GWh] |
|---|---|---|---|---|
| 60 min $\Delta t$ BC Method 2 | 312.4 | 219.0 | 93.4 | 531.4 |
| 60 min $\Delta t$ BC Method 3 | 290.4 | 196.6 | 93.8 | 487.0 |
| 60 min $\Delta t$ WC Method 2 | 419.8 | 329.0 | 90.8 | 748.8 |
| 60 min $\Delta t$ WC Method 3 | 394.3 | 305.9 | 88.4 | 700.2 |
| 15 min $\Delta t$ BC Method 2 | 115.8 | 21.4 | 94.4 | 137.2 |
| 15 min $\Delta t$ BC Method 3 | 115.1 | 20.7 | 94.4 | 135.8 |
| 15 min $\Delta t$ WC Method 2 | 227.2 | 130.6 | 96.6 | 357.8 |
| 15 min $\Delta t$ WC Method 3 | 219.0 | 125.9 | 93.1 | 344.9 |

From Table 5.17 it can be seen that the difference in energy ($E_{diff}$) is as expected more or less the same for all scenarios. It can also be seen that Method 2 is selling more energy to the market, but also buying more. This confirms that the regulation for Method 2 is much more aggressive than that of Method 3. The sum of the bought and sold energy ($E_{sum}$) shows that for all scenarios Method 2 requires a

substantial amount more energy to be transferred in the DC-grid to uphold the stability. Because of the more and higher magnitude of the power being transferred in the DC-grid, a larger percentage of the cable capacity will be used for regulation purposes.

# Chapter 6

# Discussion and Conclusions

---

*This chapter comprises the discussion related to the control methods, its robustness and uncertainties as well as the general strategy of using a BESS as primary controller in a DC-grid.*

---

## 6.1 Discussion

### 6.1.1 Control strategies

As the results show, by utilizing voltage regulation in combination with the control methods for interacting with the intraday market both the short and long term power discrepancies in the DC-grid are mitigated. However, by comparing the BESS capacity needed, to reach both the target of partial and full internal voltage regulation in the DC-system, a major difference between the more simple Method 1 and more complex Method 2 and 3 are found. Since Method 1 base an MI one time-unit forward on exclusively the current SOC-value, this result was expected. The fluctuations from the WPPs have shown to be too uncertain to use this method. Considering this, it is fair to argue that either Method 2 or Method 3 is preferred for solving the initial challenge of regulating the DC-grid under the circumstances in this report. While Method 2 and 3 would require an MI at roughly half of the possible occasions during the year for both time-basis, the average power setpoint of the MIs is rather low. Calculating this with maximum FC error for the 60 min time-basis this figure is 146 MW for Method 2 and 117 MW for Method 3. That equals less than 5% of the rated cable capacity since two BESSs are used. If instead calculated as an estimate over the full year the figure is 85 MW for Method 2 and 80 MW for Method 3, or close to 2.5% of the cable capacity. Reducing the time-basis to 15 min, the figure would be roughly half of this. However, since the simulations have been performed for the full year, the resolution has been less than ideal. Method 2 and 3 have been strongly dependent on the upcoming energy balance in the system. While the data this has been calculated from had the exact answer, this has not been utilized fully. Only four segments for the midpoint rule have been considered to speed up simulations. That means that the predicted SOC-value for one time-unit forward has a built-in error even for the best case scenario when no additional

forecast error is used. Since the SOC-value at further time-units forward is based on this, the error multiplies. Additionally, the power balance in the DC-system is based on the power output from the WPPs and OCPs at the connection point to the system. Thereby not considering the losses in the transmission lines. However, all of these have been seen as reasonable simplifications to test out the function of the control strategies.

### Robustness

When implementing a control method the robustness is of utmost importance. Since Method 1 only observes the current SOC-level and no consideration to future forecasts are needed the method is very robust. Method 2 and 3 are theoretically also robust since continuous calculations are performed to find if an MI is needed and to what extent. However, since the implementation in this work has been limited to only consider a certain amount of measurement points, e.g four segments for the midpoint rule, and only the SOC at time t+1 and t+2, the robustness has been suffering. While Method 3 has shown great potential in terms of a better strategy related to deciding the MIs it does not perform as well as expected when it comes to reducing the BESS capacity and AC-grid dependency. Logically, directing the SOC towards a higher value when an underproduction is predicted should decrease the risk of depleting. Since Method 3 both gives a larger amount of times and a longer total length of the year that the AC-grid has to perform the voltage regulation this has proved not to be the case. One explanation is that even though the predicted energy balance might be within the margins of error, no consideration of what the actual power curve looks like are taken. Assume, for instance, an underproduction for time t+2 until t+3 are predicted and the SOC-value $SOC_{t+2}$ is directed towards a high SOC-target. If the power balance, although correctly predicting an energy deficit for the time-basis, is giving a high power surplus at the beginning of the time-basis, the risk of reaching the maximum SOC-limit is increased. Because of this, the positive effects are cancelled out. This has been seen when studying the difference in performance between Method 2 and Method 3. A solution that should increase the robustness is to track the predicted SOC-value in real-time. Then, if at any point in time the SOC is predicted to reach the outer limits, the SOC-target for the MI should be set to a different value that diminishes this risk. Another solution is simply to decrease the width of the NOB. However, the more it is decreased, the less positive effects Method 3 will have on the MI.

### Increasing the time-span

The methods are gradually increasing the time-span considered, where for Method 1 only the present time is considered, for Method 2 two time-units forward are considered and for Method 3 three time-units forward are considered. The logical next step for this strategy is to implement one or more time-units further. While this is something that has not been performed in this work, it could potentially improve the MI further. If knowing the energy balance for one additional time-unit, $SOC_{t+3}$ could be directed to a more beneficial value, instead of the centre of the usable capacity. However, since the power balance is constantly fluctuating, it would

require even more knowledge about the predicted SOC-value to not reach the outer limits. Additionally, it would increase the complexity of the implementation since more possible scenarios would need to be considered. Complexity is a feature that is far from desired in this kind of applications. Furthermore, the MI can only be realized for the next time-unit. Thereby, knowledge about the energy balance in the DC-system at a long time forward might not make any difference in outcome. This is because the addition of intraday market from elsewhere will not be known until the latest one time-unit before the powerhour.

#### Decreasing the response time

The planned decrease of the Elbas intraday market time-basis from 60 min to 15 min have shown in this report to have a major impact on the result. Firstly, it has been shown that the power discrepancy with a large share of electricity from RES is decreased with the shorter time-basis. This, in turn, has made the BESS capacity needed for primary control in the DC-system much smaller. Relating this result to the primary control in the AC-grid, it would be logical to expect a similar outcome. By decreasing the time-basis it should mean that the primary reserve in the AC-grid could be sufficient for a longer time even though the share of intermittent electricity production increased. Continuing, by decreasing the time-basis, it can be seen as a decrease of the response time of the secondary storage since this storage is the AC utility grid in this work. If the time-basis would decrease even further, it would be logical to expect that even smaller BESS capacities would be needed for the primary control. It might not be reasonable to expect the Elbas time-basis to decrease lower than 15 min in the near future. But a small physical secondary storage with the right characteristics to complement both the BESS and the MI could be a solution to further decrease the BESS capacity. However, this has not been touched upon in this work.

### 6.1.2 Sizing and design

Firstly, while both Method 2 and 3 shows great results in terms of MI and AC-grid dependency even for smaller BESS, the number of SOC-cycles, although very roughly estimated, shows that the lifetime of them will not be very long. By comparing the results and Figure 2.17 it can be seen that for 0.3 DoD, which is the SOC-range considered, roughly 10 000 cycles can be expected. Since the results show that each BESS does roughly 1000-2000 cycles when the BESS capacity is minimized, they have a lifetime of closer to 5-10 years. It should be said, however, that the actual lifetime of Lithium-ion batteries has not been determined with certainty. While the usable capacity might decrease with deeper and more SOC-cycles, the batteries might be usable for far longer than the graph shows.

Secondly, while the objective of this report is not to explicitly determine what size of BESS is needed to implement this system, a few key points can be taken. By weighing in the result in section 5.4.3 about how the number of SOC-cycles depend on the BESS capacity, it is highly possible that the minimum BESS capacity from an economic point of view differs from the minimum BESS capacity from a theoretical

point of view. Theoretical in this case meaning fulfilling the requirement of 3% AC-grid dependency. Assuming the worst case scenario for a 15 min time-basis and with a doubled BESS capacity to increase the predicted lifetime to closer to 20 years. Then two BESS each with 90 MWh capacity would be needed. With this as the standpoint, a few questions related to the implementation can be answered.

### Physical implementation

As mentioned earlier in the report, reusing battery packs from the vehicle industry is a both economic, technical and environmentally viable option. Assuming the battery packs of today's vehicle industry will be used in the implementations in 10 years. Modern battery packs for vehicle applications have reached a capacity of 100 kWh as previously mentioned. For two BESS of 90 MWh, a total number of 900 battery packs of said capacity would be needed for each unit. Approximating that each battery pack holds roughly $0.15m^3$ of volume, then a total volume of $135m^3$ would be needed. Further, assuming that only 10% of the volume in a 40 ft shipping container could be used due to cooling and other equipment, a total of 20 containers would be needed for each BESS. Comparing the estimation to a project by Vattenfall, where 16.5 MWh of battery packs were fitted in five shipping containers [60], the figure seems to be in the right range. Considering the total size of the WPP cluster, the physical size of the BESS is thereby very small.

### Cost of implementation

By assuming above conditions a very rough estimate of the investment cost can be made. The figures used in this approximation are from similar projects and should only be seen as a hint towards the actual cost. To implement the BESS, cables with a rated capacity of 1.5 GW, battery packs and a DC/DC converter are needed. Assuming that the BESS has a technical capacity of providing 1.5 GW of power, then the DC/DC converter would need the same rated output. These converters have never been implemented in any project today, thereby no price information exist. However, comparing DC/DC with DC/AC for other projects, it has been found that DC/DC is usually cheaper. A 30% lower cost of DC/DC than DC/AC has been assumed. Furthermore, the increase in cost between a 1 GW converter and a 1.5 GW converter has been assumed to not have a linear price increase. An increase of 25% more expensive has been calculated for. It should also be noted that the figure is from the BritNed project, and is thereby roughly 10 years old.

**Table 6.1:** Rough estimate on the cost of investment of BESS

| Cost item | Cost/unit | Nbr of units | Total cost [MSEK] |
|---|---|---|---|
| Battery pack | 150 kSEK[61] | 1800 | 270 |
| Cables | 7 MSEK [62] | 5 km | 35 |
| DC/DC converter | 1900 MSEK [63] | 2 | 3800 |
| **Total** | | | **4105** |

In this work, maximum power outputs from the BESS of 800 MW have been noticed.

If this is technically possible or not for the BESS capacity determined in this report is outside of the scope of this work. However, assuming the DC/DC converter would only need to be rated for this, the price could be assumed to be slightly lower. No matter what, the BESS capacity could easily be larger without substantially incurring on the total price.

A development of the Swedish power grid would be an alternative to installing an ESS to handle the increase in intermittent electricity production. While a refurbishment is inevitable even with the ESS, the width of it could be less. According to Svenska kraftnät, the refurbishment is strongly dependent on how much intermittent electricity production is installed as well as where it is installed [38]. In this case, the DC-system is very far from the closest primary controlling hydropower plant. Assuming the distance to this hydro plant is somewhere in the range of 1000 km, an estimate of the cost for strengthening the grid can be found. Svenska kraftnät estimates that 1 km AC 400 kV transmission line cost 7 MSEK to build and install [62]. If only one transmission line is calculated for this leads to a cost of 7000 MSEK. As seen in the challenges, the fluctuations are sometimes above 1.5 GW, meaning that two transmission lines likely would be needed. While this might not automatically incline that the price will be double, the figure would at least be above 7000 MSEK. Additionally, if 1.5 GW of power should be mitigated, the current 600 MW of primary reserve will not be near enough. This entails a large and expensive development of hydropower or likewise.

Comparing the two figures it can be seen that installing two BESS units for mitigating the fluctuations would be an economically superior option. To continue on this reasoning, while the HVDC technology and Lithium-ion Batteries are fairly new and under extensive development, these prices are expected to decrease. The HVAC, on the other hand, are more matured and thus have more stabilized prices.

### Implementation in DC or AC-grid

The BESS in the simulations of this work has been implemented in the DC-system. By implementing it in the DC-system the cost is decreased since DC/DC converters of needed capacity are less expensive than the corresponding DC/AC converter. The BESS can provide ancillary services for both the DC-system and the AC-system in normal operation no matter where it is implemented. However, when DC-connected and a fault in the DC-system occurs, it cannot give any power to help preventing a voltage-dip and blackout to the AC utility grid. However, if a DC-breaker is installed at a strategic place in the DC-system so that the multiterminal connection act as a two-terminal connection, at least one line would continue to function. If an additional DC-breaker is installed on the DC-grid side of the BESS, the BESS on the faulty line could still continue to provide the AC-grid with power to prevent a power outage. Implementing extra DC-breakers is not a desirable option right now because of the high cost. If connected to the AC-grid, the BESS can always discharge for a period of time depending on its fullness until the secondary control has started. This would be of great service for the rest of the AC utility grid. However, further incentives related to this implementation would come with an enhancement of the ancillary services market.

## 6.2 Concluding remarks

In this work, the possibility of using a BESS to perform the primary control in a DC-grid with 4.8 GW installed capacity of wind power was discussed. The proposed strategy of letting a BESS perform the primary control by DC-droop voltage regulation initial problem regarding the balancing of the DC-grid with no or very little AC utility grid dependency. Additionally, by utilizing different control methods regarding the intraday market interactions the problem regarding the large storage capacity needed has been solved. Simulations for different scenarios with the different market interaction methods created have led to a few conclusions.

The methods created have differed greatly in terms of complexity with the parameters used ranging from current data only to predicted data for three time-units forward. While the very simple Method 1 has solved the initial problems, a method where forecasts for the upcoming power balance is used has shown more potential. The more complex Method 2 and 3 have outperformed the very simple Method 1 in all aspects. Method 3 has performed better than Method 2 in terms of MI, where the total amount of energy transferred due to regulation has been reduced. This is of large benefit since it is desirable that less of the cable capacity is utilized for regulating purposes. Method 2 has performed better when it comes to the dependency on the AC-grid for voltage regulation, which has opposed the expectations. Further research of Method 3 where the predicted future SOC-value are measured in real-time with higher resolution could improve the result.

Allowing some AC-grid dependency has vastly decreased the capacity of the BESS for all methods. However, the allowance-limit of 3% of the year related to the amount of time the AC-grid is performing the primary control has shown to require the BESS to go through more SOC-cycles than desired. From an economic point of view, a larger capacity is likely to be beneficial. This would, in turn, drive down the AC-grid dependency even further.

The time-basis of the Elbas intra-day market is another highly important factor. While this time-basis has already been decreased to 15 min in certain areas in Europe, it is necessary to be changed in others as well to allow the intermittent electricity generation to increase. This report has shown that the BESS capacity needed to provide the system with primary control has been largely dependent on the time-basis.

## 6.3 Future work

Since the work in this Master thesis has been based on one specific scenario, the range of future work is wide.

Firstly, Method 2 and 3 are the two methods showing the greatest potential. Since Method 3 requires much higher resolution of the future predicted SOC-value to reach its full potential, this would be a good starting point as a continuation of the work in this Master thesis. Continuing on this, evaluating the need for considering more time-units for the market interaction would be interesting.

Secondly, At times when the DC-grid is dependent on the AC-grid for voltage regulation, the systems are vulnerable since the fluctuations are very large. Thereby, decreasing the AC-grid dependency is always desirable. Implementing a physical secondary energy storage, like a hydrogen storage, could improve reliability. Another interesting strategy to test would be to always let the AC-grid perform a small share of the voltage regulation to potentially decrease the maximum fluctuations.

Thirdly, This work has considered a largely underused system with no trans-boundary market. With large HVDC-transmission lines connecting three countries, the ability to increase the market between these exist and is desired. With an increased market interaction, the use of the transmission lines would be heavily increased. However, since the primary regulation in the DC-grid is of utmost importance, a priority schedule between trans-boundary market as well as MI from the BESS would be needed.

Fourthly, In this work, the BESS has been directly connected in the DC-system. Thus, the BESS can only provide primary control to the DC-system. Future work in this field could include connecting the BESS to the AC-system to see what advantages this could have for both the DC-system and the AC-grid. For instance, when no ancillary services are needed in the DC-grid, the BESS could provide for the AC-grid instead.

Fifthly, the economic calculations in this work have been very roughly estimated. Proper work in this field would be needed to appropriately decide the cost of the investment and the profitability of the implementation. Related to this both the economics of the intraday market and the ancillary services market are areas that have not been touch upon in this work but would be needed to decide its economic profitability.

# Bibliography


[1] United Nations. *What is the Paris Agreement?* 2018. URL: https://unfccc.int/process-and-meetings/the-paris-agreement/what-is-the-paris-agreement. (accessed: 23.10.2018).

[2] IRENA. *Renewable capacity statistics 2018*. Abu Dhabi: International Renewable Energy Agency (IRENA), 2018.

[3] A. Berglund. *Markbygden - Svevind*. 2018. URL: https://svevind.se/Markbygden. (accessed: 23.10.2018).

[4] Svenska Kraftnät. *TSO:erna bekräftar ändring från 60 minuter till 15 minuters avräkningsperiod*. 2018. URL: https://www.svk.se/om-oss/nyheter/elmarknad-allmant/tsoerna-bekraftar-andring-fran-60-minuter-till-15-minuters-avrakningsperiod/. (accessed: 23.10.2018).

[5] Q. Wu, Z. Xu, and J. Østergaard. "Grid integration issues for large scale wind power plants (WPPs)". In: *IEEE PES General Meeting*. 2010, pp. 1–6.

[6] Baltic Integrid. *About Baltic InteGrid*. 2018. URL: http://www.baltic-integrid.eu/index.php/about-baltic-integrid.html. (accessed: 23.10.2018).

[7] N. Blazauskas et al. *Towards a Baltic Offshore Grid: connecting electricity markets through offshore wind farms*. 2018.

[8] Fino2. *Meteorological measurements on FINO 2*. 2016. URL: https://www.fino2.de/en/research/meteorology.html. (accessed: 19.03.2019).

[9] Energimyndigheten. *Energiläget 2017*. Bromma, Sweden: Statens Energimyndighet, 2017.

[10] Nordpool. *The Nordic Electricity Exchange and The Nordic Model for a Liberalized Electricity Market*. Lysaker, Norway: Nord Pool Spot AS.

[11] Svenska Kraftnät. *Sydvästlänken*. 2016. URL: https://www.svk.se/natutveckling/stamnatsprojekt/sydvastlanken/om-projektet/?id=649. (accessed: 19.11.2018).

[12] L. Bergman. *De svenska energimarknaderna – en samhällsekonomisk analys*. Stockholm, Sweden: Statens offentliga utredningar, 2014.

[13] R. Scharff and M. Amelin. "Trading behaviour on the continuous intraday market Elbas". In: *Energy Policy* 88 (2016), pp. 544–557.

[14] Nordpoolgroup.com. *Elbas 4*. URL: https://www.nordpoolgroup.com/trading/Intraday-market-Elbas/elbas-4/. (accessed: 28.02.2019).

[15] Vattenfall. *Sverige delas in i elområden*. 2011. URL: https://corporate.vattenfall.se/press-och-media/nyheter/import-nyheter/sverige-delas-in-i-elomraden/. (accessed: 20.11.2018).

[16] Nordel. *Nordic Grid Code 2007*. 2007.

[17] Svenska kraftnät. *Vägledning för anslutning till stamnätet*. Sundbyberg, Sweden, 2016.

[18] ENTSO-E. *Frequency ranges ENTSO-E guidance document for national implementation for network codes on grid connection*. Brussels, Belgium, 2018.

[19] C. Hamon, M. Perninge, and L. Söder. *Frequency Control Operation of Frequency Control Schemes in Power Systems with Large Amounts of Wind Power*. Stockholm, Sweden: Energiforsk AB, 2016.

[20] J. Duncan Glover, S. Sarma, and T. Overbye. *Power System, Analysis and design*. 5th ed. Cengage, 2012, pp. 238–341. ISBN: 81-3151635-0.

[21] S. Persic. "Frekvensreglering i det nordiska kraftsystemet". Master's Thesis. Stockholm, Sweden: Kungliga Tekniska Högskolan, 2007.

[22] P. Kundur. *Power System Stability and Control*. 1st ed. McGraw-Hill Education, 1994, pp. 627–287. ISBN: 978-0070359581.

[23] O. Peake. "The history of high voltage direct current transmission". In: *Australian Journal of Multi-disciplinary Engineering* 8.1 (2010).

[24] Siemens. *Fact Sheet High-voltage direct current transmission (HVDC)*. 2012.

[25] J. Song-Manguelle, S. Gunturi, and M. Harfman Todorovic. "Power Transfer Capability of HVAC Cables for Subsea Transmission and Distribution Systems". In: *IEEE Transactions on Industry Applications* (2014).

[26] ABB. *Why HVDC Economic and environmental advantages - Why choose HVDC over HVAC*. URL: `https://new.abb.com/systems/hvdc/why-hvdc/economic-and-environmental-advantages`. (accessed: 04.12.2018).

[27] F. Wang, L. Bertling, and T. Le. *An Overview Introduction of VSC-HVDC: State-of-art and Potential Applications in Electric Power Systems*. Bologna: Cigré, 2011.

[28] M. Callavik et al. "The Hybrid HVDC Breaker An innovation breakthrough enabling reliable HVDC grids". In: *ABB Grid Systems* nov (2012).

[29] M. Bahrman and B. Johnson. "The ABCs of HVDC Transmission technologies". In: *IEEE power and energy magazine* (2007).

[30] Å. Halvorsdatter Kjørholt. "HVDC Transmission Using a Bipolar Configuration Composed of an LCC and MMC". Master's Thesis. Trondheim, Norway: Norwegian University of Science and Technology, 2014.

[31] T. Vrana et al. "A classification of DC node voltage control methods for HVDC grids". In: *Electric Power Systems Research* 103 (2013), pp. 137–144.

[32] Y. Liu, L. Zhang, and H. Liang. "DC Voltage Adaptive Droop Control Strategy for a Hybrid Multi-Terminal HVDC System". In: *Energies* 12 (2019), pp. 137–144.

[33] W. Fruergaard. *V164-9.5 MW Archives | MHI Vestas Offshore*. URL: `http://www.mhivestasoffshore.com/category/v164-9-5-mw/`. (accessed: 07.03.2019).

[34] J. Manwell, J. McGowan, and A. Rogers. *Wind energy explained : theory, design, and application*. 2nd ed. Wiley, 2009, pp. 4–54. ISBN: 978-0-470-01500-1.

[35] H. Thiesen et al. *The Provision of Synthetic Inertia by Wind Turbine Generators: An Analysis of the Energy Yield and Costs*. 2017.

[36] H. Holttinen, J. Miettinen, and S. Sillanpää. *Wind power forecasting accuracy and uncertainty in Finland*. Espoo, Finland, 2013.

[37] D. Hart, W. Bonvillian, and N. Austin. "Energy Storage for the Grid: Policy Options for Sustaining Innovation". In: (2017).

[38] Svenska Kraftnät. *Anpassning av elsystemet med en Stor mängd förnybar elproduktion*. Sundbyberg, Sweden, 2015.

[39] P. Vanýsek and V. Novák. "Redox flow batteries as the means for energy storage". In: *Journal of Energy Storage* 13 (2017).

[40] IRENA. *Electricity Storage and Renewables: Costs and Markets to 2030*. Abu Dhabi: International Renewable Energy Agency, 2017.

[41] L. Wingren and J. Johnsson. "Battery Energy Storage Systems as an alternative to gas turbines for the fast active disturbance reserve". Master's Thesis. Lund, Sweden: Lund university, 2018.

[42] US Department of energy. *Cost and Price Metrics for Automotive Lithium-Ion Batteries*. Washington DC, USA, 2017.

[43] L. Ahmadi et al. "A cascaded life cycle: reuse of electric vehicle lithium-ion battery packs in energy storage systems". In: *The International Journal of Life Cycle Assessment* (2015).

[44] Tesla. *Model S Specifications*. 2017. URL: `https://www.tesla.com/support/model-s-specifications`. (accessed: 07.12.2018).

[45] H. Berg. *Batteries for Electric Vehicles: Materials and Electrochemistry*. Cambridge University Press, 2015, pp. 83–101. ISBN: 9781316090978.

[46] Greentechmedia. *NEC to Deploy 60MW of Energy Storage in PJM*. URL: `https://www.greentechmedia.com/articles/read/nec-to-deploy-60mw-of-energy-storage-in-pjm#gs.25vwdf`. (accessed: 13.03.2019).

[47] R. Rüther et al. *Strategies for Plug-in Electric Vehicle-to-Grid (V2G) and Photovoltaics (PV) for Peak Demand Reduction in Urban Regions in a Smart Grid Environment*. Springer, Singapore, 2015, pp. 179–219. ISBN: 978-981-287-298-2.

[48] M. Javad Jannati et al. "ADALINE (ADAptive Linear NEuron)-based coordinated control for wind power fluctuations smoothing with reduced BESS (battery energy storage system) capacity". In: *Energy* 101 (2016), pp. 1–8.

[49] A. Suzdalenko and I. Galkin. "Instantaneous, Short-Term and Predictive Long-Term Power Balancing Techniques in Intelligent Distribution Grids". In: *IFIP Advances in Information and Communication Technology* 394 (2013).

[50] L. Valverde et al. "Energy Management Strategies in hydrogen Smart-Grids: A laboratory experience". In: *International Journal of Hydrogen Energy* 41 (2016), pp. 13715–13725.

[51] H. Kanchev et al. “Energy Management and Operational Planning of a Microgrid With a PV-Based Active Generator for Smart Grid Application”. In: *IEEE transactions on industrial electronics* 58 (2011), pp. 4583–4592.

[52] H. Mahmood, D. Michaelson, and J. Jiang. “A Power Management Strategy for PV/Battery Hybrid Systems in Islanded Microgrids”. In: *IEEE journal of emerging and selected topics in power electronics* 2 (2014).

[53] L. Xin et al. “Energy management strategy of battery in isolated micro-grid based on state of charge(SOC)”. In: *7th International Conference on Biomedical Engineering and Informatics* (2014), pp. 879–884.

[54] F. Kbidi et al. “Energy Management System in Micro-Grid with Storage and Hydrogen Production”. In: *IECON 2018 - 44th Annual Conference of the IEEE Industrial Electronics Society* (2018), pp. 5044–5049.

[55] C. Eu-Tjin, C. Huat, and L. Seng. “Control strategies in energy storage system for standalone power systems”. In: *4th IET Clean Energy and Technology Conference* (2016), pp. 1–8.

[56] A. Keeli and R. Sharma. “Optimal use of second life battery for peak load management and improving the life of the battery”. In: *2012 IEEE International Electric Vehicle Conference* (2012), pp. 1–6.

[57] G. Graditi, R. Ciavarella, and M. Valenti. *An Innovative BESS Management for dynamic frequency restoration*. Napoli, Italy: ENEA, 2017.

[58] *Welcome to OpenModelica - OpenModelica*. 2019. URL: `https://www.openmodelica.org`. (accessed: 21.01.2019).

[59] M. Petrollese et al. “Real-time integration of optimal generation scheduling with MPC for the energy management of a renewable hydrogen-based microgrid”. In: *Applied Energy* 166 (2016), pp. 96–106.

[60] *Largest co-located battery installed in the United Kingdom*. 2018. URL: `https://group.vattenfall.com/press-and-media/news--press-releases/pressreleases/2018/largest-co-located-battery-installed-in-the-united-kingdom`. (accessed: 15.03.2019).

[61] C. Curry. *Lithium-Ion battery costs and market*. 2017.

[62] Svenska Kraftnät. *Planerad 400 kV-ledning Nybro - Hemsjö*. Sundbyberg, Sweden, 2017.

[63] Pöyry management consulting. *Western HVDC final funding review*. 2012.

# Appendix A

# Complete models in OpenModelica

Figure A.1 shows the full OpenModelica model before any implementation of the BESS was made. Figure A.2 shows the model after two BESS and two control units (EMS) was implemented.

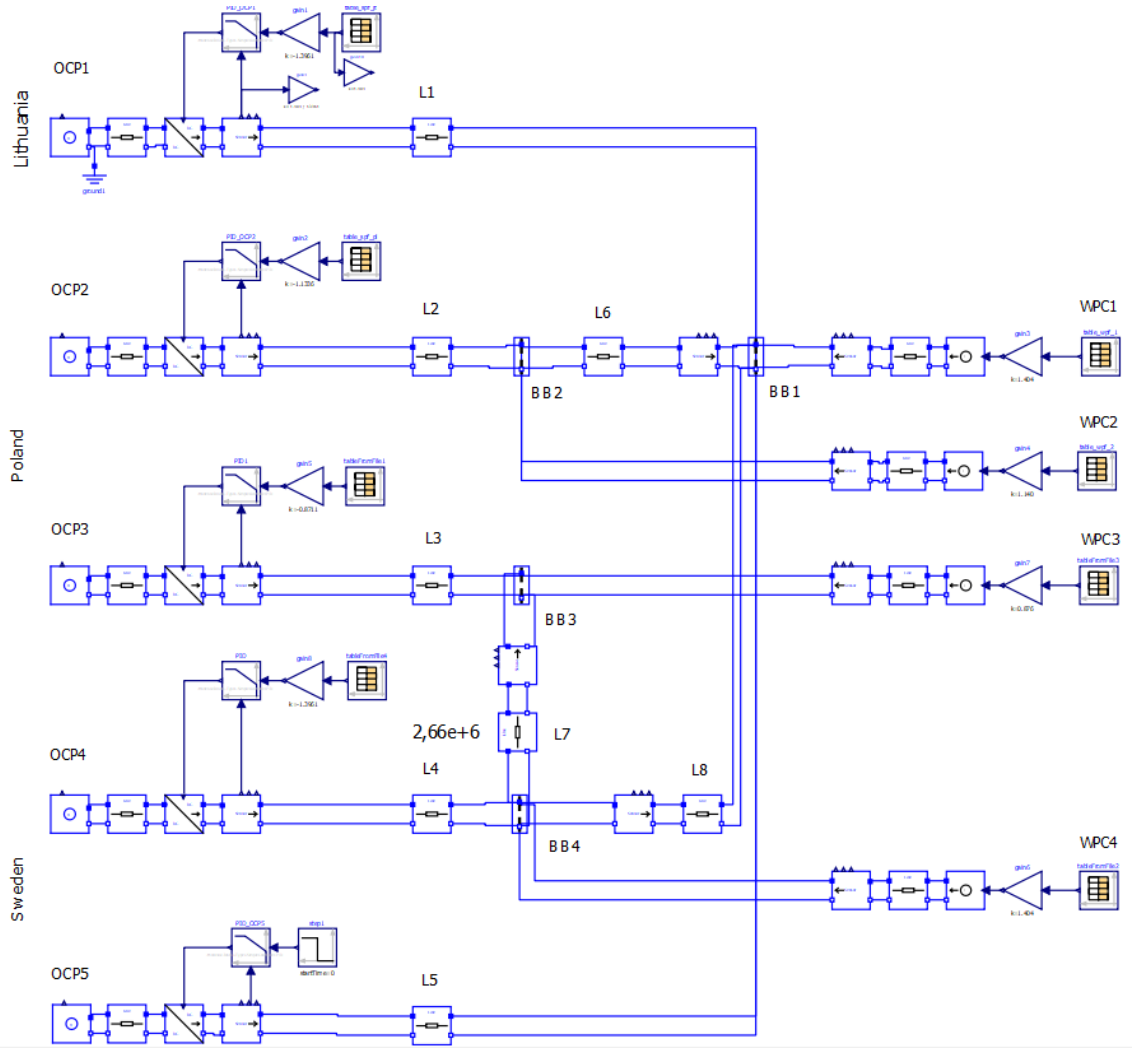


**Figure A.1:** Baltic InteGrid as modelled in OpenModelica - OCP is the Onshore Connection Points and WPP the Wind Power Plant power inputs.

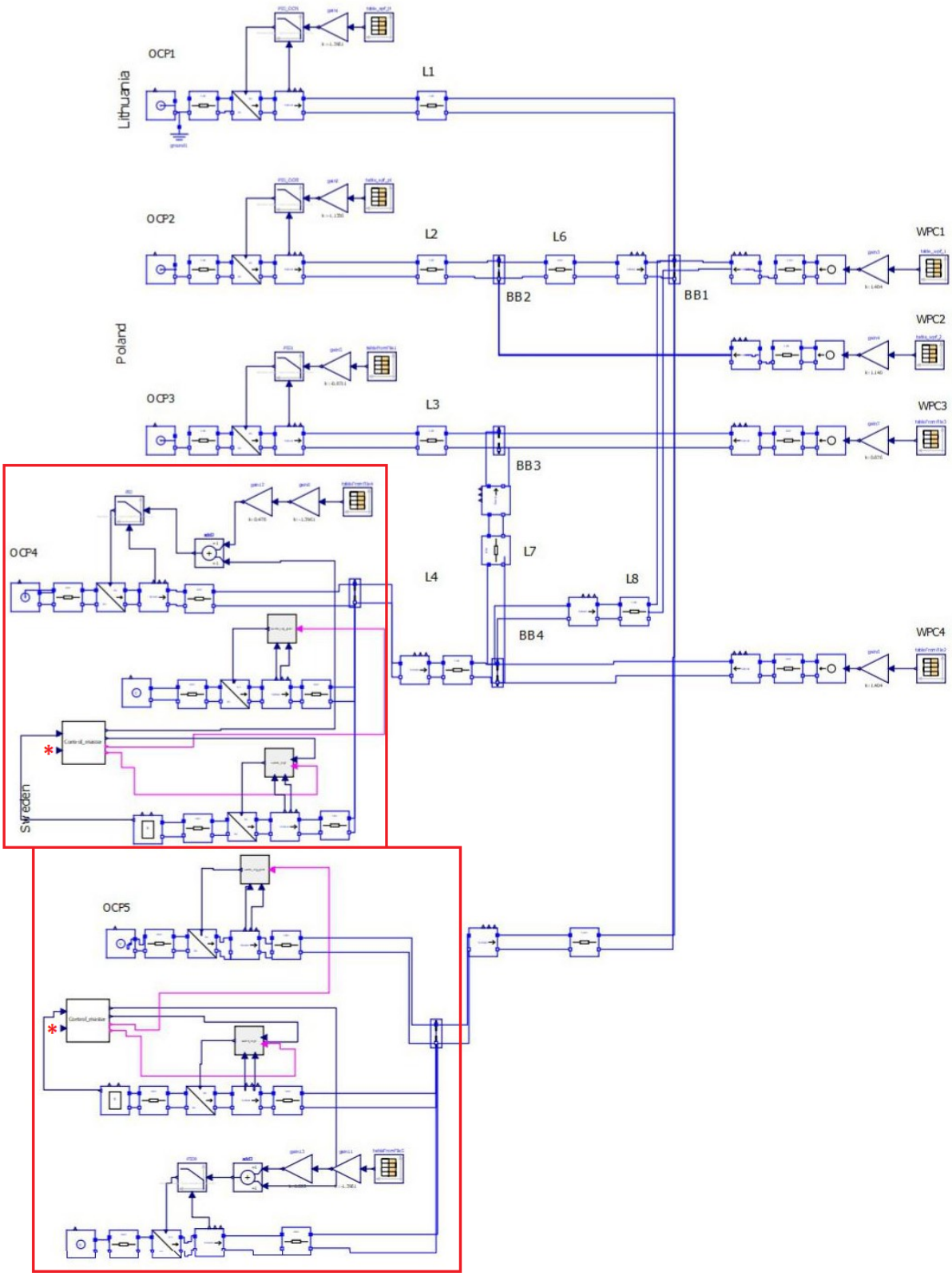


**Figure A.2:** Extended version of Baltic InteGrid as modelled in OpenModelica - OCP is the Onshore Connection Points and WPP the Wind Power Plant power inputs. The red lines mark the extension of the model to implement the BESS. The red (*) is where the addition of all WPP inputs and OCP outputs are connected. In the model this has been omitted to enhance the overview.

# Appendix B

# Extraction of Modelica-code for Method 3

```
if SOC_t2 > SOC_T_low2 and SOC_t2 < SOC_T_high2 and
SOC_t3 > SOC_T_low and SOC_t3 < SOC_T_high then

ynxt1 = 0;
state1 =0;

elseif SOC_t2 < SOC_T_high2 and SOC_t2 > SOC_T_low2 and
  SOC_t3 < SOC_T_low then

mit3 = (SOC_T_mid-SOC_t3) * batSize * 1000000;
mit2 = (SOC_T_high-SOC_t2) * batSize * 1000000;


    if mit3 < mit2 then
    state1 = 1;

        if mit3 < MI_limh then
        ynxt1 = mit3;
        else
        ynxt1 = MI_limh;
        end if;
    else
    state1 = 2;
        if mit2 < MI_limh then
        ynxt1 = mit2;
        else
        ynxt1 = MI_limh;
        end if;
    end if;


elseif SOC_t2 > SOC_T_low2 and SOC_t2 < SOC_T_high2 and
```

```
  SOC_t3 > SOC_T_high then

mit3 = (SOC_T_mid-SOC_t3)* batSize * 1000000;
mit2 = (SOC_T_low-SOC_t2)* batSize * 1000000;

    if mit3 < mit2 then
    state1 = 3;
        if mit2 > -MI_limh then
        ynxt1 = mit2;
        else
        ynxt1 = -MI_limh;
        end if;
    else
    state1 = 4;
        if mit3 > -MI_limh then
        ynxt1 = mit3;
        else
        ynxt1 = -MI_limh;
        end if;
    end if;


elseif SOC_t2 < SOC_T_low2 and SOC_t3 > SOC_T_low and
  SOC_t3 < SOC_T_high then

ynxt1 = (SOC_T_low-SOC_t2)* batSize * 1000000;
state1=5;


elseif SOC_t2 > SOC_T_high2 and SOC_t3 > SOC_T_low and
SOC_t3 < SOC_T_high then

  ynxt1 = (SOC_T_high-SOC_t2)* batSize * 1000000;
  state1=6;

elseif SOC_t2 > SOC_T_high2 or SOC_t2 < SOC_T_low2 and
  SOC_t3 < SOC_T_low or SOC_t3 > SOC_T_high then

ynxt1 = (SOC_T_mid-SOC_t2)* batSize * 1000000;
state1=7;

else
ynxt1 =0;
state1 = 0;

end if;
```